INFORMATION TO USERS

This manuscript has been reproduced from the microfilm master. UMI films the text directly from the original or copy submitted. Thus, some thesis and dissertation copies are in typewriter face, while others may be from any type of computer printer.

The quality of this reproduction is dependent upon the quality of the copy submitted. Broken or indistinct print, colored or poor quality illustrations and photographs, print bleedthrough, substandard margins, and improper alignment can adversely affect reproduction.

In the unlikely event that the author did not send UMI a complete manuscript and there are missing pages, these will be noted. Also, if unauthorized copyright material had to be removed, a note will indicate the deletion.

Oversize materials (e.g., maps, drawings, charts) are reproduced by sectioning the original, beginning at the upper left-hand corner and continuing from left to right in equal sections with small overlaps.

Photographs included in the original manuscript have been reproduced xerographically in this copy. Higher quality 6" x 9" black and white photographic prints are available for any photographs or illustrations appearing in this copy for an additional charge. Contact UMI directly to order.

University of Alberta

Characterization of Commercial Linear Low Density Polyethylenes by TREF, SEC, DSC, and Cross-Fractionation

By

Mingqian Zhang ©

A thesis submitted to the Faculty of Graduate Studies and Research in partial fulfillment of the requirements for the degree of **Master of Science**

In

Chemical Engineering

Department of Chemical and Materials Engineering

Edmonton, Alberta

Fall, 1999

National Library
of Canada

Bibliothèque nationale
du Canada

Acquisitions and
Bibliographic Services

Acquisitions et
services bibliographiques

395 Wellington Street
Ottawa ON K1A 0N4
Canada

395, rue Wellington
Ottawa ON K1A 0N4
Canada

The author has granted a non-exclusive licence allowing the National Library of Canada to reproduce, loan, distribute or sell copies of this thesis in microform, paper or electronic formats.

L'auteur a accordé une licence non exclusive permettant à la Bibliothèque nationale du Canada de reproduire, prêter, distribuer ou vendre des copies de cette thèse sous la forme de microfiche/film, de reproduction sur papier ou sur format électronique.

The author retains ownership of the copyright in this thesis. Neither the thesis nor substantial extracts from it may be printed or otherwise reproduced without the author's permission.

L'auteur conserve la propriété du droit d'auteur qui protège cette thèse. Ni la thèse ni des extraits substantiels de celle-ci ne doivent être imprimés ou autrement reproduits sans son autorisation.

0-612-47123-3

Canada

University of Alberta

Library Release Form

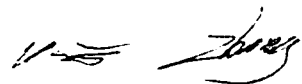**Name of Author:** Mingqian Zhang

Title of Thesis: Characterization of Commercial Linear Low Density Polyethylenes by TREF, SEC, DSC, and Cross-Fractionation

Degree: Master of Science

Year this Degree Granted: 1999

Permission is hereby granted to the University of Alberta Library to reproduce single copies of this thesis and to lend or sell such copies for private, scholarly or scientific purposes only.

The author reserves all other publication and other rights in association with the copyright in the thesis before provided, neither the thesis nor any substantial portion thereof may be printed or otherwise reproduced in any material form whatever without the author's prior written permission.

Mingqian Zhang

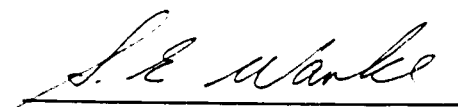608E, Michener Park
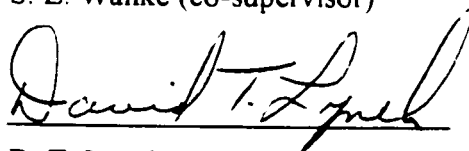Edmonton, Alberta
Canada T6H 5A1

Date: _Sept. 28, 1999_

University of Alberta

Faculty of Graduate Studies and Research

The undersigned certify that they have read, and recommend to the Faculty of Graduate Studies and Research for acceptance, a thesis entitled **Characterization of Commercial Linear Low Density Polyethylenes by TREF, SEC, DSC, and Cross-Fractionation** By **Mingqian Zhang** in partial fulfillment of the requirements for the degree of **Master of Science** in **Chemical Engineering**.

S. E. Wanke (co-supervisor)

D. T. Lynch (co-supervisor)

P. Choi

H. Uludag

Date: Sept 27, 1999

ABSTRACT

The molecular structure of various grades of Ziegler-Natta and metallocene LLDPEs was investigated by TREF, thermally fractionated DSC, SEC, TREF-SEC and TREF-SNA-DSC cross-fractionations. ATREF analyses demonstrated that Ziegler-Natta LLDPEs had a characteristic bimodal distribution of short chain branches (SCB), while the metallocene LLDPEs exhibited a narrower single-peaked distribution. Quantification of short chain branching was proposed through the use of number-average and weight-average SCB concentrations. DSC results of different LLDPEs treated with varying crystallization conditions indicated that the DSC analyses depended heavily on the thermal history of LLDPE samples. Successive nucleation/annealing (SNA) is a more effective and resolved thermal procedure than step-crystallization (SC) for segregating LLDPE with respect to methylene sequence length (MSL), and can provide complementary information to TREF. Quantitative analysis of the SNA-DSC showed that the average SCB contents estimated from the normalized heat of fusion were very close to those from TREF for the Zieger-Natta LLDPEs, but the average SCB contents for the metallocene LLDPEs were higher than those obtained from TREF. The cross-fractionation techniques were used to further investigate the molecular structure of different types of LLDPEs, of particular interest is the TREF-SNA-DSC cross-fractionation which allowed a direct observation of methylene sequence distribution and so SCB distribution. TREF-SEC cross-fractionation showed that the molar mass of the Ziegler-Natta LLDPE increased monotonically with decreasing SCB, while the plot of M_w versus SCB for the metallocene LLDPEs showed a maximum. TREF-SNA-DSC cross-fractionation clearly indicated that the metallocene LLDPE possessed only intramolecular heterogeneity in SCB distribution, whereas the Ziegler-Natta LLDPE showed both intramolecular and intermolecular heterogeneity.

ACKNOWLEDGMENTS

TABLE OF CONTENTS

LIST OF TABLES

LIST OF FIGURES

NOMENCLATURE

ATREF	Analytical temperature rising elution fractionation
CCD	Chemical composition distribution
^{13}C-NMR	Carbon-13 nuclear magnetic resonance
C_n	Number average short chain branch content
C_w	Weight average short chain branch content
ΔH_u or ΔH_f	Enthalpy of fusion
DSC	Differential scanning calorimetry
$\overline{F}_1$	Average mole fraction of monomer type 1
FTIR	Fourier transform infrared spectroscopy
HDPE	High density polyethylene
$[H_2]$	Hydrogen concentration
k_β	β-hydride elimination rate constant
k_p	Propagation rate constant
k_{tH_2}	Transfer to hydrogen constant
k_{tm}	Transfer to monomer rate constant
L	Lamellar thickness
LCB	Long chain branching
LDPE	Low density polyethylene
LLDPE	Linear low density polyethylene
$[M]$	Monomer concentration

M_1, M_2	Molar mass of the comonomers
MI	Melt index
MM	Molar mass
MMD	Molar mass distribution
M_n	Number average molar mass
M_w	Weight average molar mass
MSL	Methylene sequence length
n	Polymer chain length
$\bar{n}_n$	Instantaneous number-average chain length
$\bar{n}_w$	Instantaneous mass-average chain length
PE	Polyethylene
P_d	Polydispersity
PTREF	Preparative temperature rising elution fractionation
r_1, r_2	Reactivity ratios
SC	Step-crystallization
SCB	Short chain branching
SCBD	Short chain branch distribution
SEC	Size exclusion chromatography
σ_e	Surface energy of chain folding
SNA	Successive nucleation/annealing
τ	A parameter which represents the broadness of the composition distribution.
T_e	TREF elution temperature

T_m	Melting or elution temperature
T_m^0	Melting temperature of the pure polymer of infinite chain length
T_{onset}	Onset temperature of the primary peak on DSC endotherm
T_{peak}	Melting temperature of the primary peak on DSC endotherm
TREF	Temperature rising elution fractionation
ULDPE	Ultra low density polyethylene
VLDPE	Very low density polyethylene
$w(y)$	Composition distribution
X or X_a	Mole fraction of crystallizable ethylene units
X_c	Crystallinity
y	Deviation of an instantaneous composition from the average copolymer composition

INTRODUCTION

1.1. Classification of Polyethylene

Polyethylene (PE) is the major commodity polymer worldwide. Conventionally, polyethylene is classified into three types according to its density: high density polyethylene (HDPE), low density polyethylene (LDPE), and linear low density polyethylene (LLDPE). The world production capacity of polyethylenes in 1998 was approximately 45 million tons. The consensus of numerous studies shows that the global market demand is projected to increase by a healthy 5%+ per annum over the period to 2001, reducing to ~3.5% per annum in the early part of the next decade (2001-2005). It is also anticipated that LDPE will at best show low growth, while LLDPE will grow at ~10% per annum (Richards, 1998). Canada is a major producer and exporter of polyethylene, and its production capacity, particularly of LLDPE, is being expanded considerably.

Table 1.1 summarizes some characteristics of the three types of polyethylenes. It is evident that each type of PE is associated with a characteristic molecular structure, production process, density range, and applications. HDPE is a homopolymer of ethylene possessing a linear chain structure with no or very few branches, and up to 70% of the polymer can be in the crystalline phase, resulting in a high density of about 0.960 g/cm^3. LDPE is also a homopolymer of ethylene, but has a branched structure with long chain branches (LCB) and short chain branches (SCB) as depicted in Table 1.1. The branches disrupt the ordered arrangement of the macromolecular chains. A high SCB or LCB content means a large amount of crystal defects which lead to a lower crystallinity with a lower density and melting temperature. In general, LCBs have a profound effect on solution viscosity and melt rheology because of molecular size reduction and entanglements, while SCBs are particularly critical in influencing the morphology and solid-state properties of polyethylene.

Table 1.1. Density range, molecular structure, synthesis, and applications of various types of polyethylenes.

Type of PE	density range (g/cm³)	molecular structure	synthesis	common uses
HDPE	0.945 - 0.965		Polymerization of ethylene on Phillips, Ziegler-Natta and metallocene catalysts.	Gas pipe, car gas tanks, bottles, rope, and fertilizer bags.
LDPE	0.890 - 0.940		Free radical polymerization of ethylene at high temperature and high pressure.	Packaging film, bags, wire sheathing, pipes, waterproof membranes
LLDPE (VLDPE, ULDPE)*	0.910 - 0.925		Copolymerization of ethylene with α-olefins on Ziegler-Natta or metallocene catalyst.	Shopping bags, stretch wrap, greenhouse film.

* A family of LLDPE with density of 0.87-0.915 g/cm³.

The polymer commonly known as LLDPE is a copolymer produced by copolymerizing ethylene with α-olefins such as propylene, 1-butene, 1-hexene, 1-octene, and 4-methyl-1-pentene. LLDPE possesses a linear molecular structure with SCBs distributed nonuniformly along the backbone of polyethylene chain. The amount and distribution of SCBs have a profound effect on the thermal, physical, and mechanical properties of LLDPE. The diversity of the various LLDPE grades is primarily a result of variations in distributions of molar mass and short chain branches.

The topic of the current thesis is the characterization of different types of commercial LLDPEs. Development of fast and reliable LLDPE characterization techniques is of great interest for both industry and academia. First, the identification of the grade of new LLDPE and the prediction of its properties depends largely on such techniques. Second, the characterization of LLDPE with respect to molar mass and short chain branching by new and improved techniques is indispensable for obtaining a better understanding of the relationship between performances and molecular structure. In particular, the ever-growing advent of the new grades of LLDPEs and new applications entails effective characterization techniques to identify the difference in molecular structures and properties between different LLDPEs (e.g. between Ziegler-Natta and metallocene LLDPEs). Third, the characterization of LLDPE is also a good way to gain insight into polymerization mechanism and the effect of polymerization conditions on molecular structures of polymers. Such investigation has become important for obtaining kinetic characteristics of polymerization of ethylene on heterogeneous catalyst systems and the effect of polymerization conditions.

1.2. Ziegler-Natta and Metallocene Catalysts and LLDPEs

The end-use properties of LLDPE depend largely on the molecular structure. It is the variations of such molecular parameters as molar mass (MM), molar mass distribution (MMD), short chain branches (SCB), and short chain branch distribution (SCBD) which provide the various properties of LLDPE that meet the requirement for different applications. Catalysts play a key role in the synthesis of LLDPE with various molecular

structures. Hence, it is appropriate to give an introduction to catalysts used to produce LLDPEs. Traditionally, LLDPE is produced by Ziegler-Natta catalyst. In the past decade, the advent of metallocene catalyst and other single-site catalysts is revolutionizing LLDPE production and diversifying the grades of LLDPEs and their applications (Richards, 1998; Morse, 1998). Because of the major advance in LLDPE production technology, very low density polyethylene (VLDPE) and ultra low density polyethylene (ULDPE), a family of LLDPE that bridges the density gap between LLDPE of 0.915 g/cm^3 to ethylene/propylene rubber (EPR) of 0.85 g/cm^3, are available nowadays as a new materials for the packaging industry. The applications of different grades of LLDPEs are principally defined by their properties which are in turn determined by their characteristic molecular structures. For the production of commercial LLDPE, it is catalysts that have played an important role in defining the molecular structures of different grades of LLDPEs. Consequently, Ziegler-Natta LLDPE and metallocene LLDPE are commonly used presently to distinguish LLDPEs according to the nature of their parent catalysts.

In its broadest definition, Ziegler-Natta catalysts are composed of transition metal salts of metals from Group 4 to 8 (known as catalyst) and a metal alkyl of a base metal from Group 1, 2, 3 (known as cocatalyst). For industrial use, most Ziegler-Natta catalysts are based on titanium salts and aluminum alkyls. Ziegler-Natta catalysts are inherently heterogeneous although homogeneous Ziegler-Natta catalyst such as vanadium-based catalysts exists. In addition to being heterogeneous with respect to the number of phases present during polymerization process, i.e. solid catalyst and liquid or gaseous reactants, the catalytic sites in Ziegler-Natta catalysts are also "heterogeneous", namely, Ziegler-Natta catalysts have chemically different catalytic sites which are active for polymerization. The multiple active sites, each having a different structure and activity toward different monomers, translate to a great variation in MMD and chemical composition distribution (CCD) (Huang and Rempel, 1995; Reddy and Sivaram, 1995; Hamielec and Soares, 1996).

The most important innovations introduced in the manufacture of polyolefins with Ziegler-Natta catalysts lie in the synthesis of linear low density polyethylene by the copolymerization of ethylene with α-olefins. The incorporation of α-olefins into the backbone of polyethylene introduces comonomer units that contain short chain branches which disrupt the order of the linear polyethylene chain. As a consequence, the density, crystallinity, and rigidity of the polymer are decreased. By varying the amount and type of α-olefin, the type of catalyst, and the polymerization conditions, one can produce several grades of copolymers with different properties to meet specific market demands.

Metallocene catalyst are organometallic coordination compounds in which two cyclopentadienyl rings or substituted cyclopentadienyl rings are bonded by a π-bond to a Group 4 transition metal atom. The nature and the number of the cyclopentadienyl rings, the type of transition metal, and the cocatalyst type determine the catalytic behavior of metallocene catalyst towards the polymerization of olefins. Methylealuminoxane (MAO) has been found to be the best cocatalyst for the Group 4 metallocene catalysts which are being used commercially.

There are two major aspects in which metallocene catalyst differs from conventional heterogeneous Ziegler-Natta catalysts (Reddy and Sivaram, 1995; Hamielec and Soares, 1996; Morse, 1998):

(1) All transition metal atoms are active in homogeneous metallocene systems.

(2) Only a "single-site" is present in a homogeneous system under proper conditions.

Due to the single-site nature, metallocene catalysts can produce polymers with a sharp melting temperature, narrow molar mass distribution approaching the theoretical polydispersity value of 2.0 predicted by the Schultz-Flory mechanism. As well, for the copolymerization, metallocene catalyst can produce copolymers with an almost random incorporation of comonomers, which results in a maximum decrease in polymer crystallinity for a given amount of comonomer incorporation (Reddy and Sivaram, 1995; Hamielec and Soares, 1996).

5

Another primary advantage of metallocene catalysts is that it is possible to "tailor" the molecular architecture of the LLDPE by varying ligands in catalyst or polymerization conditions to provide the properties that are required for a particular application. This represents a major advance in capability for the polymer production, from a situation with Ziegler-Natta and Phillips catalyst development which was largely empirical. Although the metallocene LLDPE suffers from processability problems due to the narrower MMD, it is likely that the problems will be overcome by blending such polymers with LDPE or incorporating long chain branching in the polymer backbone. It is predicted that metallocene LLDPE with much improved product performance will gradually replace high pressure low density polyethylene and Ziegler-Natta linear low density polyethylene, particularly in film applications (Richards, 1998).

1.3. Relationship between Molecular Structure and Properties of LLDPE

The properties of a polymer in solid state and also in the molten state depend on its molecular structure. Specifically, the properties of a LLDPE depend on such molecular parameters as molar mass, molar mass distribution, short chain branching, and short chain branch distribution. As an example, the high flexibility of a LLDPE stems from its short chain branches. For a given average SCB content, a broad SCBD indicates a greater amount of low SCB molecules with low flexibility. As a result, the metallocene LLDPE with narrow SCBD has higher flexibility than Ziegler-Natta LLDPE.

In industry, polyethylene grade specifications are given in terms of the melt index (MI) and density. MI refers to the flow rate, usually expressed in g/10 min., measured at a specific temperature, e.g. 190°C, and a very low shear stress of $\tau = 1.966 \times 10^4$ Pa using a very short capillary. Density is related to the fraction of polymer which is crystalline. Albeit both indexes convey no information about molecular structure, they are related to the structural parameters. MI is a function of molar mass and branching. Density is mainly a function of crystallinity and therefore short chain branching to a larger degree. Density and MI are good indicators of LLDPE properties, but they cannot uniquely

define the properties. Ultimately, the properties of LLDPE are determined by its molecular structure.

Sugawara (1994) provided an interesting comparison of properties among the various branched polyethylenes produced by different technologies. Ziegler-Natta LLDPE is superior in blown film properties in terms of impact strength, tear strength, and stability to LDPE produced at high pressure, but is inferior to metallocene LLDPE. However, the HP-LDPE shows much better processability due to the broader MMD and the much higher levels of long chain branching. The performance-processability relationships are shown in Figure 1.1. It seems that the target LLDPE made with catalyst systems should have narrow molar mass distribution but contain high levels of long chain branching to further improve processabillity.

Todo et al. (1996) investigated the relationship between molecular structure and physical properties of LLDPEs produced with Ziegler-Natta and metallocene catalysts. They found that the comonomer content of Ziegler-Natta LLDPE varies according to the length of the main chain of the polymer. Small LLDPE molecules tend to have a higher concentration of comonomers than large LLDPE molecules. The small molecules are undesirable fractions that decrease performance such as high blocking characteristics and low clarity of the film. In comparison, metallocene LLDPE shows very narrow molar mass distribution and composition distribution, and exhibits improved properties such as high impact strength, high stress crack resistance, high clarity, and low heat seal temperature.

The superior properties of metallocene LLDPE to Ziegler-Natta LLDPE are probably a result of SCB distribution. Takahashi et al. (1995) conducted a comparative investigation of the relationship between properties and the structure of different LLDPEs. Based on their temperature rising elution fractionation (TREF) and n-decane extraction experiment, a model for catalytic active sites and the corresponding molecular structures were proposed as shown in Figure 1.2. The Ziegler-Natta catalyst possesses multiple active sites which produce LLDPE molecules of different MM and SCB content,

and MM increases with decreasing SCB. Metallocene catalysts are single-sited and produce LLDPE molecules with the same average SCB content. The difference in the molecular structure between Ziegler-Natta and metallocene LLDPE results in the remarkable difference in blown film properties, as shown in Figure 1.3. Overall, the metallocene LLDPE exhibits superior properties to the Ziegler-Natta LLDPE.
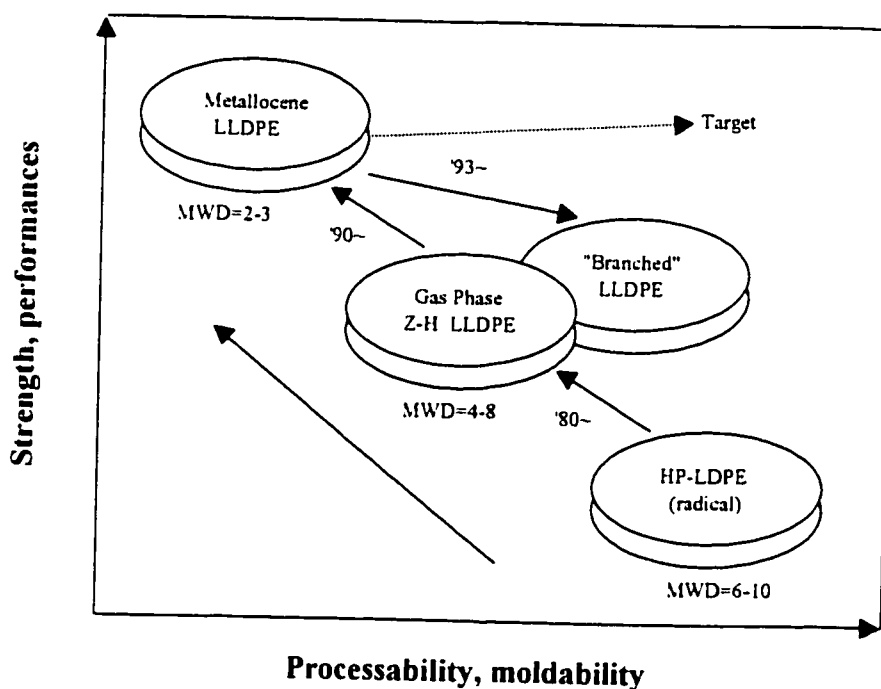
Figure 1.1. Balance of strength versus processability and moldability for polyethylenes synthesized using different polymerization processes (Sugawara, 1994).

The structure-properties relationships of homogeneous ethylene/1-butene copolymers made using DOW INSITE Technology, also called constrained geometry catalyst technology (CGCT), were studied by Kale et al. (1996). The copolymers contain 1.77-4.17% comonomer and have a polydispersity of around 2. It has been found that the physical properties of this type of LLDPE are enhanced with increasing α-olefin branch length, that is, ethylene/1-octene copolymers produced by CGCT have improved tear,

8
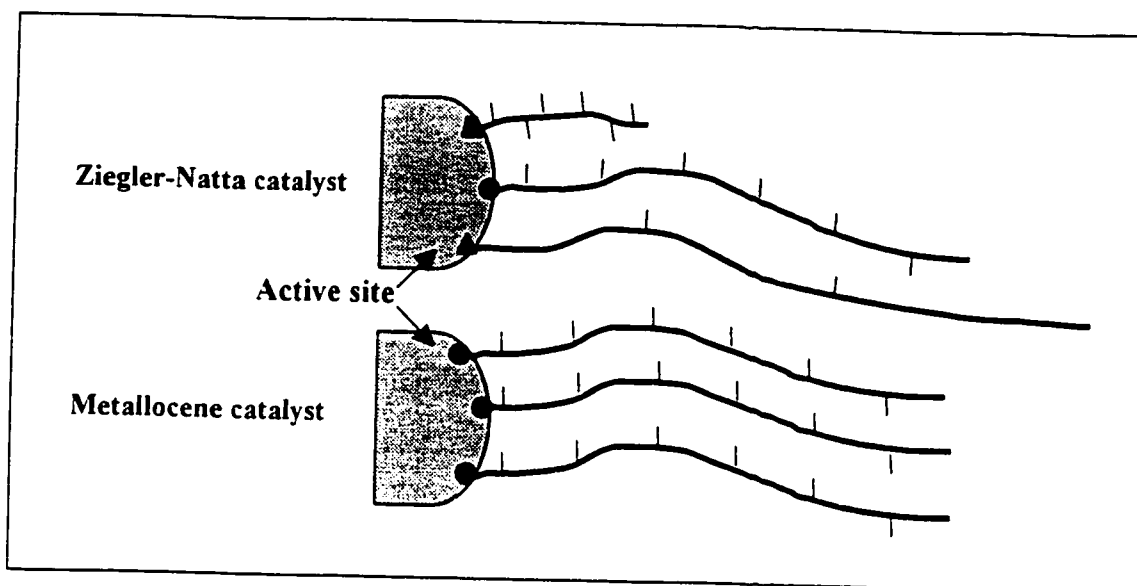
Figure 1.2. Structure model of catalytic active sites and corresponding LLDPE for Ziegler-Natta and metallocene catalyst (Takahashi, 1995).
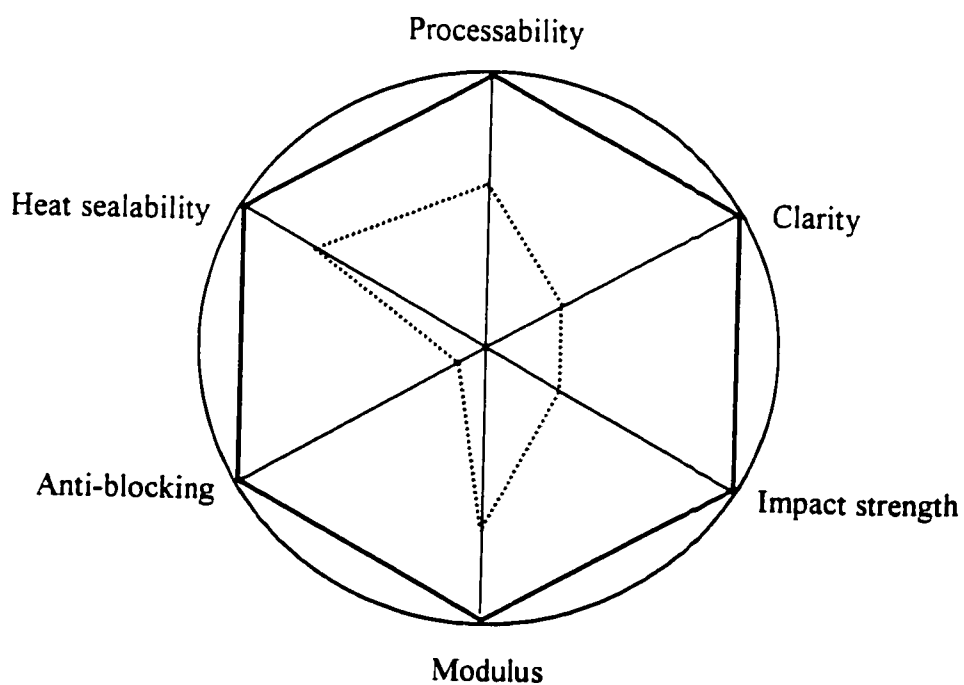
Figure 1.3. Radar chart of blown film properties of Ziegler-Natta LLDPE (dashed line) and metallocene LLDPE (solid line) (Takahashi, 1995).

impact and tensile properties compared to ethylene/1-butene copolymers produced via the same technology. These improved physical properties were observed in both compression molded plaques and blown film samples. With the characterization of these LLDPEs, it is assumed that the tie-molecules are the key factor in producing the superior tear and impact properties, suggesting that the octene comonomer is more effective than butene in producing tie-molecules.

Kim et al. (1996) investigated the processability of various types of commercial polyethylenes with respect to their molecular structure by measuring their melt rheological and thermodynamic properties. The results show that short chain branching mainly controls the density and thermodynamic properties, but it has little effect on the melt rheological properties. On the contrary, long chain branching has little influence on the density and thermodynamic properties, but it drastically affects the melt rheological properties by reducing the viscosity in processing and thus improving the processability. It is also concluded that very small amount of LCB in metallocene LLDPE can effectively reduce the viscosity and improve the flow stability in processing.

In summary, the physical, thermodynamic, and rheological properties of LLDPE are a strong function of its molecular structure. Two LLDPEs could exhibit widely different properties even if they have similar MI, density, or average SCB content (Kale et al., 1996). That is primarily due to the fact that some other molecular parameters such as SCBD may have a significant impact on the properties. Hence, the interpretation of the structure-property relationship would largely depend on the detailed characterization of molecular structure of LLDPEs.

1.4. LLDPE Characterization

Owing to the very different nature of the Ziegler-Natta and metallocene catalyst systems, a variety of LLDPEs which differ in properties are being produced worldwide. As indicated in the preceding section, the end-use properties of these commercial LLDPEs depend upon not only average molar mass and chemical composition but also

10

upon molar mass distribution and chemical composition distribution or short chain branch distribution. For example, two metallocene LLDPEs produced by different manufacturers could have similar average MM and SCB, but they may exhibit considerably different properties, which could result from the structural difference in SCBD. As a consequence, the molecular structure of LLDPE should be investigated in terms of average comonomer content, monomer sequence distribution along a polymer chain (intramolecular distribution of comonomer), and distribution of comonomer among polymers (intermolecular distribution of SCB) besides average molar mass and molar mass distribution.

Fractionation of LLDPE in terms of molar mass and short chain branch has been identified to be the best way to characterize the molecular structure of LLDPE. Size exclusion chromatography (SEC) has long been employed to measure molar masses and molar mass distributions of polymer. Temperature rising elution fractionation, a technique which fractionates semicrystalline polymer according to crystallizability, has been widely used for the characterization of LLDPE with respect to SCB. Although TREF has been considered as the most reliable technique available for the characterization of LLDPE in terms of SCB, it suffers from being solvent-involved and time-consuming. In the past decade, thermally fractionated differential scanning calorimetry (DSC) has been emerged as an alternative technique for the compositional characterization. Since LLDPE can be very heterogeneous on the molecular level in terms of SCBD, the thermal segregation process, which occurs during isothermal and dynamic crystallization of polymer from melt, can segregate LLDPE molecules according to the crystal size or the methylene sequence distribution. Although the thermally fractionated DSC is solvent-free and faster compared with TREF technique, the results are debatable, for the melting behaviors of LLDPE strongly depend on its thermal history. Furthermore, it is very difficult to obtain quantitative results from the thermally fractionated DSC.

The extended use of TREF is the combination of TREF with another fractionation technique to further separate the molecular species according to their different structures.

11

The cross-fractionation can, in essence, provide more detailed information about the molecular structure of LLDPE. TREF combined with SEC, or TREF-SEC cross-fractionation, has been extensively utilized to investigate the relationship between SCB and molar mass of LLDPE. The method has also become useful recently for obtaining kinetic characteristics of polymerization of ethylene on heterogeneous catalyst system.

Detailed information about SCB distribution, in particular, the intermolecular and intramolecular distribution of SCB, is of paramount important in determining thermodynamic and crystallization behaviors of LLDPEs. Such information can be obtained by compositional cross-fractionation. However, owing to the lack of another compositional fractionation technique, relatively little has been reported on the intra- and inter-molecular SCB distribution of TREF fractions and their generation mechanism. With the development of thermally fractionated DSC into a compositional fractionation technique, it should therefore be possible to combine TREF with DSC to obtain additional information on the molecular structure of different types of LLDPEs.

It should also be recognized that the TREF mechanism of separation is not fully understood. Although it is generally agreed that TREF fractionates semicrystalline polymer based on crystallizability, and so most of the TREF calibrations have been based on the average SCB generated from preparative TREF (PTREF), there has been suggestions that TREF separates macromolecules based on the length of crystallizable sequence. This can be easily understood by considering a crystallized molecule in TREF column, a sufficiently high rise in temperature above the crystallization temperature will first cause the molecule parts with the shortest crystallized sequence to dissolve. Upon a further increase in temperature the longest crystallized sequence will ultimately become unstable in the crystals, and the whole molecule will dissolve and elute from the column. Only then can a change in concentration in solution be detected. The signal obtained represents the entire molecule, but at a temperature that is characteristic of the longest crystallized sequence in that molecule. Therefore, the longest methylene sequence length may dictate the separation of TREF. However, there has not been any direct experimental evidence for the mechanism. On the other hand, the mechanism of the thermally

fractionated DSC is almost undoubtedly believed to be based on lamellar thickness and so methylene sequence length. Hence, TREF-DSC cross-fractionation of different LLDPEs may serve as a means to provide insights into the TREF mechanism.

The objective of this study is to present results of the molecular structure of commercial LLDPEs produced by the Ziegler-Natta and metallocene catalysts. A variety of crystallization methods were employed to study the effect of the thermal treatment on the behavior of different LLDPEs. TREF and thermally-fractionated DSC were the primary techniques for the characterization of the treated LLDPEs in terms of SCB and SCBD. Attempts were also made to quantify DSC analysis. The LLDPEs were further characterized by cross-fractionation techniques. TREF-SEC cross-fractionation was employed to characterize the relationship between SCB and molar mass. The TREF fractions were also segregated based on methylene sequence length by using DSC coupled with the successive nucleation/annealing (SNA) to reveal the heterogeneity of SCB distribution.

LITERATURE REVIEW

2.1. Techniques for LLDPE Characterization

The preceding section indicated that for LLDPE, it is not only the average level of molecular mass and the amount of short chain branches, but also their distributions which have a significant effect on the end-use properties of the material. It comes as no surprise that the development of fast and reliable techniques for the characterization of LLDPE in terms of MM and SCB is of great interest in both industry and academia. Table 2.1 lists techniques most-commonly used for LLDPE characterization. Size exclusion chromatography (SEC) has become a mature and routine technique for the determination of MM and MMD, although some other techniques are available. For the characterization of short chain branches, techniques such as ^{13}C NMR and FTIR are available, but only capable for the determination of the average SCB content. Carbon-13 NMR, although frequently used for sequence distribution analysis of LLDPE, cannot distinguish the distribution of ethylene block length in runs longer than three ethylene units (Keating et al., 1994). Thus, the best way to characterize LLDPE in terms of comonomeric composition and branching is to fractionate it according to its structural parameters (Francuskiewicz, 1994). As a result, temperature rising elution fractionation (TREF), a fractionation technique based on crystallizability resulting from SCB, emerged and has quickly become the most commonly-used method for characterizing short chain branch distribution, even though TREF equipment is not commercially available at present. However, just like any other analytical techniques, TREF has its own disadvantages of being solvent-involved and having tedious procedures. For the past decade, differential scanning calorimetry has been utilized as an alternative to TREF, since DSC apparatus is much more widely available than TREF equipment, and DSC analysis is solvent-free and much faster. The biggest drawback of DSC is that the DSC results of polymer depends heavily on the thermal history of samples. Also, due to the qualitative nature of DSC analyses, there have been very few quantitative results reported in the open literature.

Table 2.1. Techniques for the characterization of LLDPE

Molecular parameter	Characterization technique
Molar mass (MM)	SEC, viscometry, colligative properties
Molar mass distribution (MMD)	SEC
Short chain branching (SCB)	FTIR, ^{13}C NMR, TREF
Short chain branch distribution (SCBD)	TREF, DSC

2.2. TREF

TREF is a fractionation technique which fractionates semi-crystalline polymer based on the difference in crystallizability of macromolecules due to the variation in short chain branching level (Desreux and Spiegels, 1950). The earlier applications of TREF had been the attempt to fractionate high pressure low-density polyethylene (HP-LDPE) (Shirayama et al., 1965). The power of this technique was not fully appreciated until Wild and Ryle (1977) applied the technique to fractionate LLDPEs. The suggested approach was to obtain fractions of a narrow distribution having different SCB averages by using increasing temperature fractionation technique (later called preparative TREF) and then use them to determine a calibration curve of the SCB as a function of elution temperature for the analytical TREF (ATREF). A linear relationship between SCB and elution temperature was generally observed (Glockner, 1990; Soares et al., 1995a). In the past decade, TREF has been recognized as the most powerful and reliable technique for the structural analysis of LLDPEs and their blends (Kelusky et al., 1987; Soares et al., 1995). Several reviews devoted to various aspects of TREF analysis have been published (Wild, 1990; Glockner, 1990; and Soares et al., 1995a).

Although the TREF technique has been refined by a number of researchers by using data acquisition automation and off-line crystallization, the TREF procedure has been

15

essentially similar to those suggested earlier by Wild et al. (1977) and summarized by Francuskiewicz (1994). Monrabal et al. (1994, 1996, and 1999) proposed a technique called crystallization analysis fractionation (CRYSTAF). The technique makes use of the different crystallizabilities of semicrystalline polymer as TREF does. Instead of physically fractionating a LLDPE sample, the CRYSTAF extracts information directly during the crystallization process by monitoring the solution concentration depression. The method dispenses with the elution step of TREF but is much more time-consuming compared to the off-crystallization of TREF. CRYSTAF yields profiles similar to TREF profiles (Monrabal et al., 1994 and 1996). Other than the characterization of LLDPEs and their blends, TREF has been also expanded recently to the characterization of other olefin copolymers such as ethylene/styrene copolymer (Thomann et al., 1997) and propylene/1-butene copolymer (Abiru et al., 1998).

Perhaps one of the most important applications of TREF is its use for studying the nature of polymerization catalysts. Usami et al. (1986) compared four LLDPE samples made by different processes. The four LLDPEs show considerably broader and bimodal TREF profiles, which were ascribed to at least two different active sites present on the catalyst, one producing almost exclusively linear homopolyethylene and the other LLDPE with a broad composition distribution. Kakugo et al. (1988) used PTREF to investigate the catalytic active sites for ethylene/propylene and proplyene/1-butene copolymerization. The authors concluded that the lower isospecific catalytic sites were more active toward ethylene but that their activity did not change as much for 1-butene. Cheng and Kakugo (1991) combined PTREF with ^{13}C NMR spectroscopy to characterize compositional heterogeneity in ethylene/propylene copolymers produced by a Ti-based heterogeneous Ziegler-Natta catalyst. The triad sequences of each PTREF fraction were determined by ^{13}C NMR spectroscopy. The obtained PTREF-^{13}C NMR data were simulated by different multiple-site statistical models. A Bernoullian model containing 3 or 4 active-site types gave the best data representation.

The biggest challenge TREF is facing may be that the mechanism of TREF separation is not fully understood. This, to a larger extent, will hamper the interpretation

16

of different calibrations (Karbashewski and Rudin, 1993; Bonner et al., 1993; Mathot 1994; Borrajo et al., 1995; Elicabe et al., 1996). It is generally accepted that TREF fractionates semi-crystalline polymer based on the difference in crystallizability due to various chemical composition of the polymeric chains (molecules), thus growing SCB or increasing comonomer content results in an almost linear depression of the melting or elution temperature (Wild, 1990; Glockner, 1990; Soares et al., 1995). However, the results from some LLDPEs have indicated otherwise. Karbashewski and Rudin (1993) investigated the effect of comonomer sequence distribution on TREF branching distribution. They suggested that it is not the average branch content but rather the effective branch content that determines the crystallinity distribution of a linear low density polyethylene. As a result, the concept of a universal calibration curve for ATREF proposed by Wild et al. (1977, 1982a, and 1982b) and Mirabella and Ford (1987) is not likely to hold true over the broad class of commercially available resins. Pigeon and Rudin (1993 and 1994) employed dual IR detectors, one measuring a C-H stretching band of methyl groups and the other a C-H stretching band of methylene groups, and found that the calibration curves for two different LLDPEs are indeed slightly different.

On the other hand, there have been suggestions that TREF fractionates semi-crystalline polymer based on the length of crystallizable sequence between SCB points, commonly referred to as methylene sequence length (MSL). Based on this assumption and a modified Flory equation, Bonner et al. (1993) proposed a novel method of constructing the TREF calibration curve using five standard linear polyethylene samples. Borrajo et al. (1995) proposed a thermodynamic model for TREF based on the Flory-Huggins theory. They suggested that the TREF fractionation process is based essentially on crystallizable sequence lengths in addition to the degree of crystallinity attainable for the solid polymer after slow crystallization. Mathot (1994) indicated that there is a possibility that TREF may separate the polymer based on the longest sequence within a molecule. This is based on the fact that a polymer molecule only elutes from TREF column and is detected at a temperature that is characteristic of the longest sequence in the molecule, suggesting that the calibration curve generated by Bonner et al. (1993) would be valid, and DSC can be a useful complementary tool, since at each temperature

at which molecule parts dissolve, there is a measurable heat of fusion which is associated with sequences in molecules and between molecules.

Despite the difference in calibration curves generated with different LLDPEs (Glockner 1990; Soares et al. 1995), TREF is still the most reliable and most widely used technique for the characterization of LLDPE. Since macromolecules are physically separated and detected at elution temperatures, TREF is merely capable for evaluating intermolecular heterogeneity of SCB distribution. As a result, when it comes to the full characterization of LLDPE, TREF needs techniques such as thermally-fractionated DSC to complement the assessment of intramolecular heterogeneity of SCB distribution (Mathot, 1994).

2.3. Thermally Fractionated DSC

The segregation on crystallization of semicrystalline polymer from macromolecular melt was already recognized in the 1960s (Wunderlich, 1976). The earlier studies were focused on the effect of annealing on the reorganization of the existing crystals rather than systematically sorting crystalline polymers by crystallite size. It was observed that annealing allows the formation of crystals with lamellae that approach the equilibrium thickness at the annealing temperature. The higher the annealing temperature, the thicker the lamella. All of those earlier studies laid the basis for the application of DSC to segregating the polymer by crystal size.

DSC is a much faster technique than TREF, and it is solvent-free. Many studies have been devoted to utilizing DSC as a possible alternative to TREF. The earlier studies done by Wild et al. (1990) and Karbashewski et al. (1992) showed that DSC analyses of LLDPE samples that had been crystallized slowly gave much of the same qualitative information as analytical TREF in terms of estimating the breadth of the SCBD, but the resolution of DSC was not as good as that of TREF. These studies also indicated that the quantitative analysis of DSC is difficult due to the fact the intensity of the DSC response is a product of the amount of material melted at a particular temperature and the enthalpy

of fusion, ΔH_{melt}, of that material. In order to translate a DSC endotherm into a mass distribution, the ΔH_{melt} for each fraction has to be measured and the DSC response corrected for the differing enthalpies of melting.

The resolution of DSC endotherms can be improved by thermal treatment of LLDPE. A thermal fractionation technique, first proposed by Adisson et al. (1992), consisted of a stepwise crystallization of the polyethylene chains in melt by successive annealing at descending temperatures and the subsequent analysis of the melting behavior of the treated samples by DSC. The DSC thermograms of the semicrystalline ethylene copolymers displayed multiple melting peaks. It was concluded that each peak formed is representative of a distinct family of macromolecules or block of monomeric units with different SCB.

Keating and McCord (1994) used a similar method to examine the distribution of ethylene block lengths and distinguish the structural subtleties of a variety of ethylene copolymers. They concluded that: (a) copolymers with high comonomer content are less crystalline and the ethylene sequences are shorter, (b) the comonomer type makes a difference in fractionation if H-bonding is involved, (c) the narrow comonomer distribution or ethylene segment length distribution has fewer DSC fractions, (d) fractionation by crystallinity is affected if the molar mass is very high, (e) branch content reduces the crystallinity and shortens the ethylene block length, and (f) there is no direct relation to molar mass distribution or comonomer content.

Starck (1996) conducted a comparative study on the comonomer distribution of a series of commercial LLDPEs produced with traditional high activity Ziegler-Natta catalysts by using TREF and a segregation fractionation technique (SFT) based on a stepwise crystallization by DSC. The author concluded that the heterogeneity of the Ziegler-Natta type of commercial LLDPE and VLDPE copolymers can be evaluated in a much shorter time using DSC fractionation than using TREF, and the DSC method showed similar compositional information although the shapes of the curves were not the same. By applying the SFT, separation in different segregated species takes place, and

smaller difference in the chemical composition distribution of the polymers can be identified.

A semi-quantitative study was done by Keating et al. (1996). They used thermal fractionation, i.e., step-crystallization method, to segregate very low density polyethylene (VLDPE) and ultra low density polyethylene (ULDPE). Both copolymers showed a DSC endotherm with multiple peaks, each of which represents a family of crystallizable ethylene sequences. A series of commercially-available hydrocarbons were treated under the same conditions as polymer samples, and used to construct a calibration curve relating melting temperature to ethylene sequence length. The method gave rise to the semi-quantitative assessment of ethylene sequence length distribution of different LLDPEs.

Muller et al. (1997) applied the classical self-nucleation technique to segregate different types of polyethylenes. Based on a superposition of the self-nucleation and annealing cycles which are similar to those designed by Fillon et al. (1993) for the evaluation of the self-nucleation process in polypropylene (PP), a thermal treatment procedure referred to as successive self-nucleation/ annealing (SSA) was developed for the segregation of various types of polyethylenes. The SSA procedure was compared with the step-crystallization (SC) method in the literature. It was concluded that the SSA generally produces better fractionation than the step-crystallization and that the chain branching distributions derived from the SSA-DSC can be qualitatively comparable to those obtained by TREF. Quite recently, Feng and Jin (1999) investigated the effect of the self-nucleation on the crystallization and melting behavior of low ethylene content propylene-ethylene copolymers. The results indicated that the crystallization temperature depends on the pre-selected annealing temperature and the self-nucleation can enhance the crystallization, suggesting that the self-nucleation can offer advantages of high resolution and sensitivity for the segregation of LLDPEs.

2.4. Cross-Fractionation

ATREF or thermally fractionated DSC is a technique for obtaining the SCB distribution of LLDPEs. PTREF coupled with another fractionation technique, commonly referred to as cross-fractionation, should be a means of obtaining more detailed information on the heterogeneity of SCB distribution. In particular, the advent of metallocene LLDPE in the past decade entails the elucidation of the heterogeneous and homogeneous distribution of SCBs and the better interpretation of the difference in properties between metallocene LLDPEs and their Ziegler-Natta counterparts. Also, the cross-fractionation methods have become powerful tools for revealing the kinetic characteristics of ethylene copolymerization. Since the microstructure of LLDPE is mainly determined by the nature of catalyst and polymerization conditions, very important information can be obtained on the effects of catalyst and polymerization conditions on the molecular structure by studying the crystallization behaviors of the whole polymer and its fractions.

In principle, cross-fractionation takes advantage of another fractionation technique to further fractionate PTREF fractions according to different molecular parameters. The most commonly used cross-fractionation technique is TREF-SEC cross-fractionation. Earlier cross-fractionation conducted by Nakano and Goto (1981) and Wild et al. (1982b) focused on the identification of the relationship between molar mass and the degree of short chain branching by using TREF-SEC. A common observation has been that molar masses of LLDPEs decrease with increasing branching (Usami, 1985). Recently, SEC has also been used to analyze PTREF fraction to assess the influence of catalyst and polymerization conditions on the microstructure of polyethylene.

Schouterden et al. (1987) fractionated an ethylene/1-octene copolymer by molar mass using successive solution fractionation (SFF). The obtained fractions and the original copolymer were analyzed with ATREF. A very broad bimodal branching distribution was observed for both the non-fractionated polymer and the fractions. The average degree of branching decreased with increasing average molar mass of the

21

fractions. The melting behaviors of the isothermally crystallized samples were further studied by DSC. The observed low temperature melting endotherm was considered to be caused by the melting of smaller crystals composed of very highly branched molecules, while the endotherms above the isothermal crystallization temperature were the result of the melting of thicker crystals composed of weakly branched molecules.

Wilfong and Knight (1990) utilized TREF-SEC and TREF-DSC cross-fractionation to investigate the crystallization mechanism of ethylene/1-octene copolymers. The PTREF fractions were further fractionated by SEC. It was found that the molar masses of PTREF fractions increased with increasing TREF temperature, i.e., decreasing degree of short chain branching. This was attributed to the difference in reactivity between ethylene and 1-octene and the subsequent depletion of the ethylene comonomer in the solution process. The crystallization and melting behaviors as well as morphology of PTREF fractions were also studied by DSC, small-angle light scattering (SALS), and optical microscopy. It was demonstrated that the spherulites of the LLDPE fractions were less well developed, more uniform in size, and tended to progressively deteriorate and became smaller as the concentration of branches increased. DSC exotherms of the PTREF fractions suggested that independent crystallization of the linear ethylene rich regions and the branched octene portions of the molecules took place, as manifested by the DSC thermograms of the high temperature and low temperature exotherms.

Mirabella and Ford (1990) used TREF-SEC, along with X-ray diffraction, C^{13} NMR, intrinsic viscosity, and DSC, to study the microstructure of LDPE, HDPE, and LLDPE. It was demonstrated that the short-chain branching decreased with the increase of molar mass in a typical commercial LLDPE resin. The broad and multimodal melting envelope of the LLDPE resins was found to be due to a broad and multimodal short-chain branching distribution.

Defoor et al. (1992) used a similar method to investigate an ethylene/1-octene LLDPE with a bimodal short-chain branching distribution. TREF-SEC and TREF-DSC cross-fractionation indicated that the mass average molar mass decreased with increasing

22

the degree of branching while the polydispersity remains rather broad. The PTREF fractions exhibited a broad single melting endotherm in contrast to the multiple melting endotherms of the unfractionated copolymer.

Zhou and Hay (1993) studied three commercial LLDPE samples with ethyl, hexyl, and isobutyl by TREF-SEC cross-fractionation. It was found that the various branches are incorporated into the crystalline regions to different extents, in which the isobutyl and hexyl branches are substantially excluded while the ethyl branches are substantially incorporated, and crystallization conditions appear to play an important part in the extent of branches incorporated. It was also found that the frequency of SCB distribution is not simply increased or decreased with molar mass, and the MMD and SCB distribution are very broad. Short chain branching had a greater influence on the thermal properties such as crystallization kinetics and melting behavior than molar mass.

Karoglanian and Harrison (1996) studied the properties of ultra-low-density polyethylene (ULDPE) by PTREF-ATREF, TREF-SEC and TREF-DSC cross-fractionation. ATREF fractionation of the whole polymer revealed a heterogeneous polymer having a bimodal SCB distribution and an elution range of approximately 75°C. Individual PTREF fractions were characteristically unimodal in character and eluted over a narrow range on ATREF. TREF-SEC disclosed a noticeable decrease in molar mass with an increase in the number of SCBs, and individual fractions had a narrow molar mass distribution compared to the whole polymer. TREF-DSC of the ULDPE and its fractions provided additional evidence regarding the heterogeneous characteristics of SCB distribution of the resin.

Studies done by several recent researchers have focused on the cross-fractionation of LLDPEs made with different catalysts. Balbontin et al. (1995) used TREF-SEC and TREF-DSC cross-fractionation to investigate the microstructure of LLDPEs made by heterogeneous titanium-based and homogeneous zirconocene and vanadium-based catalysts. They found that the MMD and CCD of different LLDPEs are greatly influenced by the catalytic systems and process conditions, and 1-alkene insertion in the

polymer chain can be distinguished between intramolecular and intermolecular distributions. Homogeneous catalysts give rise to a narrow SCB distribution or a constant value of the average ethylene sequence length in all the TREF fractions. Also, the narrow MMD of the polymers suggests that only a single type of catalytic site is effective. On the other hand, LLDPE produced by heterogeneous titanium-based catalyst shows much different CCD and MMD. Mingozzi and Nascetti (1996) employed TREF-SEC cross-fractionation to characterize two ethylene/1-butene copolymers produced by heterogeneous Ziegler-Natta catalyst and two obtained on homogeneous zirconium-based catalyst. The results showed that all LLDPE samples studied were compositionally heterogeneous as a consequence of the different content and sequence distribution of 1-butene along the chains. TREF fractions from Zr-based catalyst have a narrower molar mass distribution than those from the Ziegler-Natta catalyst. Additionally, LLDPE samples can be clearly distinguished according to their ATREF profiles, which reflects the nature of the parent catalyst systems.

Quite recently, TREF cross-fractionation has become a powerful tool in studying the kinetics of ethylene copolymerization. Huang et al. (1997) used PTREF-SEC cross-fractionation, along with ATREF, SEC, and melt flow index to investigate the effects of hydrogen and 1-butene concentrations on the rates of catalytic polymerization, average molar mass, and 1-butene incorporation during the gas-phase polymerization of ethylene on a Ziegler-Natta catalyst. Based on the PTREF-SEC results, it was concluded that the different catalytic sites present in the Ziegler-Natta catalyst have different functional forms for chain termination by transfer to hydrogen, the termination rate is first order for the catalytic sites responsible for the formation of copolymer and half-order for the sites responsible for the homopolymer component of the polymer. Shaw et al. (1998) developed a methodology to estimate the kinetics parameters for ethylene copolymerization. They conceptually separated copolymer into bins corresponding to specific copolymer composition (CC) and chain length (CL) ranges. Measurement of the joint CL and CC distribution can be accomplished by off-line TREF-SEC cross-fractionation. With on-line polymerization reaction data, the methodology can be used to

estimate parameters in kinetics models describing ethylene copolymerization with multiple active site catalysts.

The cross-fractionation studies of LLDPE summarized above indicated that TREF coupled with another fractionation technique is not only an effective way to characterize the detailed molecular structure of LLDPE, but also a powerful technique of studying kinetics behaviors of olefin copolymerization. As pointed out by Mathot (1994), cross-fractionation should be able to provide more detailed information on the intermolecular and intramolecular heterogeneity of SCB distributions of different LLDPEs, for which no any other techniques could possibly be achieved. However, cross-fractionation, especially, compositional cross-fractionation is usually limited by the lack of another compositional fractionation technique. Two dimensional composition fractionation has thus been rarely reported in the literature. Although TREF-DSC cross-fractionation has been frequently employed, it provides very limited information due to the lack of resolution on DSC analyses.

2.5. Polymer Fractionation Theory

2.5.1. Melting Temperature versus Chemical Composition and Morphology

The fusion or melting of a crystalline polymer is governed by phase equilibrium. In the case of a copolymer, the noncrystallizable comonomer units and end-groups can be assumed to act as a low molecular weight diluent, which does not enter the crystal lattice, and will lower the melting temperature. By inference, the broad distribution of such diluents will broaden the melting range of a crystalline polymer. Based on Flory-Huggins statistical thermodynamics treatment, the melting-point depression of polymer by the presence of the diluents (solvent, comonomer, and end group) can be expressed as (Mandelkern, 1990):

$$\frac{1}{T_m} - \frac{1}{T_m^o} = \frac{RV_u}{\Delta H_u V_1}(v_1 - \chi v_1^2) \qquad (2.1)$$

25

Where T_m^o is the melting temperature of the pure polymer of infinite chain length; T_m, the equilibrium melting temperature of the polymer-diluent mixture; ΔH_u, the enthalpy of fusion per polymer repeating unit; V_u and V_1, the molar volumes of the polymer repeating unit and diluent, respectively; v_1, the volume fraction of the diluent; and χ, the Flory-Huggins thermodynamic interaction parameter.

For a random copolymer containing X_a mole fraction of crystallizing units, it has been shown (Mandelkern, 1990) that Equation 2.1 reduces to a simple form as:

$$\frac{1}{T_m} - \frac{1}{T_m^o} = -\frac{R}{\Delta H_u} \ln X_a \qquad (2.2)$$

The validity of Equations 2.1 and 2.2 depends on the ability of a real random copolymer system to achieve the conditions stipulated by the equilibrium assumptions. Equation 2.2 implies that the specific chemical nature of the noncrystallizing co-unit should not play any significant role in the crystallization behavior of copolymers as long as it is excluded from the crystal lattice. The relationship between melting temperature and composition indicated by Equation 2.2 has been verified on various copolymers of ethylene (Alamo et al., 1984).

There have been some other correlations which can also be used to relate melting temperature and composition. One of which is modified Flory-Tija correlation (Mills and Hay, 1984):

$$\frac{1}{T_m} - \frac{1}{T_m^o} = \frac{R}{\Delta H_u} \frac{\ln(n)}{n} \qquad (2.3)$$

where n represents methylene sequence length (MSL).

The modified Flory-Tija correlation has been used as a basis for constructing a calibration curve for TREF analysis from standard linear hydrocarbons (Bonner et al., 1993) and from narrowly distributed ethylene homopolymers (Huang et al., 1997).

It is also well known that the melting temperature of a polymer depends on its crystallite size. Thicker crystallites melt at a higher temperature than crystallites with smaller dimension. A correlation between the melting temperature and lamellar thickness can be described by the Thomson-Gibbs equation (Zhou et al., 1997):

$$T_m = T_m^o(1 - \frac{2\sigma_e}{\Delta H_u L})$$ (2.4)

where T_m is the observed melting temperature (K) of lamella of thickness L; T_m^o is the equilibrium melting temperature of an infinite crystal (T_m^o=414.5 K); σ_e is the surface energy per unit area of the basal face (σ_e=87×10^{-3} J/m^2), and is associated with the energy of chain folding during crystallization; and ΔH_u is the enthalpy of fusion for crystalline phase (ΔH_u=290×10^6 J/m^3) (Mandelkern et al., 1984; Starck, 1996).

Comparison of Equations 2.3 and 2.4 indicates that the crystallization morphology of a crystalline polymer is related to its chemical composition. Thus, information on the effect of chemical composition on the morphology of polymer can be derived by characterizing its composition or melting point distribution.

2.5.2. TREF Fractionation versus Chemical Composition of Copolymer

The theory that describes the chemical composition of copolymers is well developed for copolymers made with homogeneous catalyst systems. In the case of copolymers made with heterogeneous catalysts, it is known that these systems often produce heterogeneous copolymers, i.e. copolymers with broad compositional distribution.

The heterogeneity of chemical composition distribution has been observed in fractionation studies on linear low density polyethylenes. These LLDPE copolymers are usually made on similar titanium-based catalyst systems. It has been shown in numerous TREF studies that the copolymers of ethylene and α-olefins produced by using Ziegler-Natta catalyst gave not only broad composition distribution, but also multimodal composition distribution. No theory is available for the direct calculation of the composition distribution of copolymers made over heterogeneous catalysts. However, the calculation of the theoretical composition distribution function for copolymers made with homogeneous catalyst system would be helpful in understanding the composition of copolymer produced with heterogeneous Ziegler-Natta catalysts.

Stockmayer (1945) derived the instantaneous bivariante distribution function for chain-length and composition of linear copolymers by chain-growth polymerization. The distribution function, w(n,y), was derived from the Alfrey-Mayo model for one single-site reaction center. The function was modified later by Tacx (1988) and is given by:

$$w(n, y) = (1 + y \cdot \delta) \cdot \tau^2 \cdot n \cdot \exp(-\tau \cdot n) dn \cdot \frac{1}{\sqrt{2\pi\beta/n}} \exp(-y^2 \cdot n/2\beta) dy \qquad (2.5)$$

where,

$$\beta = \overline{F_1}(1 - \overline{F_1}) K$$

$$K = [1 + 4\overline{F_1}(1 - \overline{F_1})(r_1 \cdot r_2 - 1)]^{0.5}$$

$$\delta = \frac{(1 - M_2/M_1)}{M_2/M_1 + \overline{F_1}(1 - M_2/M_1)}$$

$$\tau = \frac{k_{tm}}{k_p} + \frac{k_\beta}{k_p[M]} + \frac{k_{tH_2}[H_2]}{k_p[M]}$$

and,

n polymer chain length

y	deviation of an instantaneous composition from the average copolymer composition
$\overline{F}_1$	average mole fraction of monomer type 1.
r_1, r_2	reactivity ratios.
k_p	propagation rate constant.
k_{tm}	transfer to monomer rate constant.
k_β	β-hydride elimination rate constant.
k_{tH_2}	transfer to hydrogen constant.
$[M]$	monomer concentration.
$[H_2]$	hydrogen concentration.
M_1, M_2	molar mass of the comonomers.
τ	a parameter which represents the broadness of the distribution and is influenced by the conditions of polymerization such as concentration of monomers, activity of catalysts etc..

For random copolymerization, the product of r_1 and r_2 is close to unity and therefore K should be close to 1. The instantaneous weight chain length distribution can be obtained by integration Equation 2.4 with respect to y, from -∞ to +∞:

$$w(n) = \tau^2 n \exp(-\tau n)$$

(2.6)

The instantaneous number-average and mass-average chain lengths are calculated as follows (Soares et al., 1995b):

$$\overline{n}_N = \left[\int_0^\infty \frac{w(n)}{n} dn \right]^{-1} = \frac{1}{\tau}$$

$$\overline{n}_W = \int_0^\infty n \cdot w(n) dn = \frac{2}{\tau}$$

Note that the single site instantaneously produces polymer with polydispersity of 2.

Similarly, the composition distribution, w(y), through the whole region of the molar masses can be derived from the integration in the limits of 0 to ∞ for chain length;

$$w(y) = \int_0^\infty w(n, y)dn = \frac{3(1 + \delta \cdot y)}{4\sqrt{2\beta\tau}(1 + y^2 /(2\beta\tau))^{5/2}}$$ (2.7)

This distribution should be related to the results of the TREF fractionation of a LLDPE sample which is synthesized using a single site catalyst. Thus a fractionation analysis of the copolymers provides not only structural information but also information about the kinetics parameters and the mechanism of copolymerization. Furthermore, single site mechanism shows narrow molar mass distribution whereas multiple site mechanism yields broad distribution (conventional polyethylene synthesized with multi-site catalyst usually has a polydispersity larger than 4).

The model has been used to simulate the TREF profiles of LLDPEs produced by multiple active site catalyst. Soares and Hamelec (1995b) used a five active site model to simulate the bimodal TREF profile of ethylene-propylene copolymer. The parameters used and the simulation results are shown in Table 2.2 and Figure 2.1, respectively. It is evident that each site produces a LLDPE having the most probable composition distribution and a polydispersity of 2 in molar mass. The superposition of the five sites gives rise to the bimodal TREF profile in composition. One of the advantages of the model is that it contains parameters relating to copolymerization conditions. Theoretically, by simulating the TREF profile of a LLDPE, one can obtain important information about the mechanism of copolymerization.

It should be pointed out that the model is only applicable to instantaneous composition and chain length of random copolymers. Also other factors such as axial diffusion effects together with crystallization kinetics may also have a significant effect
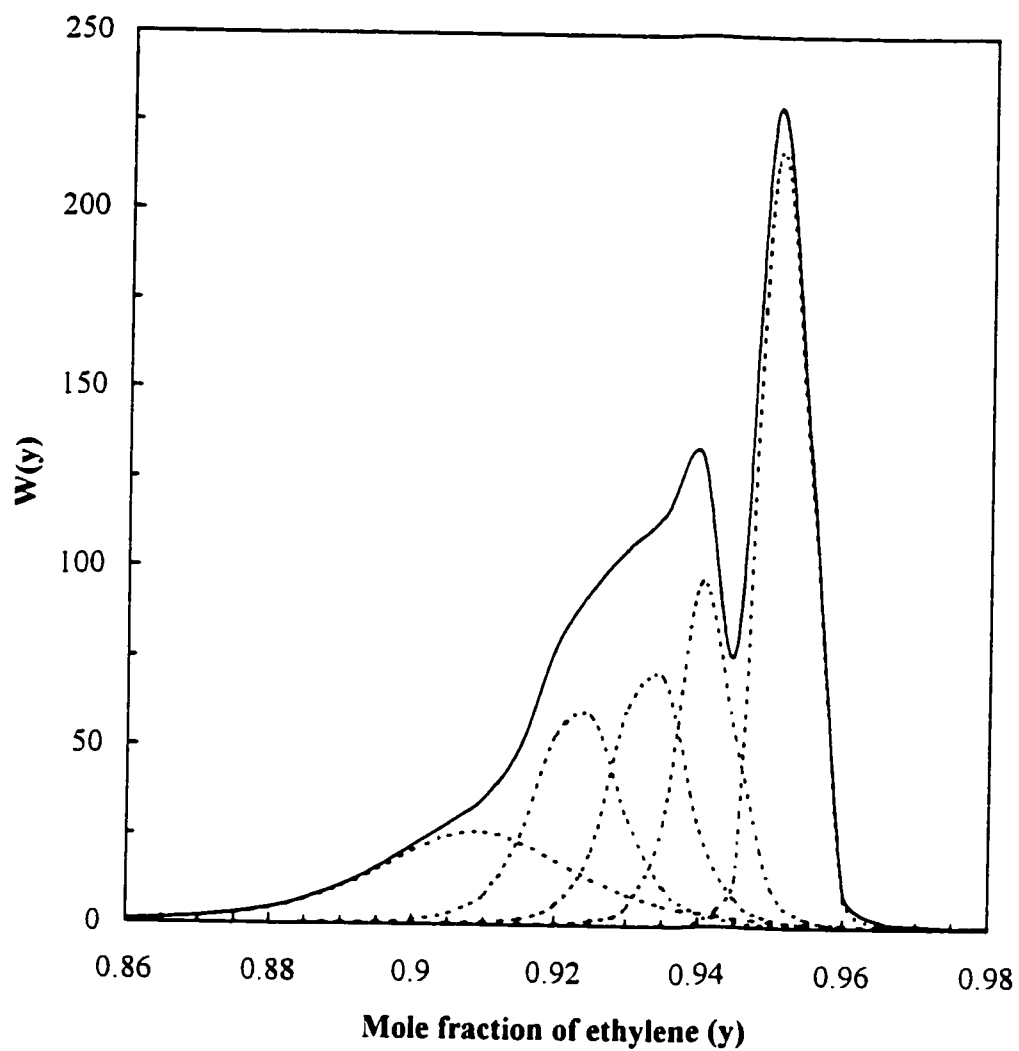
Figure 2.1. TREF profile of ethylene/propylene copolymer calculated by a five-sited catalyst model (Soares and Hamielec, 1995).

31

on peak broadening. However, even in the face of all these restrictions, the model is the first ever which is able to give a good quantitative description of TREF profile and can be applied to obtaining a better understanding of TREF data and possibly DSC data. The model has been further used to investigate the relationship between short chain branching and molecular weight based on TREF-GPC cross-fractionation data (Soares et al., 1996), and the joint chain length and copolymer composition from semi-batch ethylene copolymerization experiments (Shaw et al., 1998) on multiple-sited catalysts.

Table 2.2. TREF simulation parameters.

Active site	τ	r_1	$r_1 \cdot r_2$	$\overline{F_1}$
1	0.00500	10	1	0.909
2	0.00100	12	1	0.923
3	0.00075	14	1	0.933
4	0.00050	16	1	0.941
5	0.00010	20	1	0.952
average				0.932

A thermodynamic model based on the Flory-Huggins theory was also proposed for TREF (Borrajo et al., 1995). This model focuses on the thermodynamic aspect of TREF fractionation process by taking into account the dependence of TREF fractionation on melting temperature, melting enthalpy, average crystallinity, average crystallizable sequence length, and polymer-solvent interaction parameter. The model will help understand the TREF separation mechanism and TREF calibration, but provides little information about copoplymerization compared with the model described above.

EXPERIMENTAL EQUIPMENT AND PROCEDURE

The main objective of this study was to explore the difference in molecular structure between commercial Ziegler-Natta and metallocene LLDPEs. The identification of the heterogeneous and homogeneous distributions of short chain branches was of particular interest. TREF and thermally fractionated DSC were primary techniques employed to characterize these LLDPEs with respect to SCB. SEC was used to characterize molar masses and molar mass distributions. Further, TREF-SEC cross-fractionation was carried out to study the relationship between molar mass and SCB, and TREF-DSC cross-fractionation was utilized to obtain more detailed information about the intramolecular and intermolecular distributions of SCBs for different LLDPEs. The detailed experimental set-ups and procedures are presented below.

3.1. TREF

3.1.1. TREF System

The TREF system used in this study was a custom-built apparatus which has been described in detail elsewhere (Lacombe, 1995). A schematic representation of the TREF system is shown in Figure 3.1. The solvent pump was a DuPont Instrument 860 Chromatographic pump which can be operated with a flow rate ranging from 0.2 to 10 mL/min at a pressure up to 400 bar. The temperature chamber was a Thermotron model S-1.2C-B programmable temperature chamber with the usable volume of 34 L. The temperature chamber can control temperatures ranging from -73°C to 177°C with a precision of ± 1.0°C and has the capacity for heating and cooling rates of up to 10°C/min. The TREF column was placed inside the temperature chamber, about one meter of coiled tubing connecting the pump and the column was kept in the temperature chamber to minimize the difference between column and solvent temperatures. Two J type

33
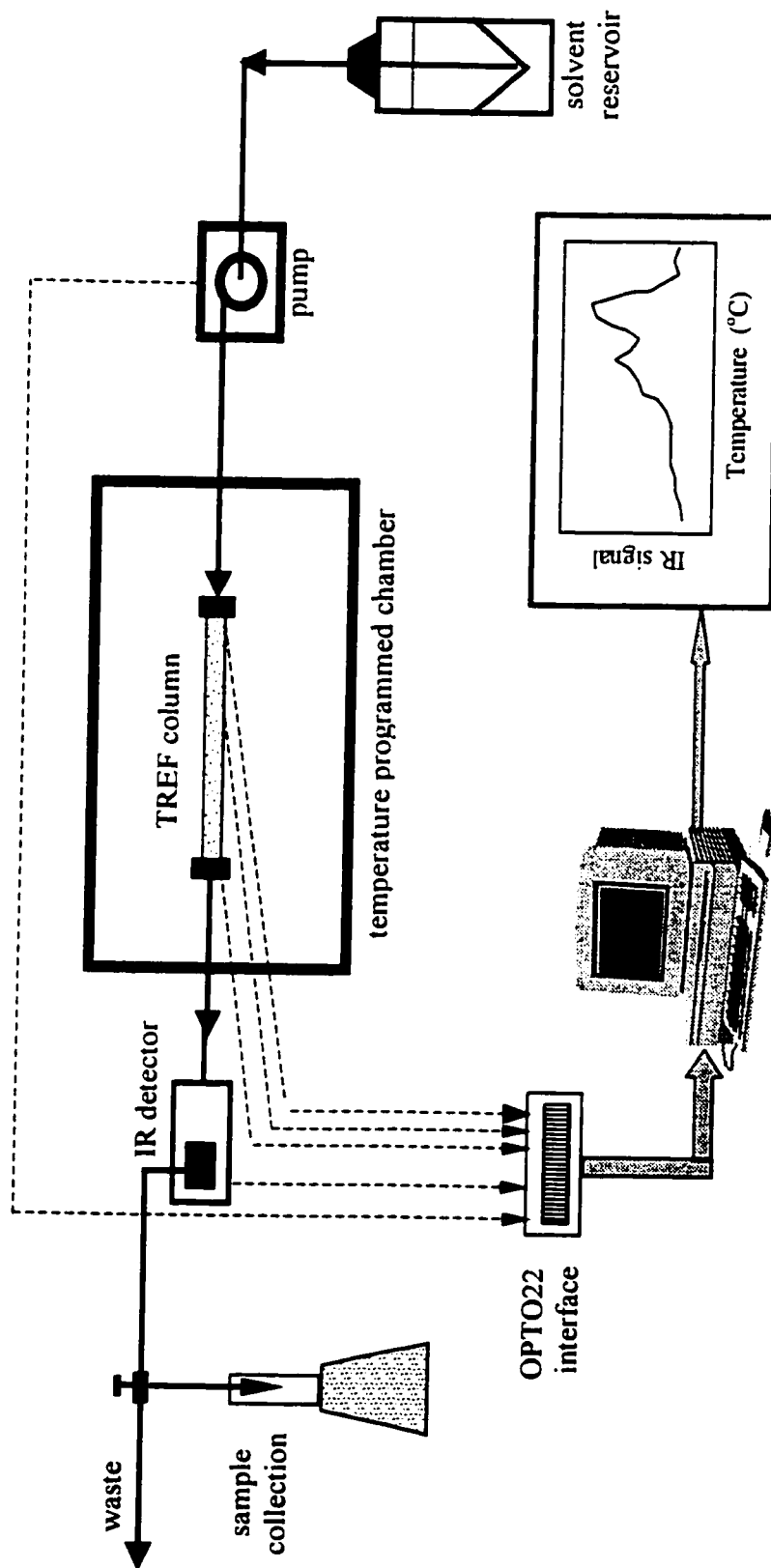
Figure 3.1. Schematic representation of TREF system

thermocouples inside the column were used to measure the inlet and outlet temperatures of the solvent. Another thermocouple was located at the middle wall of the column to measure the outside temperature of the column. The IR detector was a tunable high-temperature DuPont liquid chromatography IR detector. The IR cell was maintained at 127°C to keep the polymer in solution. The IR cell windows were two CaF_2 disks (32×3 mm) separated by a 0.5 mm Teflon™ spacer. The frequency of the IR detector was set to 3.38 μm (2959 cm^{-1}) which corresponds to the stretching frequency of the C-H bond of polyethylene. The tubing after the IR detector was tape-heated to about 100°C to avoid the polymer precipitation. A miniature quick-connection device was installed after the IR detector to direct the solvent flow to either the collecting vial or the waste vessel. The chamber temperature, column temperature, pump pressure, IR cell temperature, and IR signal were all recorded by a 486 PC computer interfaced with an OPTO22 system. The data were stored in an ASCII data file which can be imported in other application softwares for data processing.

3.1.2 TREF Procedure

The fractionation of LLDPE resins by TREF consists of crystallization and elution steps. In this experiment, crystallization was carried out off-line on separate equipment, in which as many as 24 samples can be crystallized simultaneously; this makes the TREF analyses more efficient. The crystallized samples can be eluted in two different modes, analytical TREF (ATREF) and preparative TREF (PTREF), on the TREF system described above and shown in Figure 3.1.

3.1.2.1 Crystallization Step

The crystallization step involved dissolving the LLDPE sample at high temperature in a favorable solvent and subsequently crystallizing out of the solution onto a support by slowly cooling. This step allows macromolecules to crystallize according to their crystallizability. Co-crystallization and recrystallization are undesired and are generally

avoided by using a cooling rate slower than 2°C/h (Wild, 1991). For ATREF, a sample size of 5-10 mg was normally used unless specified otherwise. The LLDPE sample was weighed in a glass bottle (15 or 20 mL) and the desired solvent (o-xylene or o-dichlorobenzene) was added at a concentration of 0.001 g PE/mL solvent. Further, about 1.5 g of glass beads (80-100 mesh) was added into the mixture. A disposable magnetic stirrer bar (12 mm × 3 mm) was put in the mixture, and the bottle was sealed with 90/10 mil Tegrabond silicon septum. The slurry was heated slowly with vigorous stirring to 125°C in a silicone oil bath and maintained at the temperature for 2 h to ensure that the polymer was completely dissolved. Then, the sample bottle was transferred to an Endcal RTE 220 ethylene-glycol bath/circulater which is controlled by a 386 PC computer. Further heating of 2 h at 125°C without stirring was carried out, followed by slowly cooling the polymer solution to about -8°C at a cooling rate of 1.5°C/h. The slow cooling process allows polymeric molecules to crystallize out of solution onto glass beads according to their crystallinity. The most crystalline fraction crystallizes first at higher temperature on the glass beads whereas, the least crystalline and more soluble one is the last to precipitate. The time required for the crystallization step is about 90 hours.

For PTREF samples, the crystallization procedure was essentially the same as above, except that larger sample sizes of 60-300 mg at a concentration of 0.005 to 0.04 g PE/mL solvent were utilized.

The crystallized sample was filtered into a TREF column. The ATREF column was a stainless steel tube having an inside diameter of 9.5 mm and a length of 63.5 mm with Swagelock fittings on both ends. An inlet filter having the pore size of 10 μm and an outlet filter of pore size 5 μm were put inside the end fittings of the column. The column was first filled to about quarter of its length with glass beads, the polymer sample was then filtered into the middle section of the column by using a glass funnel. The sample in the column was washed by flowing cold acetone through several times, followed by filling with glass beads to the top of the column. The column with the crystallized polymer was then connected to the TREF system. Similarly, the polymer samples for PTREF were

filtered into a bigger column having an inside diameter of 12.7 mm and a length of 63.5 mm. The filters used for the PTREF column on both ends had pore sizes of 7 μm.

3.1.2.2. Elution Step

The TREF elution step was carried out on the TREF system with different procedures for ATREF and PTREF. In ATREF, the column temperature was ramped up from 0°C to 125°C at a heating rate of 1°C/min while the solvent (o-dichlorobenzene) was pumped through the column continuously at a constant flow rate of 1.0 mL/min. During the heating, LLDPE molecules dissolved and were eluted by the solvent flow. LLDPE molecules with lower crystallinity, i.e. higher SCB content, dissolved first and were eluted at lower temperatures. The polymer species eluting from the column were detected with the on-line IR detector tuned at 2859 cm^{-1}. The elution step of ATREF is rather automatic, all the data (column temperatures, pressure, IR signal) were recorded by the computer. The time required for a typical ATREF run is about 2.5 hours.

In the case of PTREF, a stepwise procedure was adopted. The elution temperature range was divided into several temperature intervals based on the ATREF profile of the LLDPE sample. PTREF started from lowest temperature interval where the temperature of the column was maintained at the lowest temperature with solvent flowing through the column until a steady baseline was reached on IR signal. Then, the solvent flow was stopped and the column temperature was raised in 10 min to the level of the next temperature interval; the temperature was maintained for 10 min without solvent flow. This period of time is generally sufficient to achieve equilibrium of dissolving LLDPE. The solvent pump was then started to elute the dissolved polymer from the column. The eluted polymer was monitored by the on-line IR detector and was collected at a collecting point following the IR cell in vials for further SEC and DSC analyses. The same procedure was repeated for subsequent temperature intervals. The time required for a PTREF run is about 6 hours.

The amount of sample used for PTREF was a major factor to control the quality of PTREF, especially for SCB broadly-distributed Ziegler-Natta LLDPE. Figure 3.2 is a plot of PTREF data showing the variation of polymer concentration and column temperature as a function of time. It can be seen that the baseline of IR signal sloped up with time or increasing temperature. The significant scale-up of the baseline at high temperatures could mean that polymer fraction in a higher temperature interval could not completely dissolve due to the limited volume of solvent in the column. This seems to be the case in Figure 3.2 in which a secondary peak can be observed following each temperature interval at high temperatures. As a result, the collected PTREF fractions might be overlapped. To overcome this problem, two or more PTREF runs with varying sample sizes must be done to ensure that the PTREF fractions collected are representative. In this study, two PTREF runs with different sample sizes were performed for Ziegler-Natta LLDPE, and a single PTREF run seemed to be sufficient for SCB narrowly distributed metallocene LLDPE.

3.2. Thermally Fractionated DSC

The thermally fractionated DSC involves the thermal treatment or the crystallization of LLDPE samples from the melt prior to DSC measurement. The two thermal treatment procedures used in this study were step-crystallization (SC) and successive nucleation/annealing (SNA). Both procedures were undertaken in the temperature chamber of the TREF systems (Figure 3.1). The large space of the temperature chamber available allows the treatment of many samples at a time and under the same conditions. This is a more efficient way than the on-line treatment in the literature (Adisson et al., 1992; Keating et al., 1994; Starck, 1996; Muller et al., 1997). The treated samples were then analyzed by DSC.

3.2.1. DSC Sample Preparation

In general, about 10 mg of commercial LLDPE sample as received was directly used
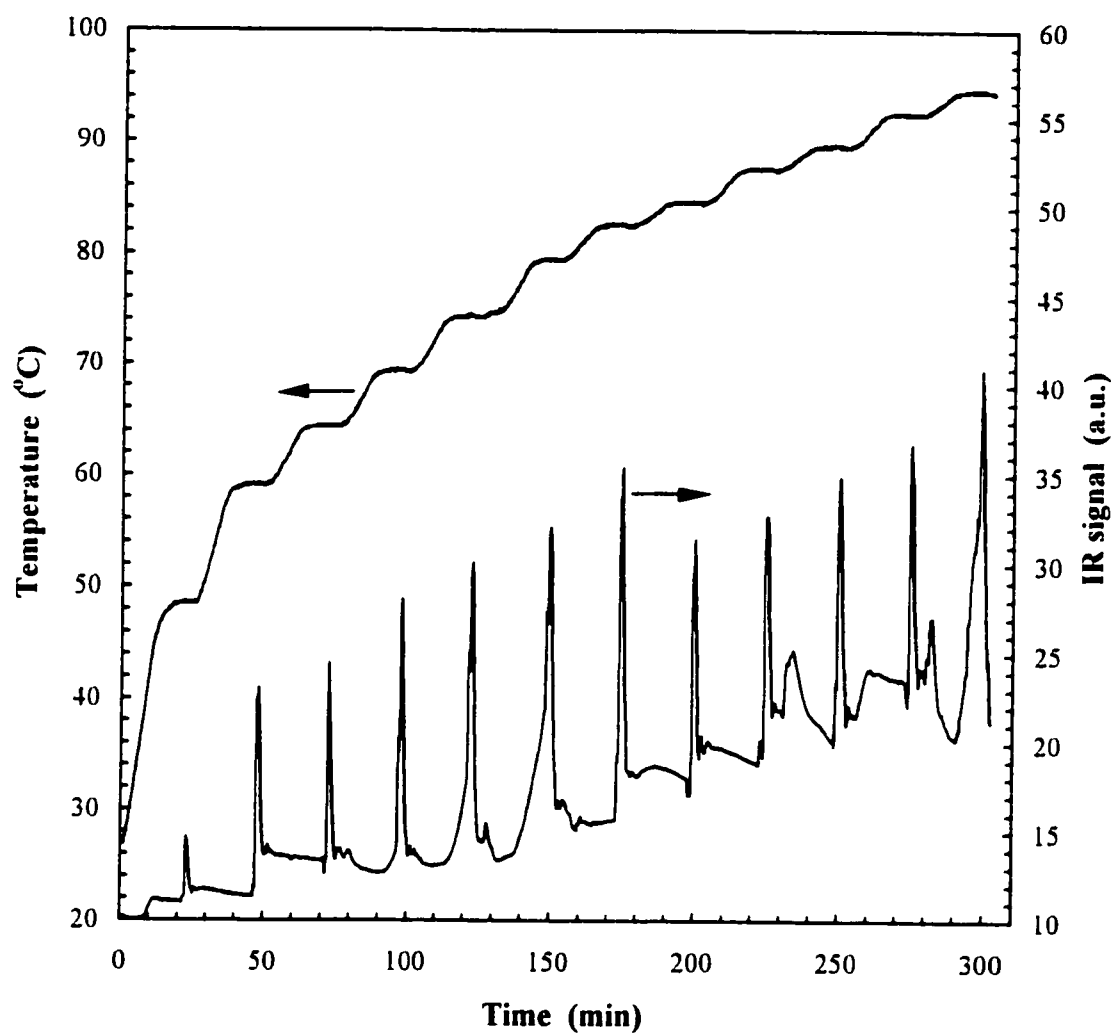
Figure 3.2. Variation of polymer concentration and column temperature during PTREF experiment.

for the thermal treatment. The granular sample was cut into slices, weighed, and encapsulated in aluminum DSC pans, duplicates were made for each type of LLDPE. The sample was then put in a 15 mL glass bottle, and was subjected to successive nucleation/annealing (SNA) or step-crystallization (SC) treatment in the temperature chamber. Repeated DSC experiment showed that there was no appreciable polymer degradation taking place for these commercial LLDPEs under study when they were treated in air at temperature as high as 150°C.

For the samples collected from PTREF, the LLDPE in the PTREF fractions was precipitated by adding equal volumes of acetone into each PTREF sample. The slurry was then filtered using 0.5 μm Teflon film. The obtained polymer was washed thoroughly with acetone and dried at ambient temperature for a few days. The solid polymer was weighed and then encapsulated in DSC pans.

3.2.2. Step-Crystallization (SC)

Step-crystallization is a stepwise thermal procedure which anneals and segregates polymer in descending temperature intervals. The polymer samples as received or PTREF fractions were grouped according to their melting temperatures, and were put in the programmable temperature chamber. The samples were first heated up to 155°C for the Ziegler-Natta LLDPE and 135°C for metallocene LLDPE, and were maintained at the temperature for 20 h. These samples annealed at temperature close to their melting temperatures were subsequently cooled to the first annealing temperature in about 2 min and was isothermally annealed at that temperature for 10 h. The long period of annealing time is recommended in the literature to ensure the equilibrium of the melting-crstallizination process, and importantly, to minimize the effect of molar mass and viscosity (Adisson et al., 1992; Keating et al., 1994). The annealing step was continued downwards with a temperature step of 10°C and annealling time of 10 h at each step at high temperatures as well as a temperature step of 15°C and annealling time of 6 h at low temperatures. The final annealing temperature was 35°C for Ziegler-Natta LLDPE and

25°C for metallocene LLDPE. Figure 3.3 shows the complete SC procedure for the Ziegler-Natta LLDPEs. The time required for the step-crystallization of Ziegler-Natta sample is typically 45 hours.

3.2.3. Successive Nucleation/Annealing (SNA)

The successive nucleation/annealing (SNA) procedure is similar to the well-known self-nucleation method for thermal treatment of polymer. The SNA method can be performed in a dynamic fashion, which should be more efficient for characterizing LLDPE with a broad crystallization range. The conventional self-nucleation method includes four major steps (Fillon et al., 1993): (a) erasure of the previous thermal history; (b) creation of a crystalline state from the melt at a temperature; (c) partial melting and annealing of the sample at the temperature; and (d) crystallization. Under the successive nucleation/annealing, steps (b-c) are repeated continuously from high to low temperatures.

To erase the previous thermal history, the sample was heated at a rate of 5°C/min to 155°C for Ziegler-Natta samples and to 135°C for metallocene samples and was maintained at the high temperature for 10 min to allow polymer to completely melt. The samples were then cooled to 25°C at a cooling rate of 5°C/min. This first step erases the previous thermal history of the LLDPE samples, and creates the initial "standard" states for samples of the same type.

The subsequent thermal treatment includes a series of continuous heating-annealing-cooling cycles. Figure 3.4 shows the complete procedure of SNA for the Ziegler-Natta samples. The samples in the standard state were heated at a rate of 5°C/min to 135°C and were maintained at this temperature for 10 min. This step results in the formation of partial melting and annealed crystal fragment. Crystallization was achieved by subsequently cooling the samples to 25°C at a cooling rate of 5°C/min. Then, the samples were heated once again at a rate of 5°C/min up to a temperature which was 5°C lower
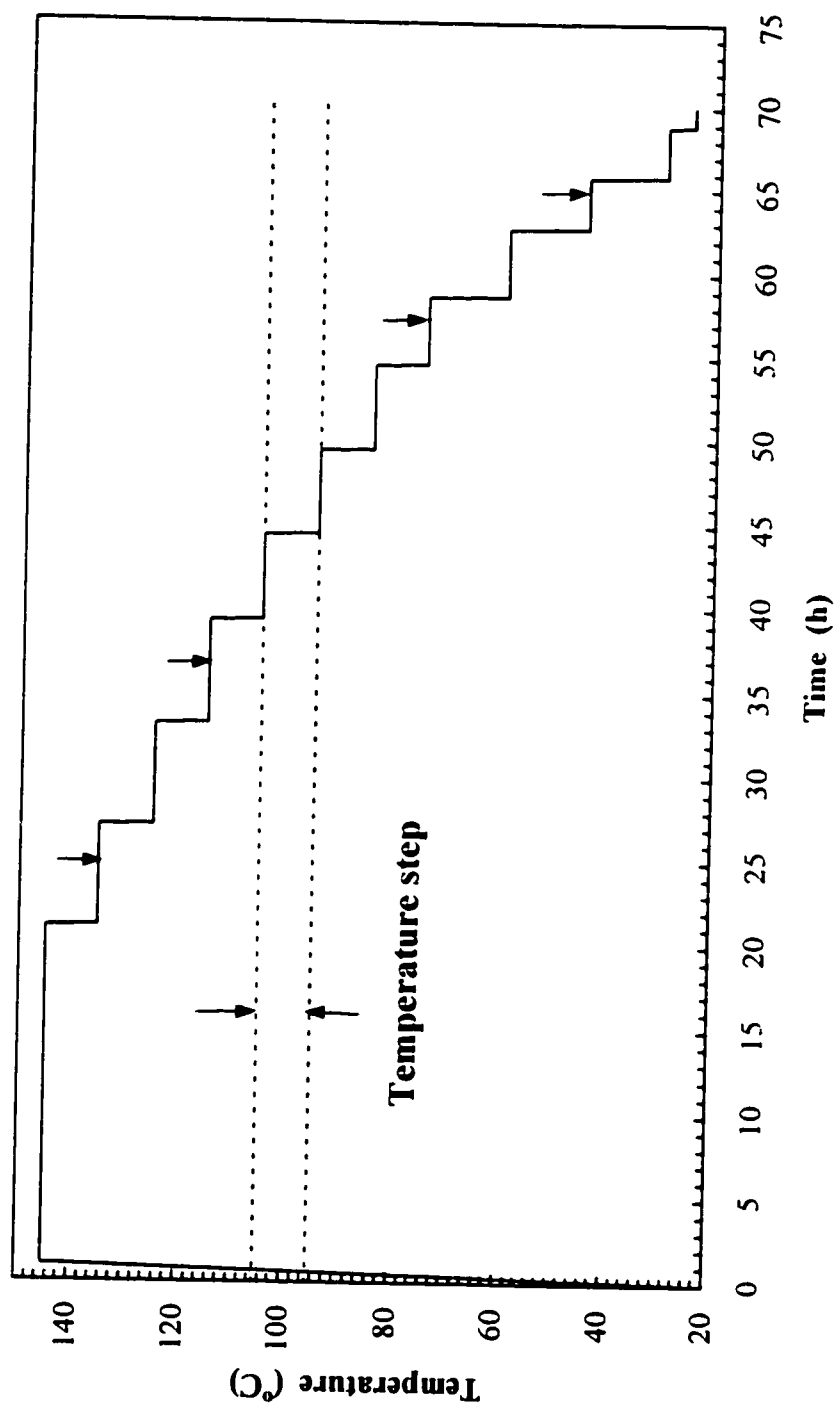
Figure 3.3. Schematic representation of step crystallization for thermal fractionation of Ziegler-Natta LLDPE.
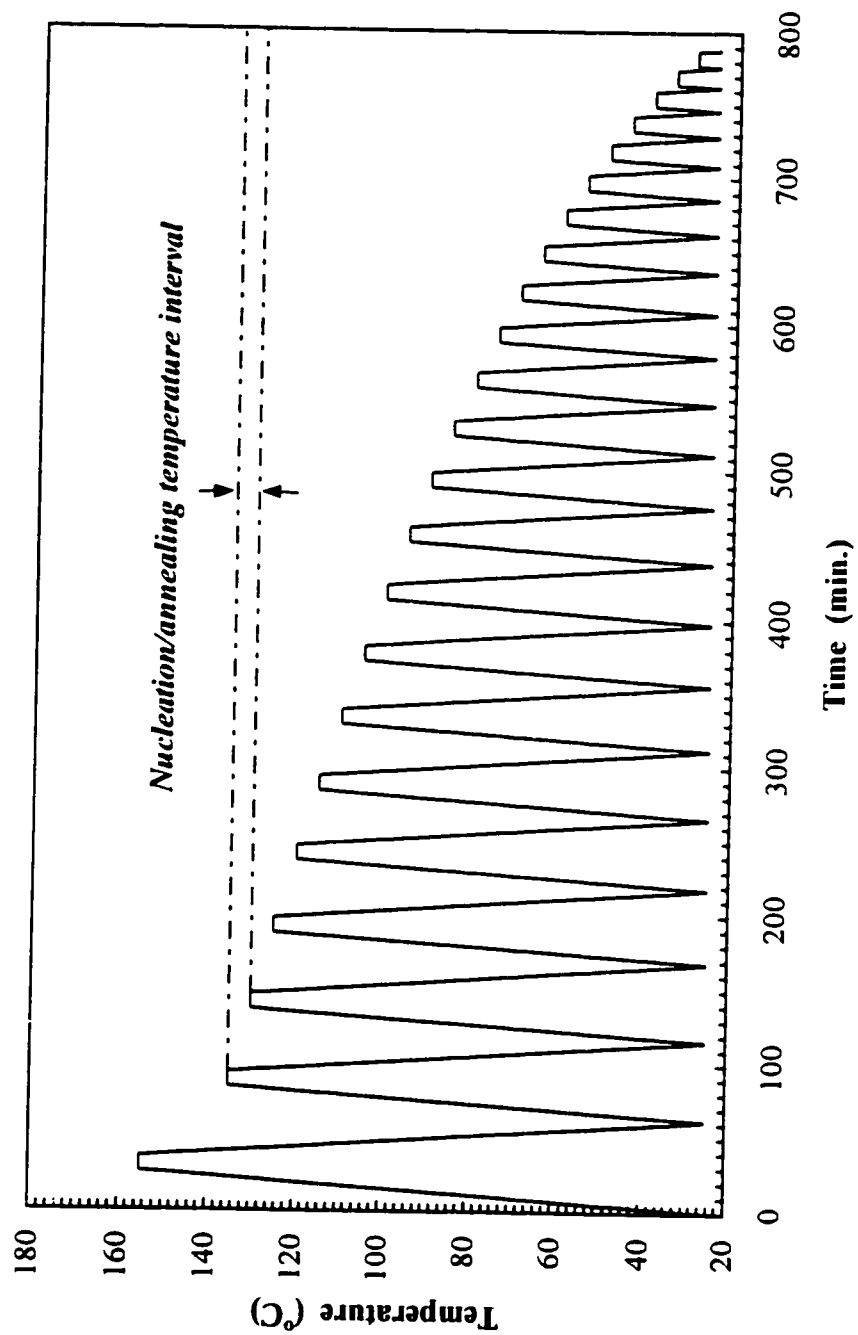
Figure 3.4. Schematic representation of successive nucleation/annealing (SNA) for thermal fractionation of Ziegler-Natta LLDPE.

than the previous annealing temperature, and were kept at this temperature for 10 min, during which the unmelted crystals annealed while the melted species isothermally crystallized after being self-nucleated by the unmelted crystals. The rest of the molten chains or chain segments would only crystallize during the subsequent cooling to 25°C. The heating-annealing-cooling cycle was repeated at a temperature interval of 5°C from 135°C to 25°C. The metallocene LLDPE samples were treated in a similar procedure except that the temperature range for SNA was from 105°C to 25°C. The time required for the SNA treatment was about 13 hours for Ziegler-Natta samples and about 8 hours for metallocene samples.

3.2.4. DSC Measurement

DSC endotherms of all the samples were measured by using a TA Instrument Model DSC2910. The instrument was calibrated with an indium standard (melting point 156.6°C). The LLDPE samples or PTREF fractions were scanned from 0°C to 160°C at a heating rate of 10°C/min, isothermally heated at 160°C for 1 min, and subsequently cooled to 0°C at a cooling rate of 10°C/min. For the purpose of comparison, a second heating and cooling cycle was also carried out at the same heating and cooling rates. All the measurements were performed in a nitrogen atmosphere. The transition temperature and the overall degree of crystallinity were analyzed by integrating the DSC endotherms using the software package TA2200.

3.3. TREF Calibration

The results of ATREF analysis is commonly presented as an elution curve of IR signal versus elution temperature. The TREF profile qualitatively represents the characteristics of crystallinity distribution of a LLDPE under investigation. It is of interest to translate the TREF profile into SCB distribution and to estimate average SCB content of the LLDPE. This is normally accomplished by using a calibration curve which relates TREF elution temperature to short chain branch content.

44

There have been a number of different ways to generate the TREF calibration curve. The most-commonly used method is the PTREF fractionation of LLDPE of interest and the subsequent analyses of SCB concentration in each PTREF fraction by FTIR or ^{13}C NMR. The calibration curve can be then obtained by plotting SCB concentration against PTREF temperature. This method, though somewhat complicated and time-consuming, has advantage of using LLDPE similar to those under investigation as a PTREF sample, and so the calibration is considered to be reliable (Wild, 1990; Glockner, 1990; and Soares et al. 1995). Pigeon and Rudin (1994) proposed a direct method for generating TREF calibration. They used dual IR detectors to measure C-H stretchings of both -CH$_2$ and -CH$_3$. The method is theoretically sound and practically convenient, particularly for those cases where a separate calibration curve is required for each polymer that is analyzed. However, due to the overlapping of -CH$_2$ and -CH$_3$ absorbance bands and sensitivity limitation of IR detector, the method tends to be unreliable at the lower end of SCB concentrations.

Another method for generating TREF calibration was proposed by Bonner et al. (1993). The method makes use of the correlation between melting temperature and crystallizable sequence length between SCBs, commonly referred to as methylene sequence length (MSL) (e.g., Equation 2.3). By measuring the TREF elution temperatures of a number of linear paraffins and standard ethylene homopolymers of known molecular weight, a calibration relating elution temperature to MSL and SCB was established. Huang et al. (1997) extended this method by PTREF-SEC cross-fractionation of a broadly distributed ethylene homopolymer. The obtained PTREF fractions covered the whole temperature range of interest for most of TREF analyses and was more reliable than the use of "standard samples" by Bonner et al. (1993).

In this study, a calibration curve relating TREF elution temperature to short chain branch content was constructed in the similar way used by Huang et al. (1997) and by Lacombe (1995) in more detail. First, a home-made ethylene homopolymer (GC93048) was fractionated by PTREF into 10 fractions in the temperatures ranging from 30 to 95°C.

This temperature range covered the elution temperature range for most of the LLDPEs studied in the present project. The molar masses of these ten PTREF fractions were subsequently determined by SEC. Knowing the molar mass of each fraction, MSL can be calculated by the following equation:

$$MSL = \frac{M_n - 30}{14}$$ (3.1)

Table 3.1 gives the results of the TREF-SEC cross-fractionation. It can be seen that the polydispersities of all ten fractions are close to unity. MSL value and PTREF temperature were fitted using Equation 2.3 with T_m replaced by the TREF elution temperature. This is another form of the equation used by Bonner et al. (1993). Figure 3.5 shows an excellent fit between MSL and PTREF temperature.

MSL is related to SCB in branches per 1000 carbons by the following equation:

$$SCB = \frac{2000}{MSL + 2}$$ (3.2)

Based on the relation between MSL and TREF temperature, a calibration curve relating SCB to TREF temperature was calculated and is plotted in Figure 3.6. It can be seen that the calibration is not linear, as expected. As shown in the next chapter, the calibration gives good estimation of average SCB content for commercial LLDPEs.

3.4. DSC Calibration

Compared with TREF, DSC data is very difficult to quantify. This is due to the fact that the signal intensity of DSC measurement is the heat which is a product of the amount of crystalline polymer melted at a specific temperature and the enthalpy of fusion. The enthalpy of fusion is in turn a function of polymer composition and the melting

Table 3.1. TREF-SEC cross-fractionation of homopolyethylene (GC93048)

Temperature range (°C)	T (°C)	M_n	P_d	MSL	ln(MSL)/MSL	1/T×1000
30 – 50	40.0	1026	1.08	71	0.05995	3.1934
50 – 60	55.0	1273	1.10	89	0.05053	3.0474
60 – 70	65.0	1759	1.16	124	0.03900	2.9573
70 – 75	72.5	2233	1.15	157	0.03215	2.8931
75 – 80	77.5	2769	1.18	196	0.02697	2.8518
80 – 85	82.5	3608	1.18	256	0.02169	2.8118
85 – 88	86.5	4610	1.19	327	0.01770	2.7805
88 – 90	89.0	5710	1.16	406	0.01480	2.7613
90 – 93	91.5	7489	1.21	533	0.01178	2.7424
93 – 95	94.0	9915	1.27	706	0.00929	2.7237
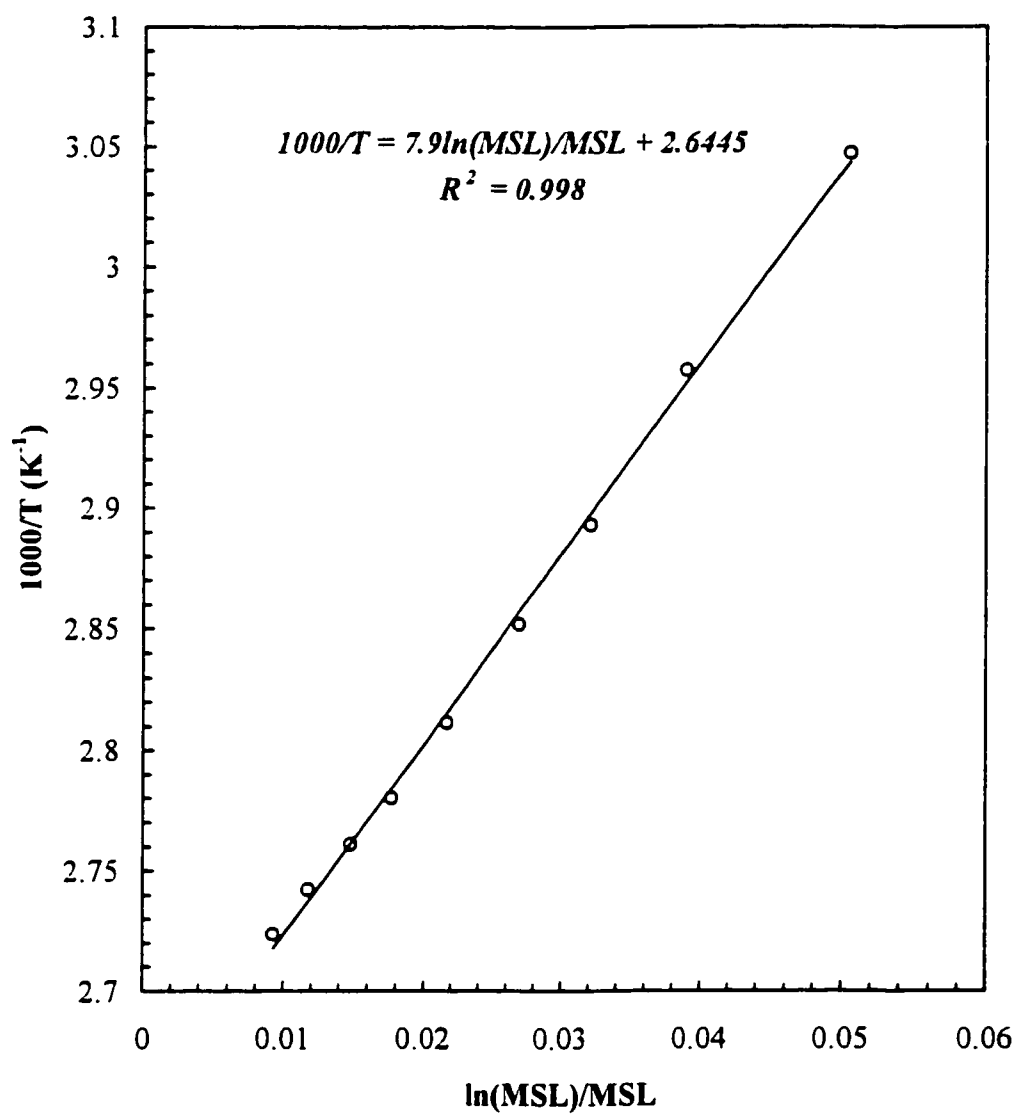
Figure 3.5. Plot of TREF elution temperature against methylene sequence length (MSL) of GC93048.

$$SCB = 0.0044T^2 - 1.1376T + 71.691$$
$$R^2 = 0.9999$$
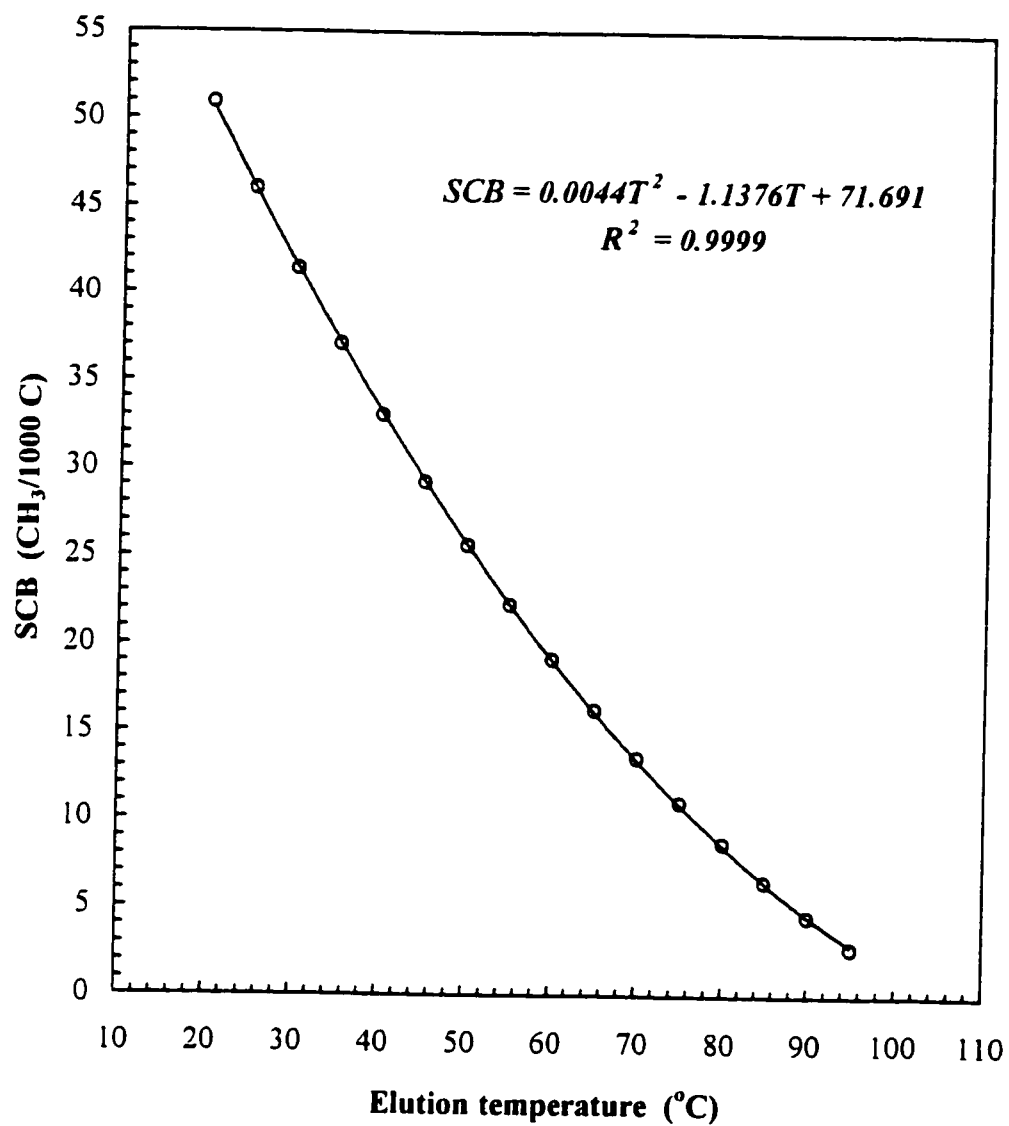
Figure 3.6.TREF calibration: short chain branch content as a function of elution temperature.

temperature. As a result, another calibration is needed to convert the heat into mass fraction, in addition to the calibration curve to convert the melting temperature into SCB. Such calibration is, however, very difficult to come by due to the lack of availability of "standard" copolymer samples. Alternatively, the normalized heat is sometimes used for quantitative analysis supposing that the dependence of the enthalpy of fusion on melting temperature is negligible. Recent studies done by Karoglanian et al. (1996) and Prasad (1998) showed that the area or height of DSC peak gave reasonably good quantitative results.

The quantification of DSC is only possible when DSC endotherms are highly resolved. This is partly because the baseline for integration of DSC data is somewhat arbitrary. An unresolved endotherm makes it difficult to draw a baseline. In the following chapter, it will be seen that the DSC endotherms of LLDPEs pretreated by successive nucleation annealing (SNA) show high resolution, and can be used for quantitative analysis.

The melting temperature of DSC data can be translated into composition by using a calibration curve, which can be constructed using standard hydrocarbons (Keating et al., 1996). In the present study, three linear paraffins and two standard ethylene homopolymers from the National Bureau of Standards were used to generate a calibration. The standard samples were treated by SNA described above, and the melting temperature of each sample was subsequently measured by DSC. Table 3.2 lists the melting temperatures and compositions of these samples. Note that the melting temperatures of the last two samples were very close in spite of more than twice difference in molar mass, indicating that molar mass is not a significant factor affecting the melting temperature when it exceeds a certain value (i.e. above about 10,000).

The composition and melting temperature can be fitted with the correlations such as Equations 2.2 and 2.3. As shown in Figure 3.7, Equation 2.2 gives the best fit between ethylene mole fraction and melting temperature. This was consistent with the results
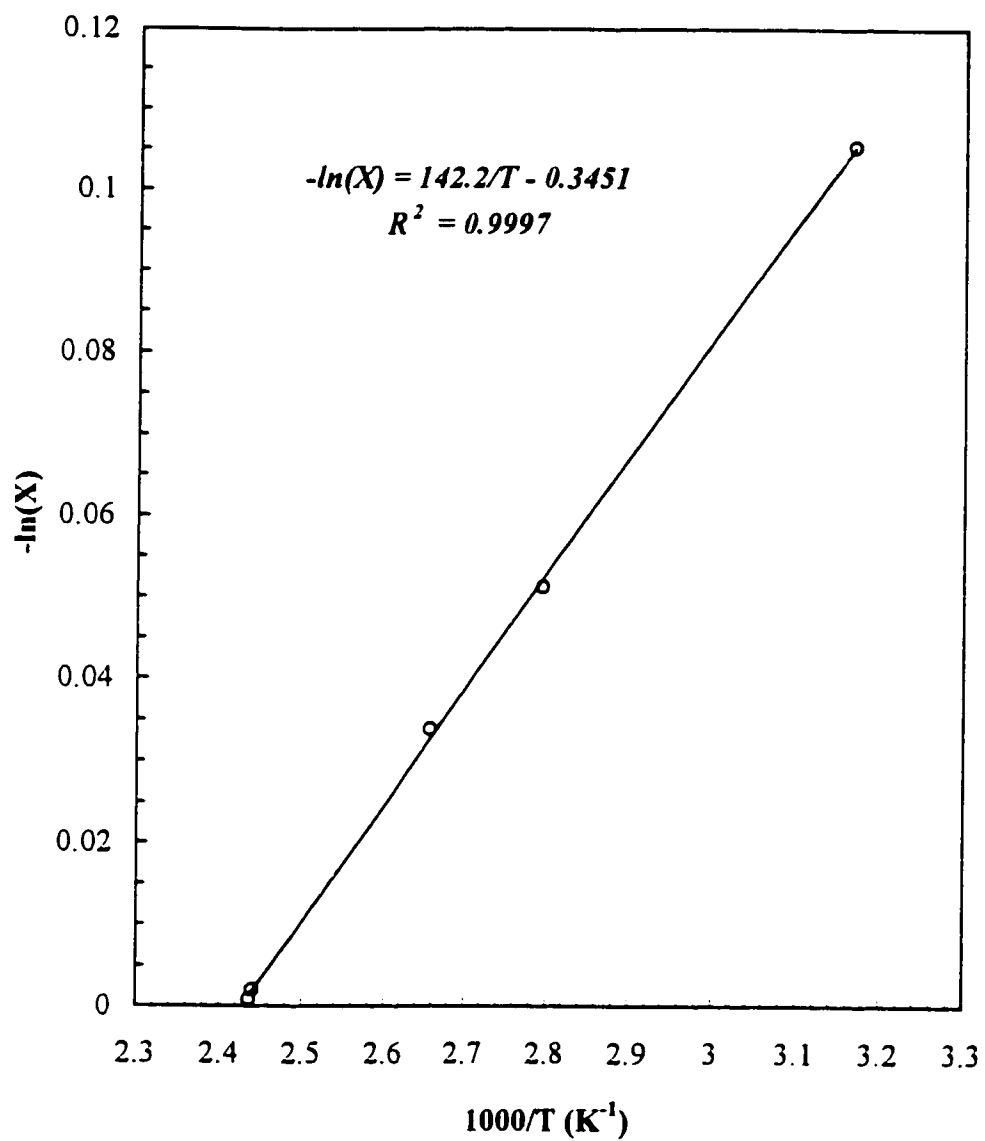
Figure 3.7. Mole fraction of crystallizable ethylene units versus melting temperature for DSC calibration.

51

obtained by Keating et al. (1996). Knowing the relationship between composition and melting temperature, the SCB content and methylene sequence length (MSL) of each peak on DSC endotherms can be calculated from the corresponding temperature.

Table 3.2. Melting temperatures of standard hydrocarbons and ethylene homopolymers versus chemical composition.

Sample	M_n	T (K)	X	1000/T (K^{-1})	-ln(X)
C$_{20}$	282	315.75	0.9000	3.1671	0.2231
C$_{40}$	562	357.85	0.9500	2.7945	0.1054
C$_{60}$	842	376.35	0.9667	2.6571	0.0690
SRM1482*	13600	409.75	0.9979	2.4405	0.0041
SRM1483*	32100	410.45	0.9991	2.4364	0.0017

* NBS standard linear polyethylene.
M_n: Number average molar mass.
T: Melting temperature
X: Mole fraction of crystallizable ethylene units.

3.5. TREF and DSC Data Processing

Analytical TREF data consist essentially of a series of polymer masses (IR signal intensities) eluted at corresponding ascending elution temperatures. The TREF profile can be obtained simply by plotting IR signal against elution temperature, while SCB distribution curve can be obtained by transforming the elution temperatures using the TREF calibration curve in Figure 3.6 into SCB contents and plotting IR signal against SCB.

The determination of average SCB content is based on the SCB distribution curve. The integration and normalization of the SCB distribution were done numerically. It is

proposed in this work to use expressions similar to molar mass distributions based on moments to calculate number-average and weight-average short chain branch contents, C_n and C_w, i.e.

$$C_n = \frac{\sum A_i C_i}{\sum A_i}$$

(3.3)

$$C_w = \frac{\sum A_i C_i^2}{\sum A_i C_i}$$

(3.4)

where A_i is the slice area of SCB distribution; and C_i is the corresponding SCB evaluated from the calibration curve. The ratio of C_w to C_n can serve as an indicator of the broadness of short chain branch distribution.

Similarly, DSC data are composed of a series of heat flow measurements at corresponding melting temperatures. DSC endotherms can be obtained by simply plotting heat flow against melting temperature. The quantitative analysis is based on the DSC endotherms of LLDPEs treated by SNA where there are multiple melting peaks. The multiple-peaked DSC endotherms were deconvoluted using commercial software (PeakFit, Version 4.06) from SPSS Science Inc.. Knowing the peak areas at the corresponding melting temperature, C_n and C_w were calculated using Equations 3.3 and 3.4.

3.6. Size Exclusion Chromatography (SEC)

The molar mass distributions of the whole LLDPEs and TREF fractions were determined by size exclusion chromatography on a Waters 150C SEC apparatus equipped with a differential refractometer. The columns used for the polymer separation were four Shodex UT 806M columns which were maintained at 140°C under operation. The carrier solvent was 1,2,4-trichlorobenzene (TCB) at a flow rate of 1.0 mL/min. Prior to injection

the samples were preheated at 160°C for 1 h. Two injections of 0.3 mL each for every sample were normally performed.

The SEC data were treated according to a universal calibration generated with narrow polystyrenes and standard polyethylenes. The molar masses were computed using Maxima 820 software provided by Waters. The operation of SEC and the data processing were done by Mrs. N. Bu.

RESULTS AND DISCUSSION

4.1. Commercial LLDPE Samples

The characterization of commercial LLDPEs in terms of chemical composition and molar mass is a challenging task. This is largely due to the fact that a variety of grades of LLDPEs are produced by different technologies and under varying polymerization conditions. As an example, metallocene LLDPEs are being produced by solution, slurry, and gas-phase polymerization technologies (Richards, 1998). The processes and polymerization conditions will surely have an effect on the final molecular structure of LLDPE even if the type of catalyst used has been considered to be a dominant factor (Huang and Rempel, 1995; Morse, 1998; Richards, 1998). Typically, little information is available about the catalyst, polymerization conditions, and post-reactor treatment for commercial LLDPEs. This makes it difficult to predict the molecular structure of a specific grade of LLDPE. Moreover, a commercial product could be a blend of LLDPEs produced in multiple reactors under different conditions, which entails the use of data deconvolution for the interpretation of the characterization results. In this study, several commercial LLDPEs made by different manufacturers have been selected on the basis that these LLDPEs possess the typical characteristics of Ziegler-Natta and metallocene LLDPEs, so that a general methodology can be developed for characterizing molecular structure of commercial LLDPEs. The difference stemming from the effect of processes and polymerization conditions, if any, has been neglected.

The seven commercial linear low-density polyethylenes used in this study are described in Table 4.1. All LLDPEs were produced by the copolymerization of ethylene with an α-olefin on either Ziegler-Natta or metallocene catalysts. At first glance, the metallocene LLDPEs may be best differentiated from their Ziegler-Natta counterparts by a lower density (~0.88) and a polydispersity of the whole polymer approaching the theoretical value of 2 for single site catalysts. The three Ziegler-Natta LLDPEs, having

Table 4.1. Commercial polyethylenes studied.

Type of PE	trade mark	manufacturer	comonomer type	catalyst system	density (g/cm^3)	$M_w \cdot 10^{-4}$	P_d
LLDPE	Exact4033	Exxon	1-butene	metallocene	0.880	11.01	2.14
LLDPE	PF0118F	NOVA	1-butene	Ziegler-Natta	0.918	10.56	3.28
LLDPE	SLP9095	Exxon	1-hexene	metallocene	0.883	8.62	2.14
LLDPE	TF0119F	NOVA	1-hexene	Ziegler-Natta	0.918	10.56	3.28
LLDPE	Attane4201	Dow	1-octene	metallocene	N/A	8.19	2.09
LLDPE	Engage8100	Dow	1-octene	metallocene	0.870	10.81	2.00
LLDPE	Sclair13J7	NOVA	1-octene	Ziegler-Natta	0.930	9.70	3.43
LLDPE	PF0218F	NOVA	1-butene	Ziegler-Natta	0.918	9.70	3.43
HDPE	19C	NOVA	-----	Ziegler-Natta	0.957	2.80	4.89
LDPE	LF-Y819-A	NOVA	-----	-----	0.919	1.55	6.45

M_w: weight average molar mass.
P_d: polydispersity (M_w/M_n).

either ethyl, butyl, or hexyl branches, had similar weight average molar masses and polydispersity, but the density of Sclair13J7 was higher than the PF0118F and TF0119F. The four metallocene LLDPEs having different types of branches were made by different manufactures with metallocene catalysts using different polymerization processes. The Dow Engage8100 and Attane4201 are products of solution polymerization, whereas the Exxon SLP9095 and Exact4033 are produced by gas-phase polymerization process (Richards, 1998). The molar masses, polydispersities, and even densities of these four metallocene LLDPEs were very close, but they certainly show different properties, as indicated in Chapter 2, which very well justifies a need to characterize these LLDPEs in terms of SCB distribution. Another Ziegler-Natta LLDPE, PF0218F, and one LDPE as well as one HDPE samples, all from NOVA, were used as references for DSC analysis.

4.2. TREF Results of Ziegler-Natta and Metallocene LLDPEs

4.2.1. Analytical TREF Profiles

For the characterization of LLDPE with respect to chemical composition or short chain branching, analytical TREF not only gives qualitative representation of crystallinity or short chain branch distribution, but also provides the basis for further quantitative analysis and PTREF. To ensure the reproducibility of ATREF analysis, at least three ATREF runs were done for each LLDPE sample. It has been found that the crystallization step was very important for obtaining reproducible TREF profiles, particularly for ethylene/1-octene copolymers. The addition of an appropriate amount of glass beads to the solution from which the polymer was crystallized was essential for obtaining reproducible TREF profiles (see Appendix C).

Figure 4.1 shows ATREF profiles of the three Ziegler-Natta LLDPEs. It can be seen that the Ziegler-Natta LLDPEs, regardless of their branch length, showed a rather broad bimodal elution temperature or crystallinity distribution. The ethylene/1-butene and ethylene/1-hexene copolymers showed a crystallinity distribution in the temperatures ranging from 20 to 100°C, while the ethylene/1-octene copolymer showed a relatively
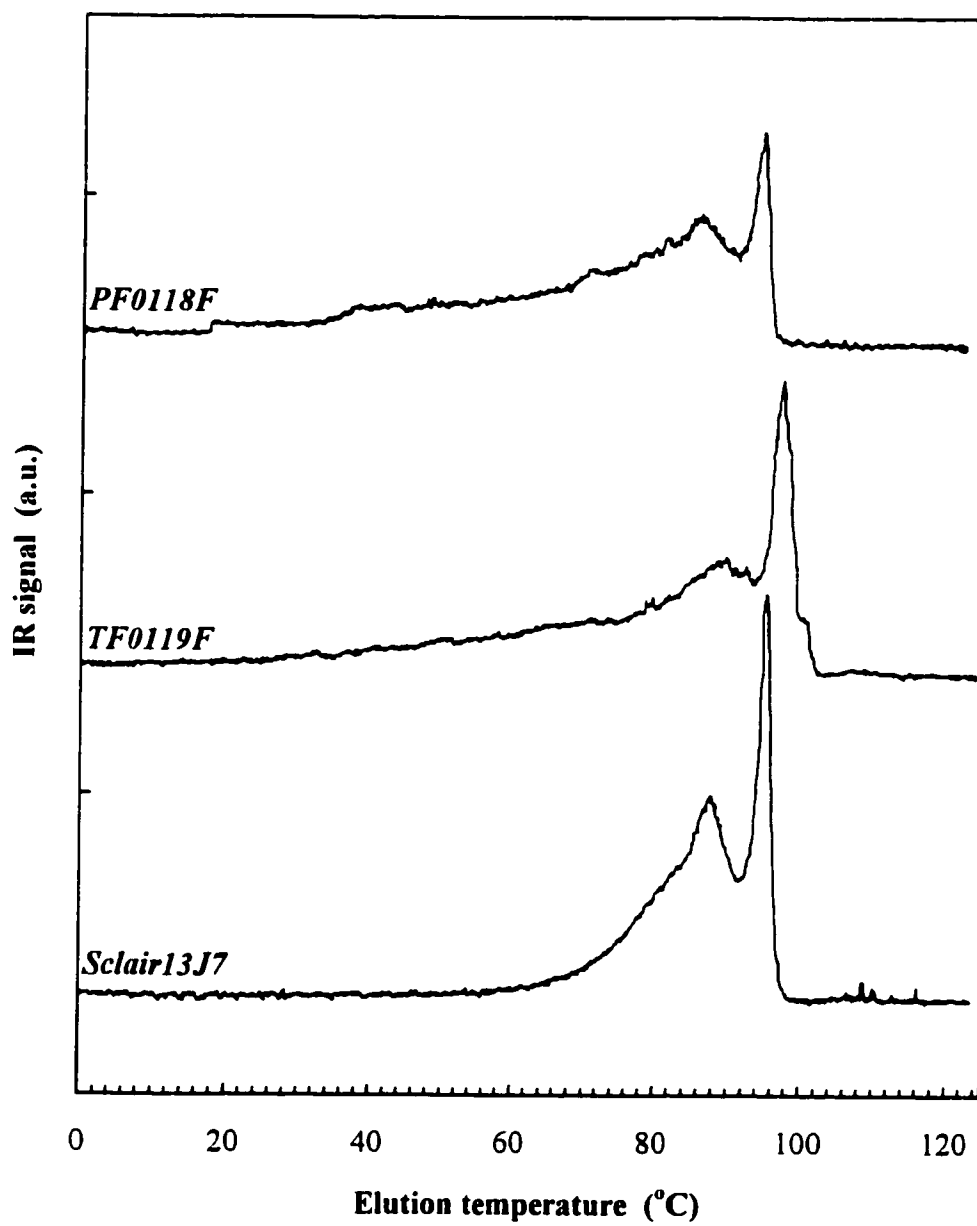
Figure 4.1. TREF profiles of various commercial Ziegler-Natta LLDPEs.

narrow distribution between 50 to 100°C. These bimodal TREF profiles are consistent with those in the literature where almost all the LLDPEs made with Ziegler-Natta catalysts, irrespective of polymerization processes and conditions, exhibit the bimodal TREF profiles (Wild, 1990; Soares et al., 1995a). The bimodal distribution has been ascribed to the presence of multiple active sites on Ziegler-Natta catalysts (Usami et al., 1986; Soares et al., 1995a and 1995b). The peak at low temperature with the long tail toward lower temperatures represents ethylene/1-olefin copolymer produced on the catalytic sites responsible for copolymerization, while the sharp peak centered at about 95°C represents ethylene homopolymer produced on the catalytic site only capable of homopolymerization. Hence, the Ziegler-Natta samples are, in a sense, a blend of copolymer and homopolymer.

The ATREF profiles of the four metallocene LLDPEs are shown in Figure 4.2. As expected, the metallocene LLDPEs showed a much narrower range of elution temperatures or crystallinity compared with the Ziegler-Natta LLDPEs shown in Figure 4.1. The distribution broadness or the range of elution temperatures varied considerably from sample to sample. Engage8100, an ethylene/1-octene copolymer, exhibited a very narrow range in elution temperatures from 15 to 40°C. Exact4033 and SLP9095 showed similar elution temperature range from 20 to 60°C, although the shapes of their TREF profiles were different. In comparison, Attane4201 had the broadest distribution among the four metallocene LLDPEs in the temperature range from 20 to 80°C. Despite the difference in the broadness of the crystallinity distributions, the overall TREF profiles of these metallocene LLDPEs seemed to have one single peak. It should be pointed out that the varying polymerization processes and conditions may have an effect on the shapes of the distribution curves of these different metallocene LLDPEs.

4.2.2. Short Chain Branch Distribution

ATREF profile can be converted to SCB distribution curve by applying the calibration curve in Figure 3.6. Figure 4.3 displays the SCB distribution of the Ziegler-Natta LLDPEs. As can be seen, the SCB distributions are essentially the reverse of the
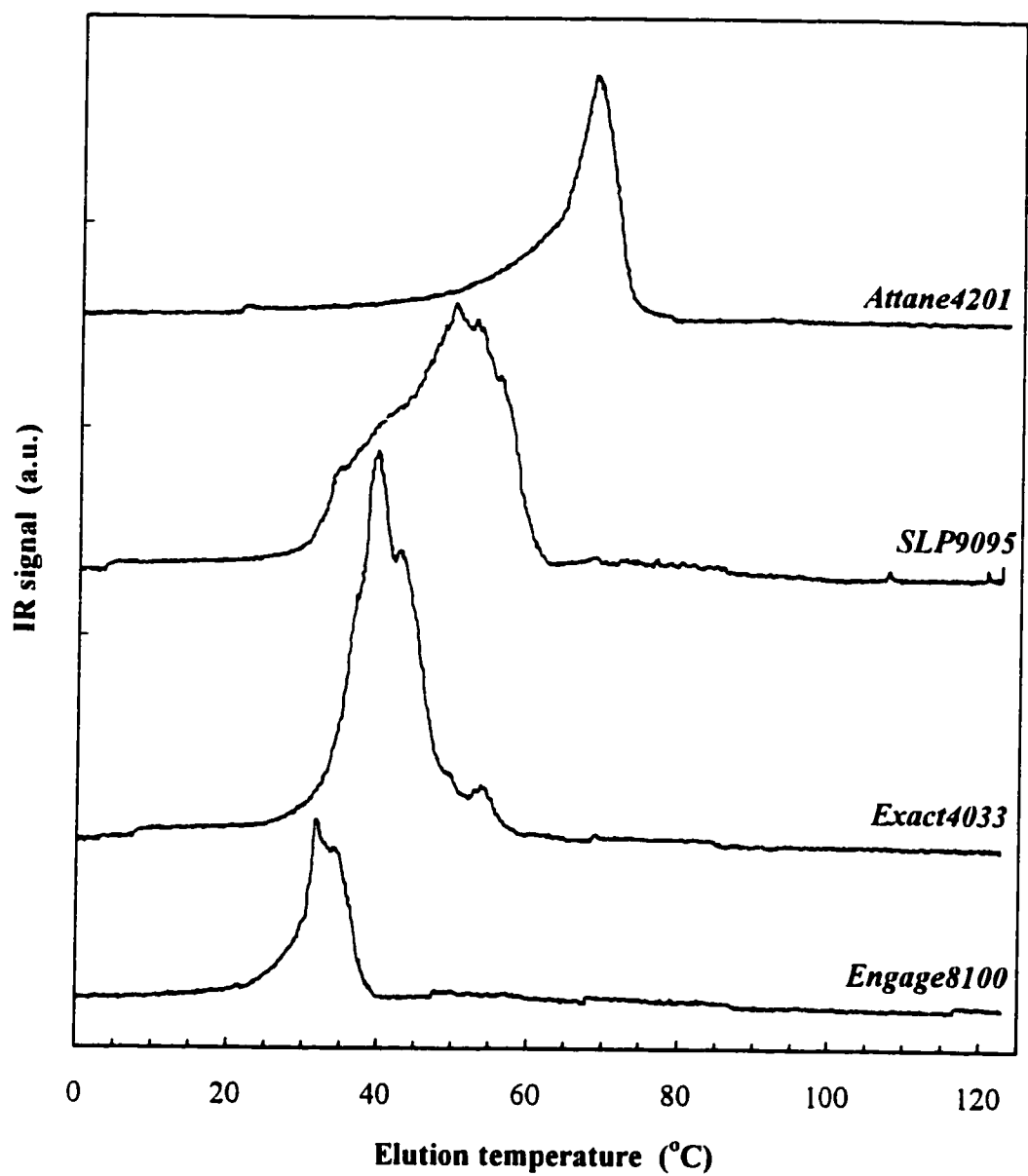
Figure 4.2. TREF profiles of various commercial metallocene LLDPEs.

60
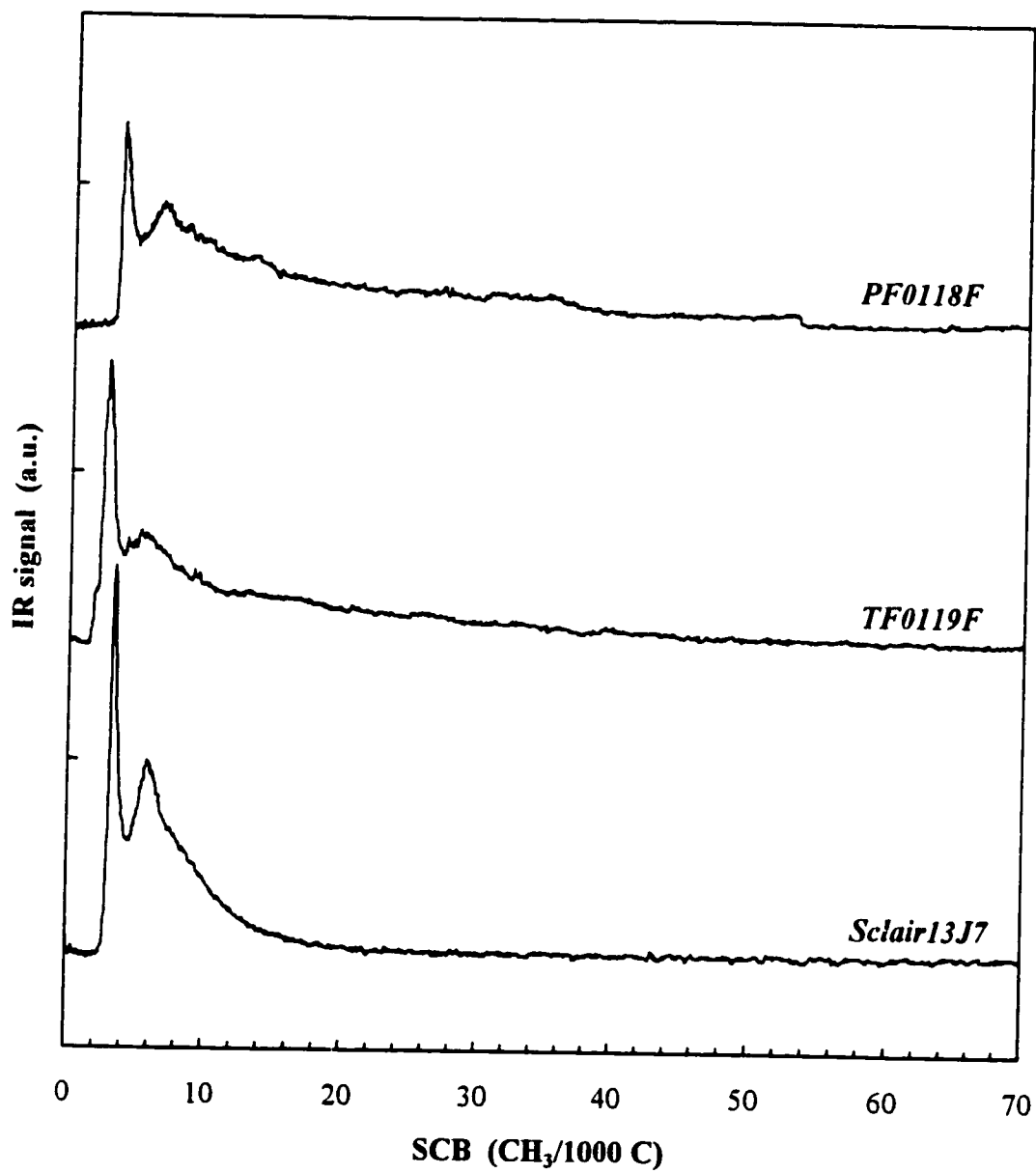
Figure 4.3. Short chain branch distribution of various commercial Ziegler-Natta LLDPEs.

TREF profiles. The bimodal SCB distribution was characteristic of the Ziegler-Natta LLDPEs. Note that the peak representing linear polyethylene contained less than 4 branches per 1,000 carbons. The ethylene/1-butene and ethylene/1-hexene copolymers were distributed from 4 to 55 SCBs per 1,000 carbons, compared to 4-40 SCBs for the ethylene/1-octene copolymer.

The SCB distribution curves of the metallocene LLDPEs are shown in Figure 4.4. In comparison to the Ziegler-Natta LLDPEs, the metallocene LLDPEs did not have low SCB content or linear polyethylene fraction. As shown in Figure 4.4, the SCB distribution of the Engage8100 appeared between 30 to 60 branches per 1,000 carbons. Exact 4033 and SLP9095 had SCB contents between 16 to 50, and the Attane4201 gave a SCB distribution between 10-50 branches per 1,000 carbons.

The average SCB content for the Ziegler-Natta and metallocene LLDPEs were calculated based on the calibration curve (Figure 3.6) and Equations 3.3 and 3.4. The results are listed in Table 4.2. Note that the Ziegler-Natta LLDPEs had much lower average SCB contents than the metallocene LLDPEs. PF0118F had about 18 branches per 1,000 carbons on the average, while Sclair13J7 had only 8 SCBs per 1000 carbons. As also compared in Table 4.2, the average SCB contents obtained from the ATREF analysis agree well with the manufacture's values. For the metallocene LLDPEs, Engage8100 possessed as many as 40 branches per 1,000 carbons on the average. Exact4033 and SLP9095 had 32 and 29 branches per 1,000 carbons. Even Attane4201, which showed least branches among the four metallocene LLDPEs, had almost 20 SCBs per 1,000 carbons.

Also note in Table 4.2 that the ratio of C_w to C_n defined in the section 3.5 was a good indication of the broadness of SCB distribution. The order of C_w/C_n values for all the LLDPE samples was in good agreement with the broadness revealed by the SCB distribution curves in Figures 4.3 and 4.4. The C_w/C_n values of the Ziegler-Natta LLDPEs were around 1.5, while those of the metallocene LLDPEs were about 1.0.
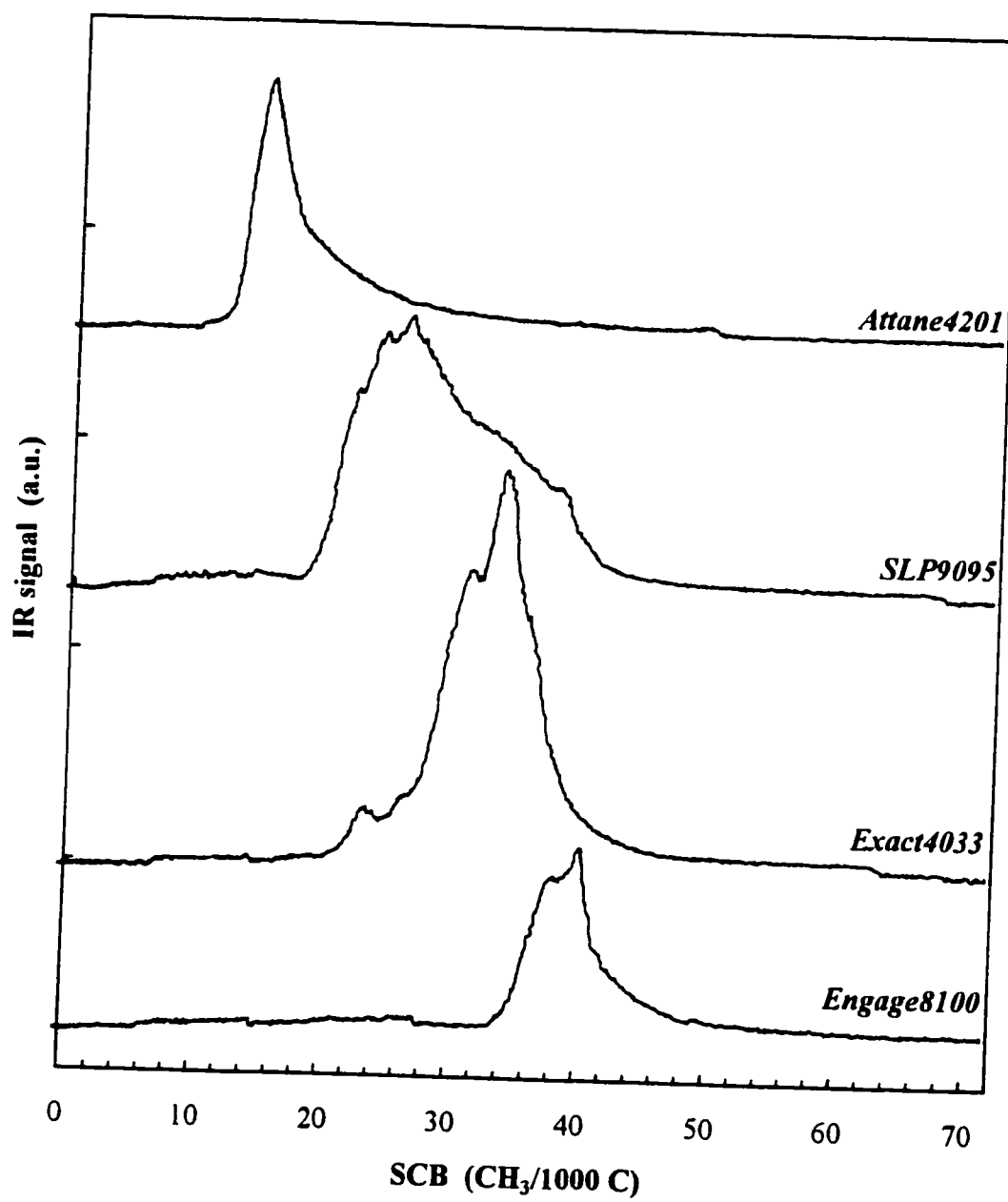
Figure 4.4. Short chain branch distribution of various commercial metallocene LLDPEs.

Table 4.2. Average SCB content obtained from the ATREF profiles of various Ziegler-Natta and metallocene LLDPEs.

LLDPE	C_n	C_w	C_w/C_n
PF0118F	17.7 (20)[*]	26.5	1.50
TF0119F	13.4 (16)[*]	21.7	1.62
Sclair13J7	8.0 (7.9)[*]	11.2	1.40
Exact4033	32.4	33.3	1.02
SLP9095	28.7	29.7	1.04
Engage8100	40.2	40.6	1.01
Attane4201	19.6	22.5	1.15

[*] Values provided by manufacturer.

In general, Ziegler-Natta LLDPE seems to have less branches distributed broadly, whereas metallocene LLDPE has more branches distributed narrowly. Statistically, the former tends to yield a heterogeneous copolymer while the latter tends to give a copolymer of homogeneous distribution (Mathot, 1994). It should however be mentioned that some grades of Ziegler-Natta LLDPEs commercially available contain average SCB content as high as that of metallocene LLDPEs, they may still be more easily differentiated from metallocene counterparts by the characteristic bimodal SCB distribution.

The results above indicate that ATREF is an effective method to characterize different types of commercial LLDPEs in terms of crystallinity and short chain branch distribution. The Ziegler-Natta LLDPEs show a characteristic bimodal distribution, while the metallocene LLDPEs generally show a narrower single-peaked SCB distribution. It is conceivable that the SCB distribution revealed by ATREF represents the SCB distribution of the overall polymer sample. For a lot of cases where the knowledge of the

average values or SCB distribution is not sufficient, the detailed molecular structure, viz. intermolecular and intramolecular distribution of SCBs, is needed. It will be shown in the later sections (Section 4.4.3) that the acquisition of such information has to rely on techniques such as PTREF-SEC and PTREF-DSC cross-fractionation.

4.3. DSC Results of Different Grades of Ziegler-Natta and Metallocene LLDPEs

DSC is not only an alternative to TREF for the characterization of LLDPEs in terms of chemical composition, but also provides complementary information about the molecular structure of LLDPEs. This is primarily because the segregation of polymer by DSC is governed by different mechanism from that by TREF. As indicated above, TREF fractionates macromolecules based on the crystallizability difference between molecules, in other words, TREF physically separates polymeric molecules. However, DSC does not physically separate molecules. Rather, it segregates molecular segments according to lamellar thickness or methylene sequence length. Hence, the difference in lamellar thickness between molecules and within individual molecule can be equally evaluated.

The results of DSC analysis depend largely on the thermal history of polymer sample (Mathot, 1994; Peeters et al., 1997 and 1999). This dependence on thermal history justifies the use of different thermal treatment procedures such as step-crystallization and successive nucleation/annealing prior to DSC measurement. The effect of different thermal treatments on the segregation of Ziegler-Natta and metallocene LLDPEs will be dealt with in this section.

4.3.1. DSC Endotherms of As-Received Samples

Figure 4.5 shows DSC endotherms of several as-received Ziegler-Natta and metallocene LLDPE samples. It is interesting to see that the DSC endotherms revealed the drastic difference in melting temperatures of different LLDPE samples. However, the DSC endotherms did not seem to provide much information about distribution of short chain branches. Comparison of ATREF profiles and DSC endotherms for as-received
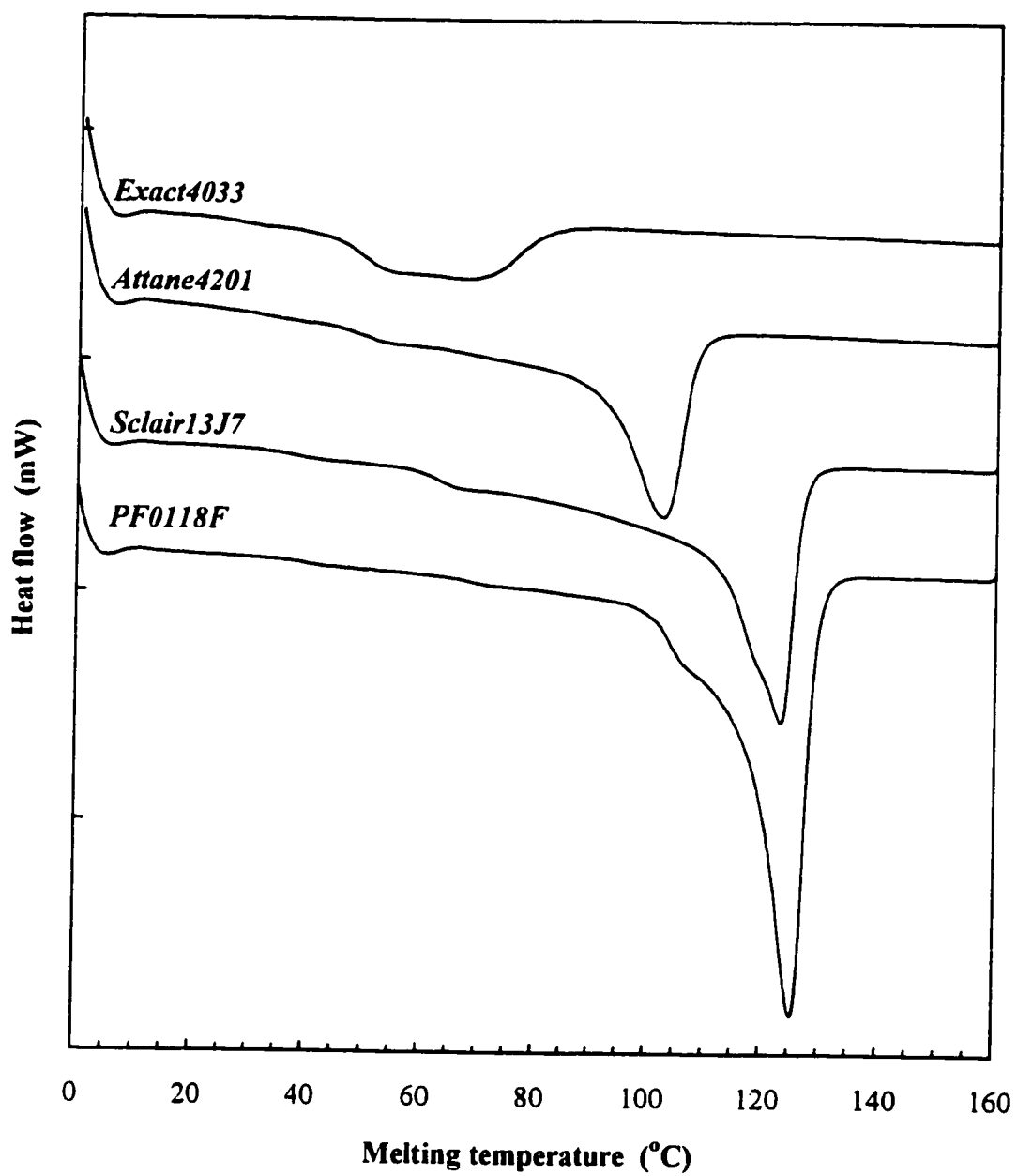
Figure 4.5. DSC Endotherms of various as-Received commercial LLDPEs.

samples showed quite different characteristics. For example, the DSC endotherm of Sclair13J7 seemed to be broader than that of PF0118F (see Figure 4.5), this is contrary to the ATREF results which indicate the profile for PF0118F was broader than that of Sclair13J7 (see Figures 4.1 and 4.3). The result is largely due to the fact that the branch content of the Ziegler-Natta LLDPE samples in this study is relatively low and the distribution is broad, which implies that DSC analyses of as-received samples are very limited in sensitivity for the detection of SCBD. The preliminary observations indicate that DSC, without prior thermal treatment of the samples, is not suitable for the characterization of LLDPE in terms of compositional distribution.

4.3.2. DSC Endotherms of LLDPE Samples Treated by Solution and Slow-melt Crystallization

Since the thermal treatment or crystallization is so important for DSC analysis of LLDPE sample, it is important to compare the effectiveness of different crystallization procedures. Crystallization of polymer from solution or melt at a very slow cooling rates are probably the simplest procedures. To study the effect of different crystallization processes on the DSC endotherms, a Ziegler-Natta LLDPE, PF0118F, was selected to be subjected to solution crystallization and slow-melt-crystallization from melt. The solution crystallization was the same as that used for TREF, i.e., the polymer solution was slowly cooled from 125°C to -8°C at a rate of 1.5°C/h. The slow-crystallization from melt was carried out by annealing the polymer sample at 145°C for 20 h, followed by slowly cooling the polymer melt from 145°C to 25°C at a rate of 1.5°C/h. Figure 4.6 shows the DSC endotherms of the LLDPE crystallized from solution and from melt. It can be noted that there was drastic difference in DSC endotherms between solution-crystallized and slowly-melt-crystallized samples. The solution-crystallized sample showed a strong shoulder peak beside the high-temperature peak, while the slowly-melt-crystallized sample had a long tail behind in the temperature range from 35 to 120°C. These results clearly show that the crystallization process has a significant effect on the DSC endotherms of LLDPE. It seems that LLDPE may be crystallized differently from solution than from melt. Even if at such a low cooling rate (1.5°C/h), the DSC

67
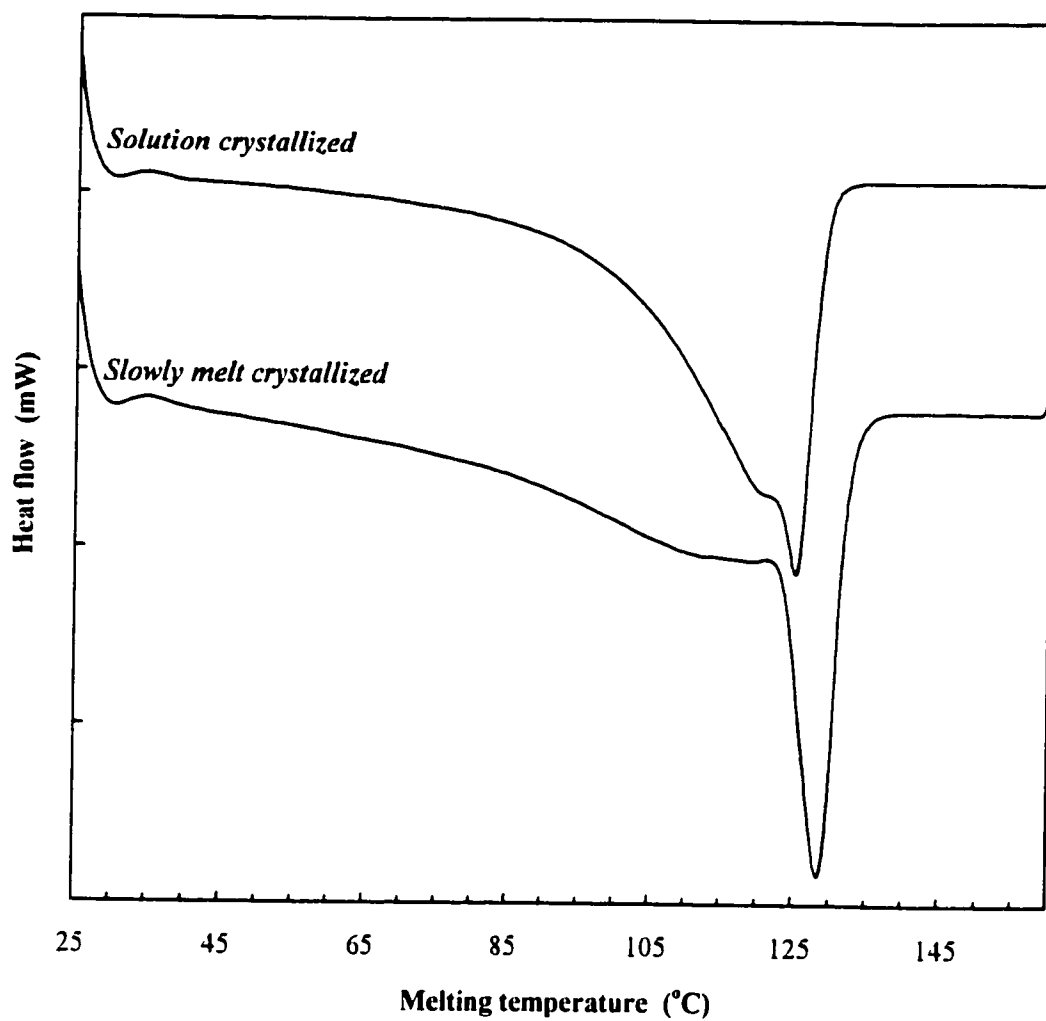
Figure 4.6. DSC endotherms of solution-crystallized and slowly-melt-crystallized
Ziegler-Natta LLDPE (PF0118F).

68

endotherms of the Ziegler-Natta LLDPE crystallized from melt was hardly double-peaked or bimodal, as observed on other Ziegler-Natta LLDPEs (Wild et al., 1990; Mathot, 1994; Karoglanian and Harrison, 1996). Again, this is probably due to the low SCB content. For this reason, the results herein do not seem to agree with the conclusion in the literature that DSC analysis of slowly-melt-crystallized LLDPE can provide much the same information as TREF (Wild et al., 1990; Karbashewski et al., 1992). This implies the necessity of more efficient crystallization procedure for DSC analysis.

4.3.3. DSC Endotherms of LLDPE Samples Treated by Step-Crystallization (SC)

In light of the dependence of DSC analysis on the thermal treatment or crystallization of LLDPE samples, it should be possible to improve the sensitivity and resolution of DSC analysis by applying appropriate thermal treatment to the LLDPE samples. Step-crystallization (SC) is one of the commonly-used thermal treatment procedures. The SC segregates molecular segments according to the lamellar structure. The long period of annealing time (Figure 3.3.) allows polymer chain segments to crystallize independently and therefore reduces cocrystallization and recrystallization. As a result, the SC treatment can enhance the crystallinity of LLDPE samples. This is equivalent to improving the sensitivity of DSC analysis, since DSC is only sensitive to the melting of the crystallized fraction of the samples.

The DSC endotherms of various LLDPEs treated by step-crystallization are shown in Figure 4.7. The DSC endotherm of each sample was composed of multiple peaks of varying intensity at different melting temperatures, each of which corresponds to a specific temperature step and represents a fraction of polymer segments that have similar lamellar thickness (Keating et al., 1996). Compared with the DSC endotherms of the untreated samples in Figure 4.5, the DSC endotherms of the Ziegler-Natta samples showed much broader distribution, the melting peaks at low melting temperatures were clearly visible. It can be seen that the distribution broadness of PF0118F, which possessed highest average SCB content among the three Ziegler-Natta samples, was close to the distribution revealed by TREF (Figure 4.1). The same was true for that of
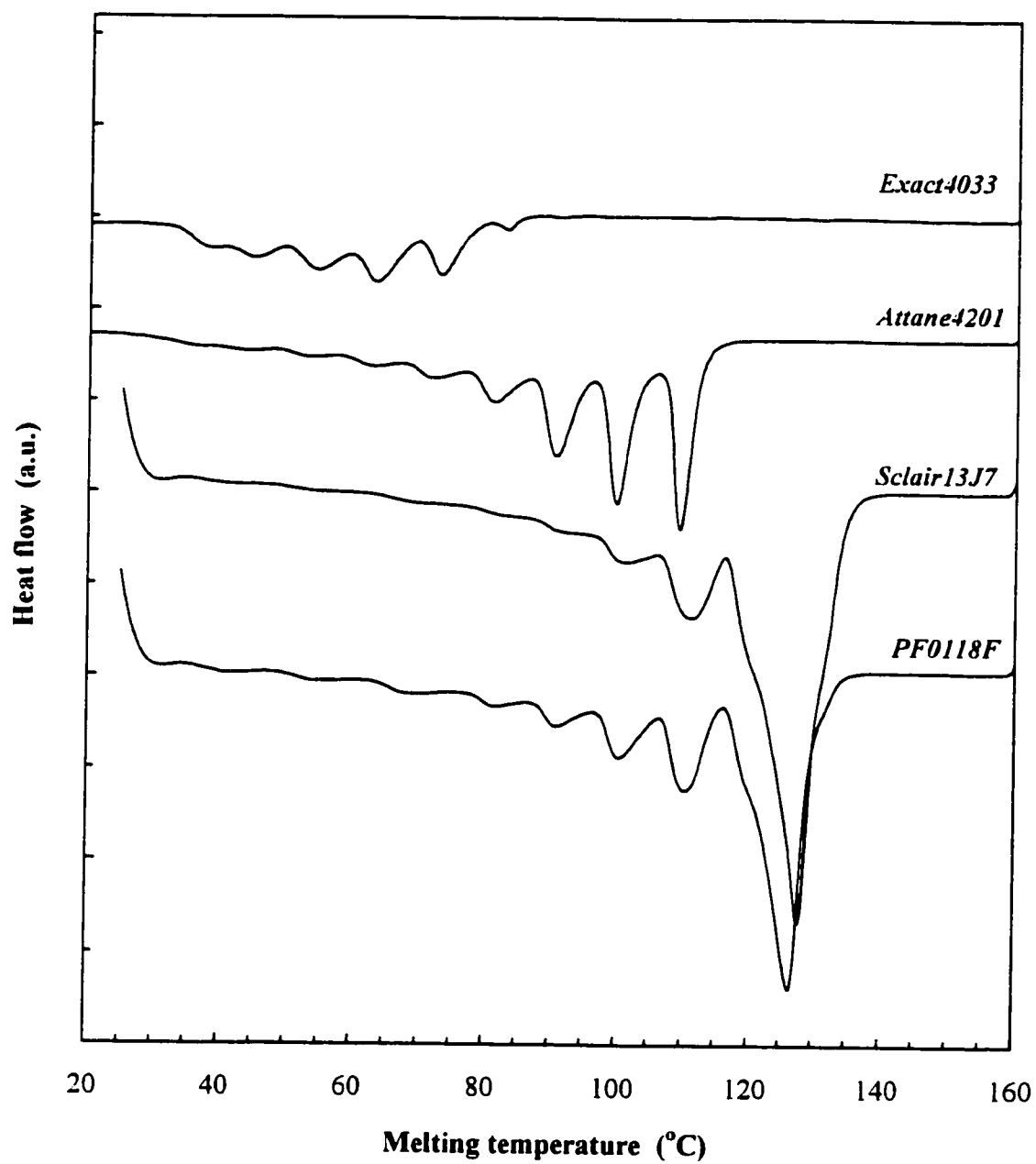
Figure 4.7. DSC endotherms of various LLDPEs treated by step crystallization.

Sclair13J7. Once again, it proves that the SC treatment can improve the sensitivity of DSC analysis for LLDPE samples of low SCB content. It can be also seen form Figure 4.7 that the resolution of DSC endotherms of the Ziegler-Natta samples, particularly at higher temperatures, was poor. This is probably because the SC thermal treatment cannot completely eliminate the cocrystallization of similar molecular segments, even after the long period of annealing.

For the metallocene samples, the SC treatment seemed to be efficient to sort out the molecular segments according to their lamellar structures. As shown in Figure 4.7, the distributions of DSC endotherms of Exact4033 and Attane4201 were similar to those indicated in TREF profiles in Figure 4.2.

4.3.4. DSC Endotherms of LLDPE Samples Treated by Successive Nucleation/Annaeling (SNA)

Successive nucleation/annealing is a continuous temperature-dependent process which segregates macromolecules based on recrystallization and reorganization of methylene sequences from the melt. The segregation mechanism is similar to that for the step-crystallization. Instead of annealing polymer isothermally at each temperature step for a long period of time, the SNA uses the precrystallized crystals as nuclei and allows polymer segments of similar methylene sequence lengthes to crystallize during each melting-annealing-crystallization cycle (Figure 3.2). The neighboring sequence on polymer chain can crystallize independently and subsequently melt at temperature corresponding to their crystallite size. As a result, each peak of SNA-DSC endotherms represents a group of chain segments having similar methylene sequence length.

As a preliminary study, three different types of commercial polyethylenes were treated by SNA, followed by DSC measurement of the treated samples. Figure 4.8 displays the DSC endotherms of the three types of polyethylenes. It can be seen that sample 19C, a NOVA high density polyethylene with molar mass of 1.37×10^5 and polydispersity of 4.89 (Table 4.1), showed a symmetrical single peak, indicating that the
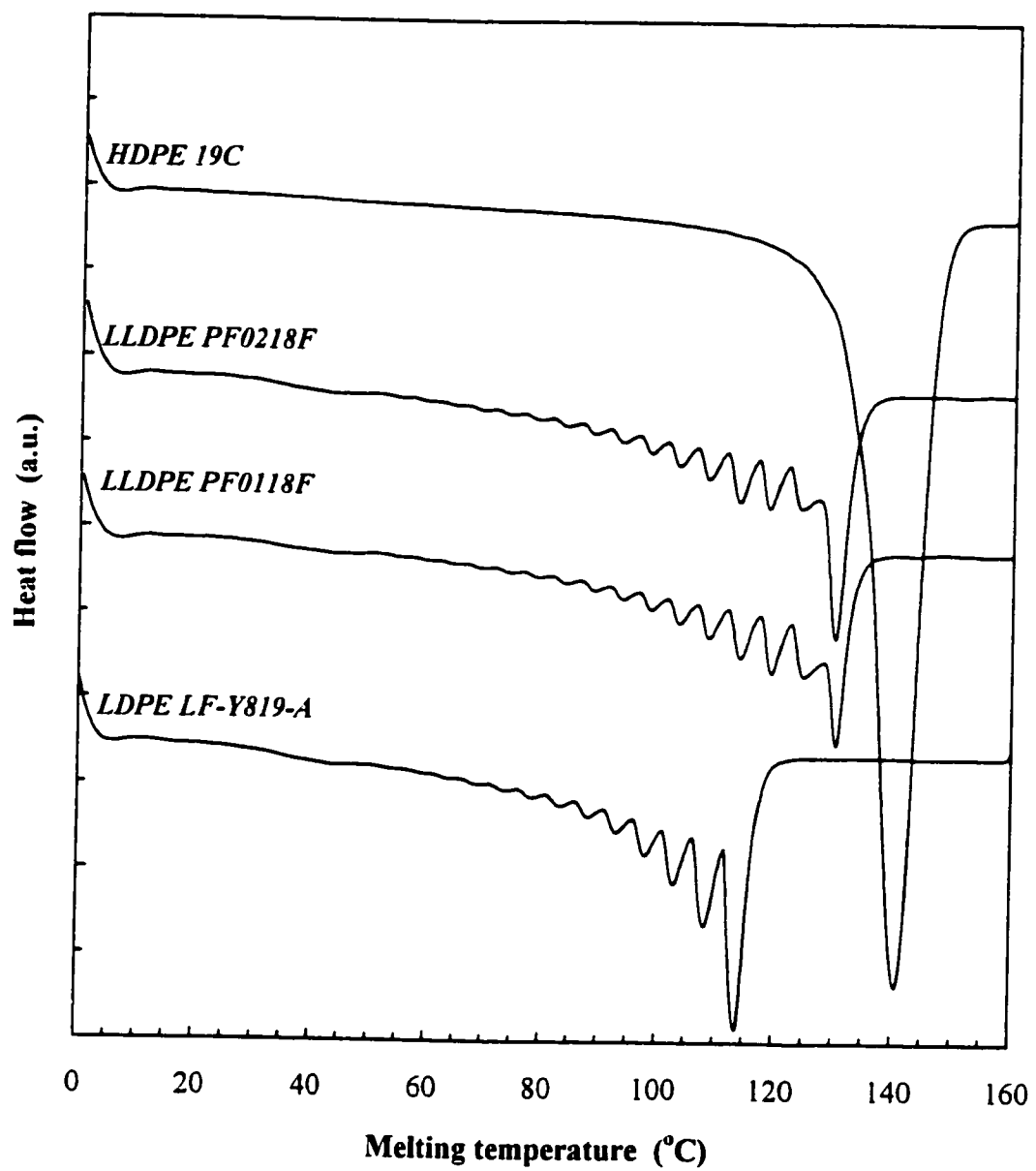
Figure 4.8. DSC endotherms of various NOVA polyethylenes treated by SNA.

SNA-DSC could not separate macromolecules from one another after the sequence length was over a certain value (~10,000 as indicated in Chapter 2). LF-Y819-A, a NOVA low density polyethylene, showed a multiple-peaked endotherm in the melting temperature ranging from about 60 to 120°C. The linear low density polyethylenes, PF0118F and PF0218F, showed a multiple-peaked endotherm with much broader distribution. The distribution seems to coincide with TREF profile in Figure 4.1. The preliminary results suggest that the SNA-DSC is effective in differentiating among polyethylenes with different chain structures.

Figure 4.9 shows DSC endotherms of three Ziegler-Natta LLDPEs treated by SNA. It can be seen that the SNA-DSC is capable of revealing the distribution difference between different samples. PF0118F and TF0119F showed a broad multiple-peaked distribution in the temperatures ranging from 60 to 135°C, while Sclair13J7 had a distribution from 80-138°C. Along with the shapes of the endotherms of these Ziegler-Natta LLDPEs, it can be concluded that the SNA-DSC is much more effective than the SC-DSC for the characterization of the Ziegler-Natta LLDPEs with low branch content, and it can provide much the same information as ATREF.

Figure 4.10 shows DSC exotherms of the three Ziegler-Natta LLDPEs following the first DSC heating. The exotherms were recorded at a cooling rate of 10°C/min. In contrast to the SNA-DSC endotherms, the exotherms showed a single sharp crystallization peak with a long tail at low temperatures.

The DSC endotherms of the metallocene LLDPEs treated with SNA are given in Figure 4.11. Again, multiple-peaked DSC endotherms were observed, which indicate different methylene sequence distributions in all the metallocene LLDPE samples. The Attane4201 showed the broadest distribution, while the Engage8100 had the narrowest among the four metallocene samples. The methylene sequence distribution curves bear much resemblance to the TREF profiles of the metallocene LLDPEs in Figure 4.2. It should be pointed out that a distinct peak with a minimum of about 40°C existed on the SNA-DSC endotherms of the metallocene LLDPEs. The cause of the low-temperature
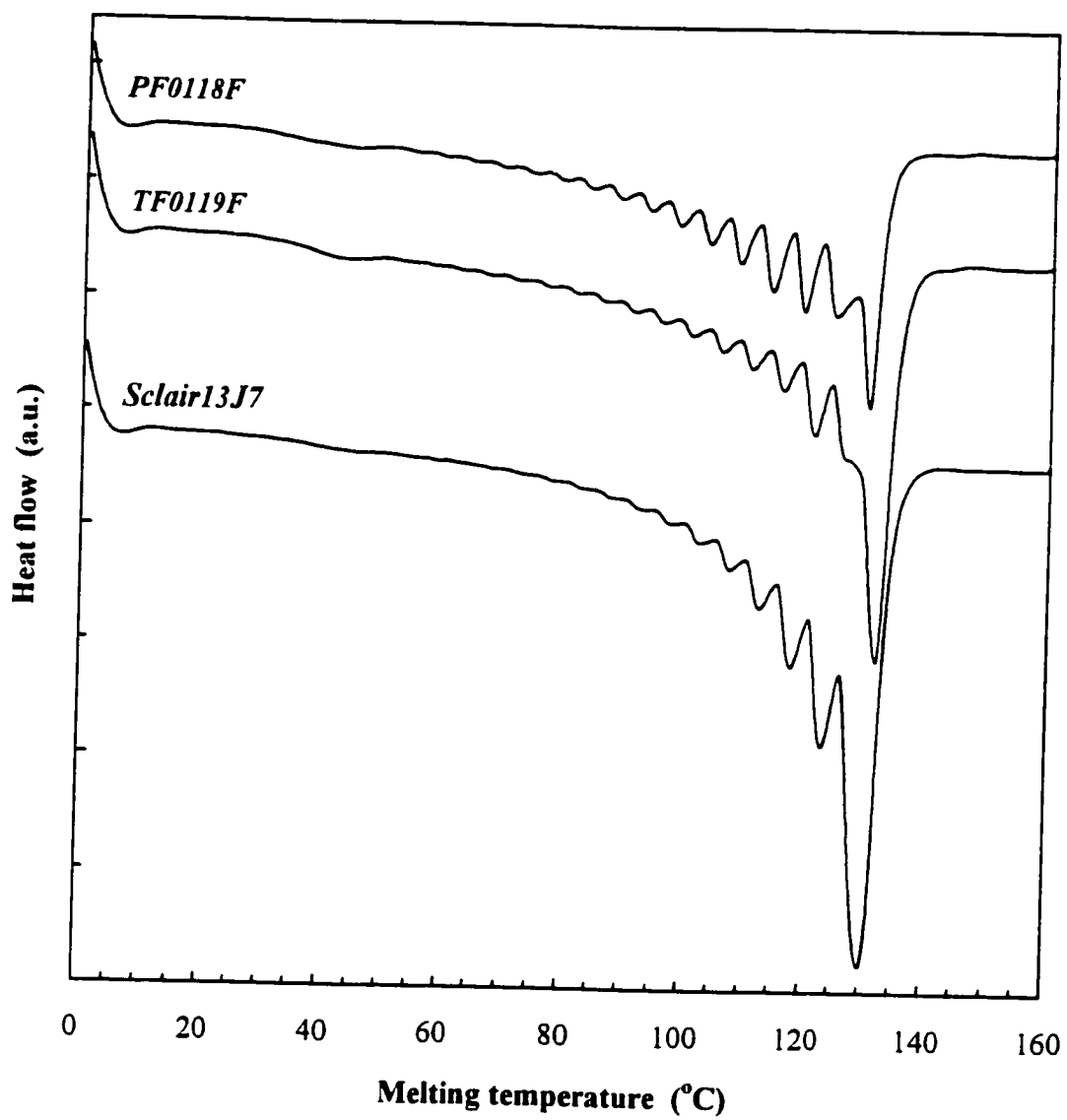
Figure 4.9. DSC endotherms of different commercial Ziegler-Natta LLDPEs.
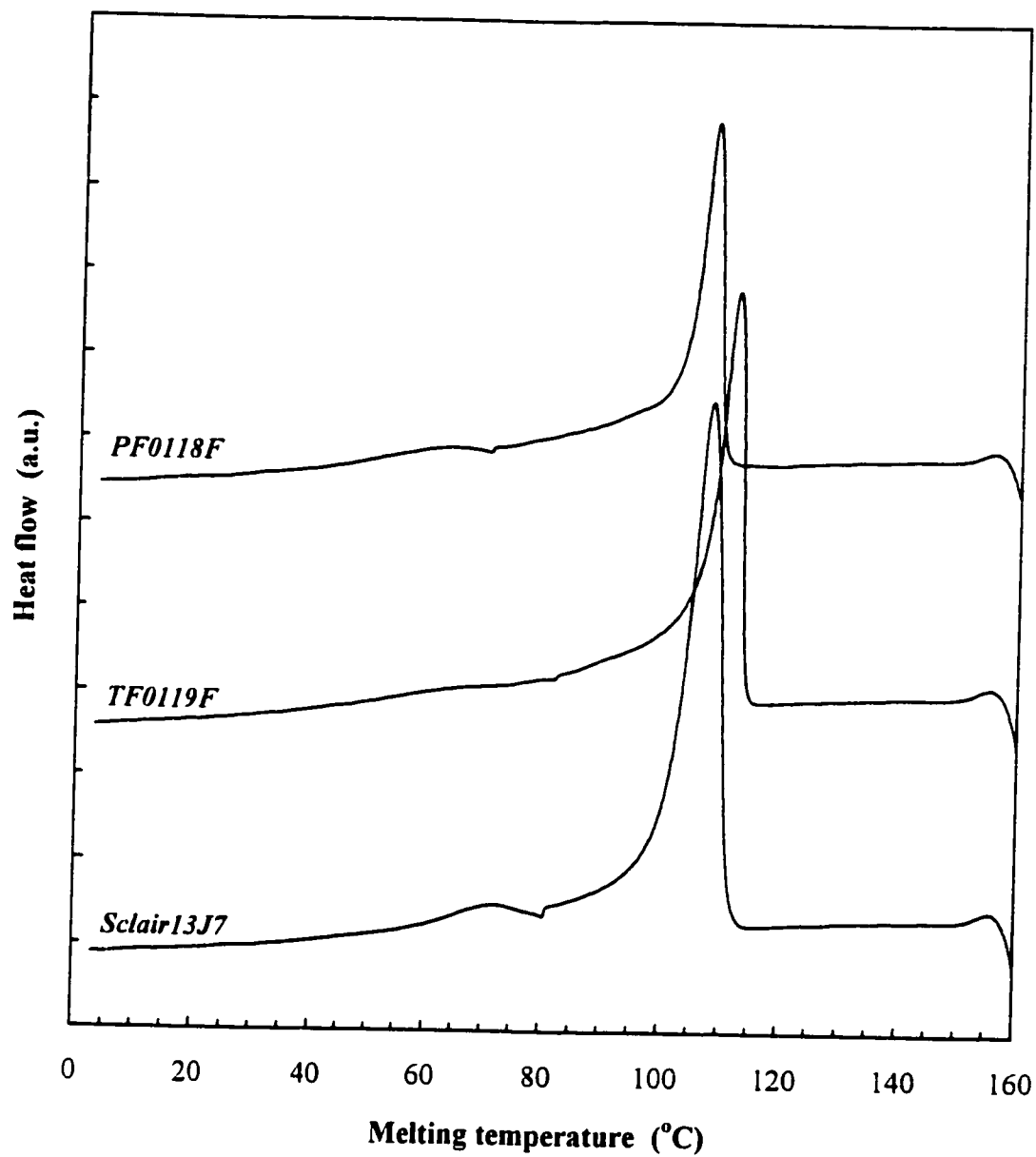
Figure 4.10. DSC exotherms of different commercial Ziegler-Natta LLDPEs.
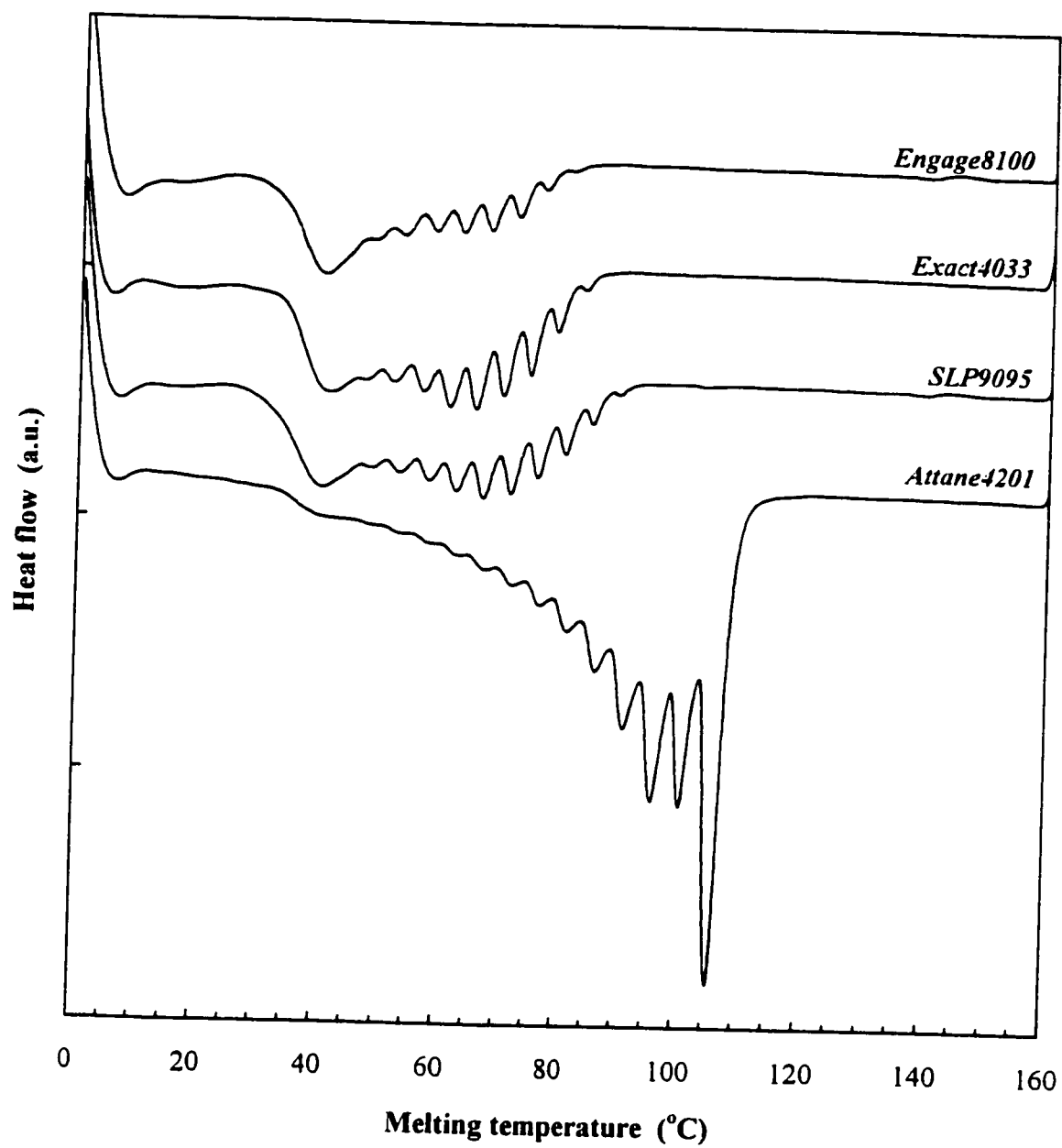
Figure 4.11. SNA-DSC endotherms of various commercial metallocene LLDPEs.

peak is not known. It is likely that the peak represents a group of "very short" methylene sequences which form fringed micelle-like nucleation structure (Mathot, 1994; Peeters et al., 1997 and 1999). The very short methylene sequences can crystallize and melt at low temperatures under favorable conditions, and may not be able to be distinguished by TREF.

Similar to those of the Ziegler-Natta LLDPEs, the DSC exotherms of the metallocene LLDPEs after the first heating were all single-peaked (Figure 4.12) with long tail at low temperatures. The different peak temperatures reflected the difference in crystallization temperature among these metallocene LLDPEs.

4.3.5. Quantitative DSC Analysis

The high resolution and good reproducibility of the SNA-DSC analysis shown above appear to provide the basis for the quantitative analysis of the short chain branch distribution of different LLDPEs. Another necessary condition for the reasonable estimation of the average SCB content is that the SNA-DSC segregation is SCB-controlled. For copolymers such as LLDPEs, the branches except methyl (propylene as comonomer) are usually excluded from the crystalline regions for energetic reasons (Mandelkern, 1989; Bonner et al., 1993). It follows that when the maximum MSL is less than the critical value for the onset of chain folding, the MSL or SCB controls the attainable crystal thickness and so the thermal segregation. The critical value for the onset of chain-folding is about 250 carbons (Ungar et al., 1987; Stack et al., 1988; Bonner et al., 1993). The MSL values calculated from the peak temperatures of the SNA-DSC endotherms, based on the calibration in Figure 3.7, were less than or close to the critical value for almost all the peak temperatures, suggesting that the SNA-DSC segregation is MSL or SCB controlled for the commercial LLDPEs under study.

The melting temperature can be translated into methylene sequence length and so SCB content by using the calibration curve in Figure 3.7. The heat flow in the ordinate of the SNA-DSC endotherm needs to be translated into weight fraction by using another

77
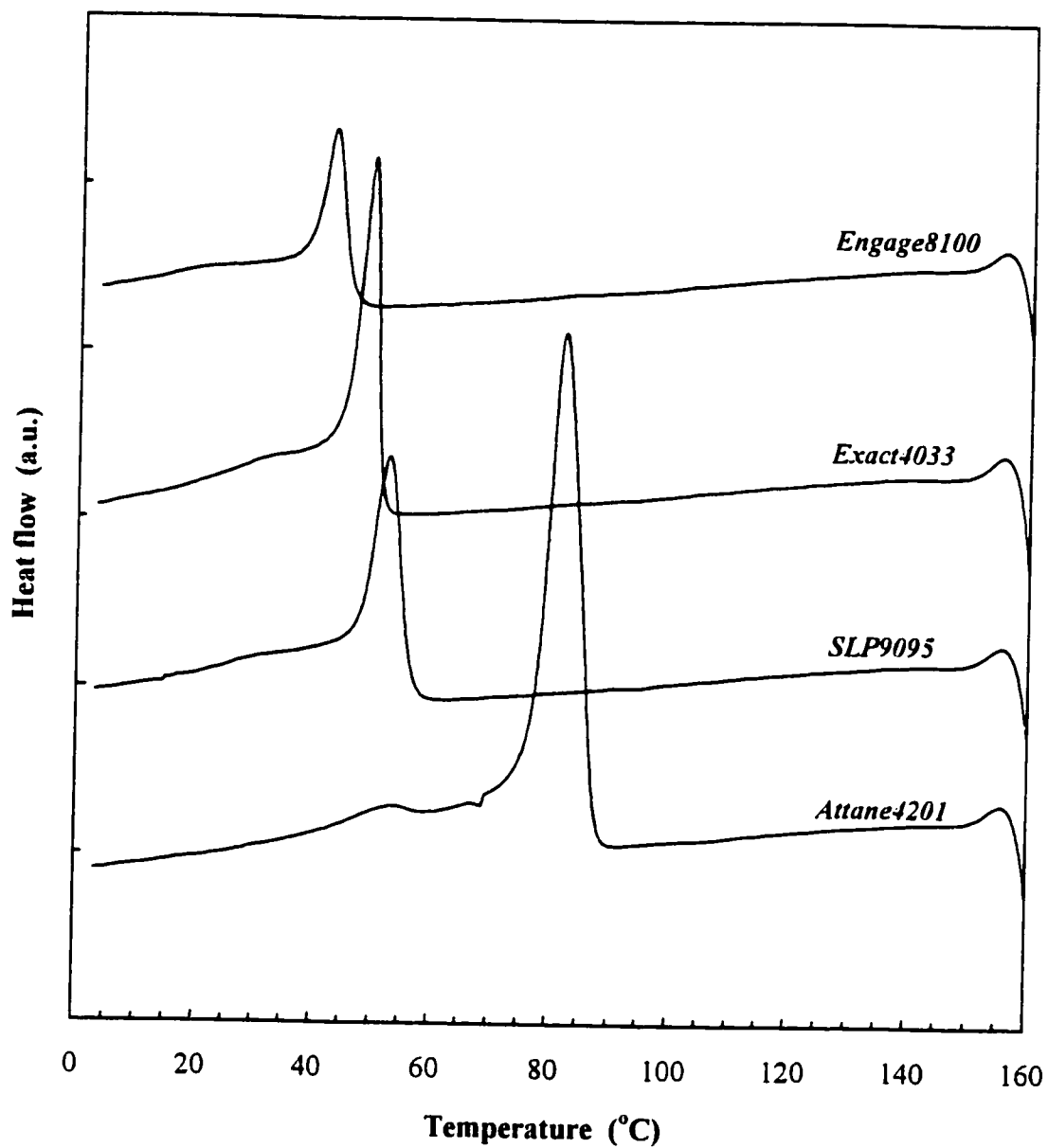
Figure 4.12. DSC exotherms of various commercial metallocene LLDPEs.

calibration relating the enthalpy of fusion to the melting temperature. However, such a calibration is very difficult to come by since it depends on the composition of polymer. With the lack of such calibration, the normalized heat flow can be used for quantitative analysis. Recent studies have indicated that the use of normalized heat flow yielded reasonably good quantitative results (Karoglanian et al., 1996; Prasad, 1998). The quantitative results below are based on the use of normalized heat flow.

The SNA-DSC endotherms of different LLDPEs were deconvoluted using commercial peakfit software (PeakFit, Version 4.06), from SPSS Science Inc.. The functions used in the fitting were the Gaussian area function:

$$y(T) = \frac{A_0}{\sqrt{2\pi}a_2} exp\left[-\frac{1}{2}\left(\frac{T-a_1}{a_2}\right)^2 \right]$$

(4.1)

or the Gaussian-Lorentzian area sum function:

$$y(T) = 2A_0\left[\frac{a_3\sqrt{\ln 2}}{a_2\sqrt{\pi}} exp\left[-4\ln 2\left(\frac{T-a_1}{a_2}\right)^2 \right] + \frac{1-a_3}{\pi a_2\left[1+4\left(\frac{T-a_1}{a_2}\right)^2\right]} \right]$$

(4.2)

where:

A_0 : peak area.

a_1 : peak centre temperature.

a_2 : peak width at half height.

a_3 : shape factor (≥ 0, ≤ 1).

T : melting temperature.

$y(T)$: heat flow.

Prior to the fitting, the DSC data was reversed into the positive peaks. A baseline was fitted and subtracted by the PeakFit software before peak fitting. Upon the selection of a fitting function, the PeakFit software automatically selected the initial parameters and performed the fitting. Figures 4.13 and 4.14 show the curve fitting results for two different LLDPEs. It can be seen that Equations 4.1 and 4.2 gave excellent fits of the SNA-DSC endotherms.

Figure 4.15 shows the cumulative distribution of melting temperatures for the Ziegler-Natta and metallocene LLDPEs calculated from the normalized area of each peak on the SNA-DSC endotherms. These distribution curves essentially reflected the methylene sequence length distribution of different LLDPEs. As expected, the slopes on the cumulative distribution curves for the Ziegler-Natta LLDPEs were lower than the slopes for the metallocene LLDPEs. This indicates a broader MSL distribution for the Ziegler-Natta LLDPEs.

Knowing the melting temperature and the peak area of each peak on the SNA-DSC endotherms, the average SCB content can be estimated based on the calibration curve in Figure 3.7 as well as Equations 3.3 and 3.4. That is, the melting temperature was translated into SCBs using the calibration curve, and the normalized areas were used for the calculation of weight fractions (procedure of the calculation is given in Appendix D). Table 4.3 lists the calculated results for all the LLDPE samples. Note that the above treatment appeared to yield reasonably good estimates for the average SCB contents of the Ziegler-Natta LLDPEs, compared with the results from TREF (Table 4.1). For the metallocene LLDPEs, the SNA-DSC seemed to somewhat overestimate the average SCB contents in comparison to the ATREF results. One of the reasons for the discrepancy could be the intense low-temperature peak at about 40°C on the SNA-DSC endotherms of the metallocene LLDPEs. Similar low-temperature peaks did not exist on the TREF profiles of these samples (Figures 4.2 and 4.4). It should be pointed out that the above treatment was an attempt to develop a methodology to estimate the average SCB contents from DSC analyses. To our knowledge, there have not been similar results reported in literature. The results could be further refined by correcting the heat flow using an
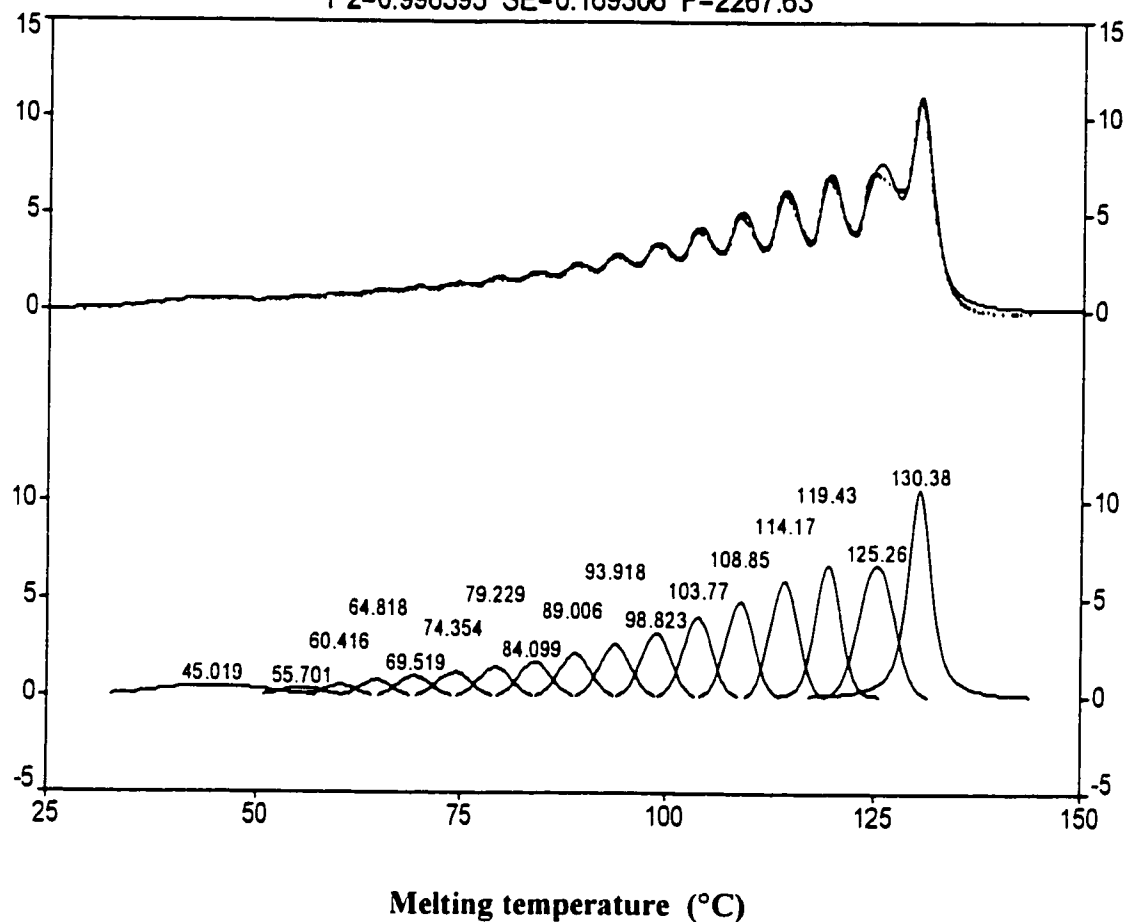
Figure 4.13. Curve fitting of SNA-DSC endotherms of Ziegler-Natta LLDPE (PF0118F). Dotted points are SNA-DSC data, solid line represents the fitted points.
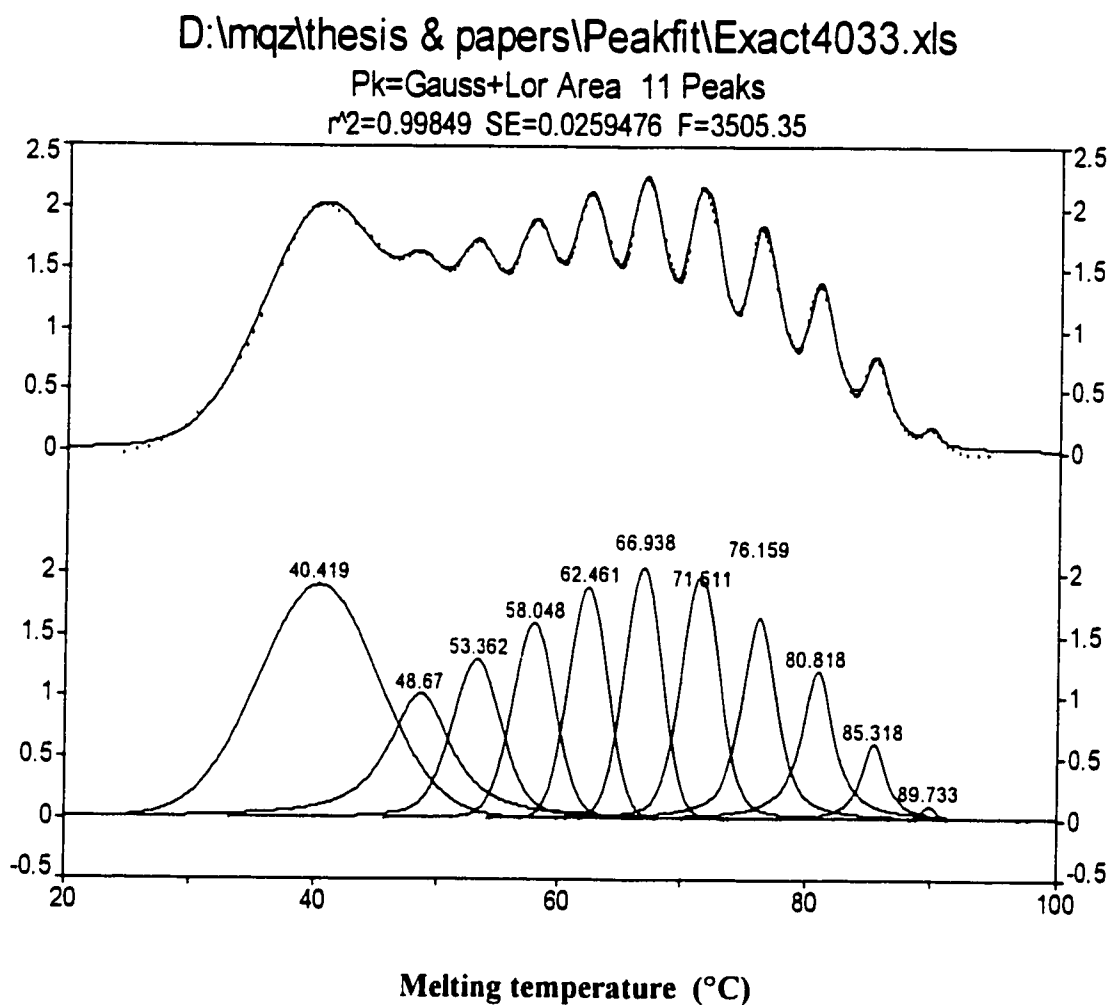
Figure 4.14. Curve fitting of SNA-DSC endotherms of metallocene LLDPE (Exact4033).
Dotted points are SNA-DSC data points, solid line represents the fitted points.
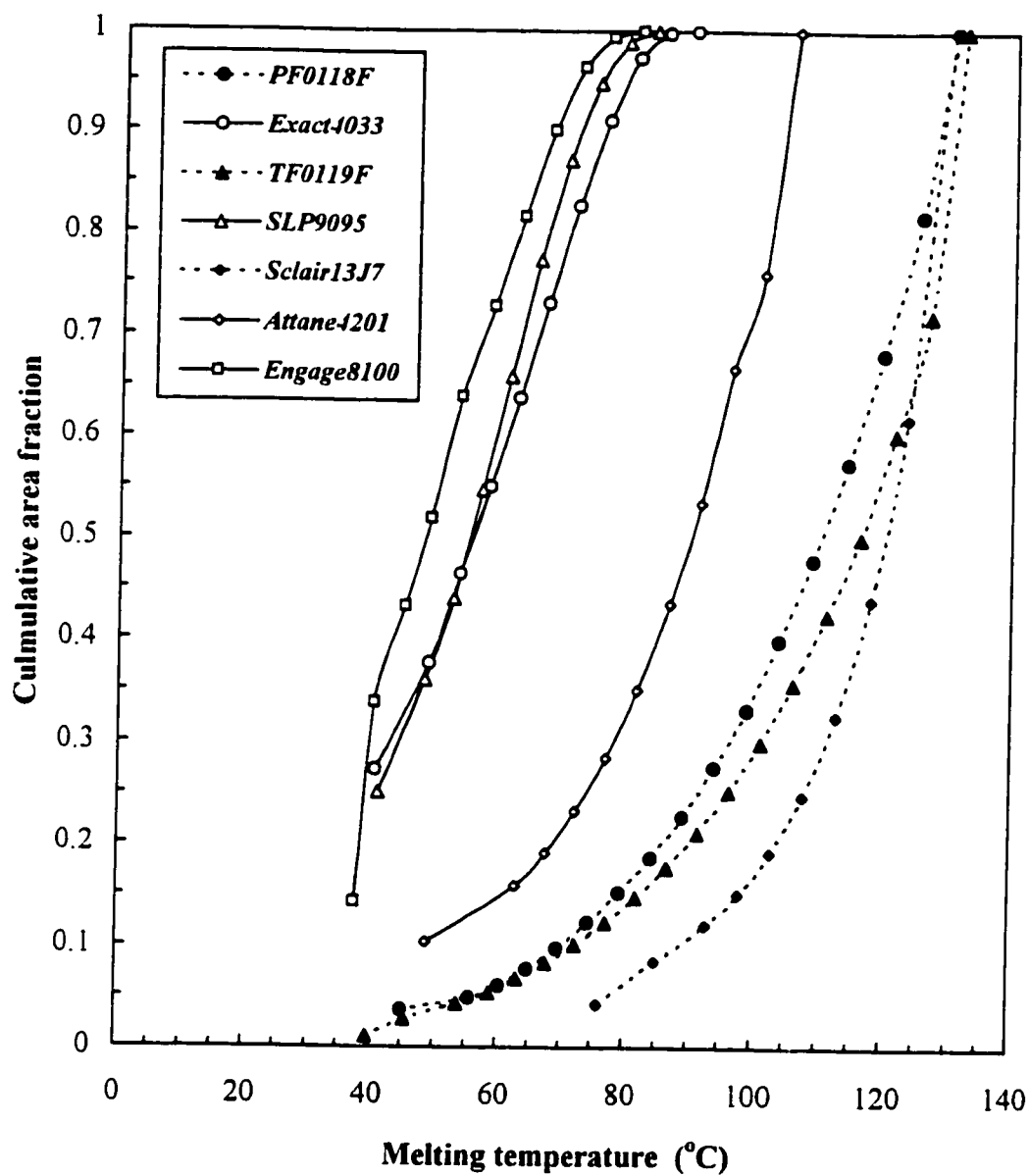
Figure 4.15. Cumulative distribution of various Ziegler-Natta and metallocene LLDPEs obtained from SNA-DSC endotherms.

appropriate calibration for variation in enthalpy of fusion with melting temperature.

Table 4.3. Average SCB content calculated from SNA-DSC endotherms of various Ziegler-Natta and metallocene LLDPEs (values in parentheses are the ATREF results from Table 4.2).

LLDPE	C_n	C_w	C_w/C_n
PF0118F	15.8 (17.7)	25.9 (26.5)	1.64 (1.50)
TF0119F	13.8 (13.4)	22.8 (21.7)	1.65 (1.62)
Sclair13J7	9.8 (8.0)	15.0 (11.2)	1.53 (1.40)
Exact4033	44.5 (32.4)	46.7 (33.3)	1.05 (1.02)
SLP9095	45.2 (28.7)	46.9 (29.7)	1.04 (1.04)
Engage8100	48.8 (40.2)	50.4 (40.6)	1.03 (1.01)
Attane4201	26.1 (19.6)	30.9 (22.5)	1.18 (1.15)

4.3.6. Relation between Lamellar Morphology and Short Chain Branches or Methylene Sequence Length

For LLDPE, the amount and type of comonomer and the short chain branch distribution are the dominant factors affecting the spherulitic texture and the lamellar morphology, and so the melting behaviors (Hosoda, 1988; Defoor et al., 1993; Peeters et al., 1997 and 1999), although the molar mass is certainly also of importance. Frequently, very complicated techniques such as small-angle X-ray scattering (SAXS) or wide-angle X-ray Diffraction (WAXD) have been used to measure lamellar morphology (Defoor et al., 1993; Marigo et al., 1996 and 1998; Peeters et al., 1997 and 1999). DSC has also been used to calculate lamellar morphology, but the dependence of DSC endotherms on thermal history introduced considerable uncertainty (Zhou and Wilkes, 1997). As shown above, the SNA-DSC treatment effectively segregates molecular segments according to their lamellar thickness, and the use of the calibration (Figure 3.7) gives reasonably good

estimation of MSL and SCB at each melting temperature. Hence, it is possible to quantitatively illustrate the relationship between lamellar morphology and SCB or MSL.

The relationship between lamellar thickness and short chain branches as well as methylene sequence length was calculated based on Equation 2.4 and the calibration curve of Figure 3.7. The melting temperatures were taken from peak temperatures of the SNA-DSC endotherms. Figure 4.16 plots the calculated lamellar thickness against SCB and MSL. It can be seen that the lamellar thickness decreased pronouncedly with increasing SCBs at low SCB range (less than 15 SCBs/1000 carbons). When the SCB content was more than 15 SCBs/1000 carbons, the lamellar thickness only gradually decreased with increasing SCBs. Also shown in Figure 4.16, the lamellar thickness increased almost linearly with increasing methylene sequence length. These results are in agreement with those obtained from SAXS (Defoor et al., 1993).

4.4. Cross-Fractionation Analysis

As demonstrated above, ATREF and thermally fractionated DSC have revealed distinct difference in SCB distribution between Ziegler-Natta and metallocene LLDPEs. To fully analyze the molecular structure of these two different LLDPEs, three characteristics must be known: One; the distribution of SCBs along polymer chains; two; the distribution of SCBs distributed across the molar mass distribution; and third the molar mass distribution of the TREF fractions and whole polymer. To obtain these inputs, PTREF-SEC cross-fractionation has been performed to explore the relationship between SCB and molar mass, whereas PTREF-SNA-DSC cross-fractionation has been used to study the intramolecular and intermolecular distribution of SCBs.

An ethylene/1-butene copolymer, PF0118F, was chosen as being representative of Ziegler-Natta LLDPE for detailed investigation by PTREF-SEC and PTREF-DSC cross-fractionation. The ATREF data in Figure 4.1 shows that for this Ziegler-Natta sample the polymer concentration eluted was very low at low elution temperatures and very high at
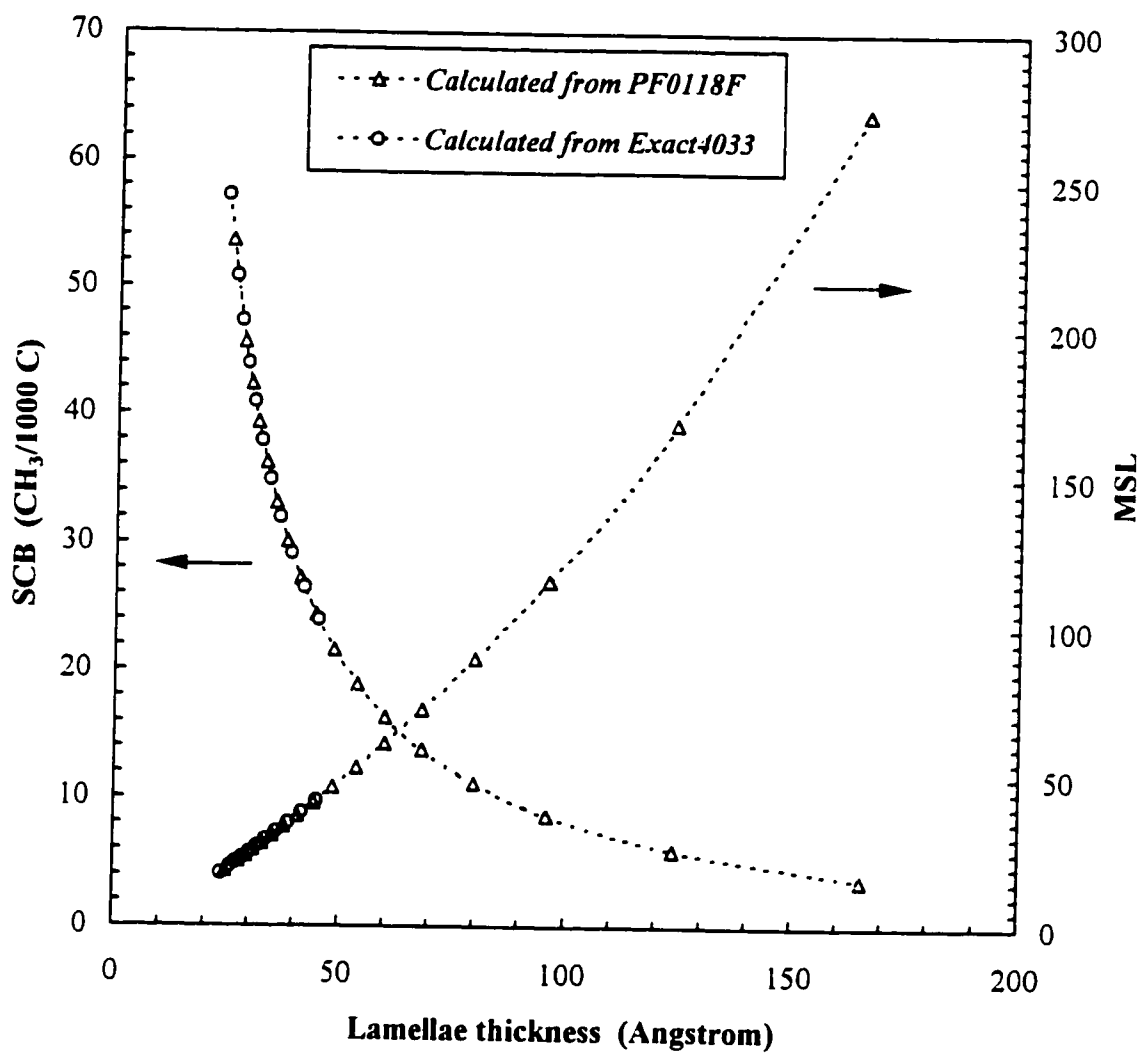
Figure 4.16. Relationship between lamellae thickness and short chain branches (SCB) and methylene sequence length (MSL) for ethylene-butene copolymers.

high elution temperatures. This presents a problem for collecting representative TREF fractions for subsequent SEC and DSC analysis in a single PTREF run. A large sample size is necessary to collect an adequate amount of sample at low temperatures for subsequent DSC analysis, but this causes problems, at high temperatures, such as solvent flow blockage and incomplete dissolving of polymer due to the limited volume of the column. To overcome these problems, two PTREF runs with different sample sizes were performed to ensure the PTREF fractions collected were representative. At first, a sample size of 300 mg was used which allowed TREF fractions to be collected in a temperature range typical of the branched polymer (0-85°C) as indicated in Figure 4.1. On the second PTREF run, a smaller sample size (60 mg) was used to collect fractions at high temperatures (85-100°C).

Similarly, an ethylene/1-butene copolymer, Exact4033, was chosen as being representative of metallocene LLDPE for detailed investigation by PTREF-SEC and PTREF-DSC cross-fractionations. Unlike the Ziegler-Natta sample, the whole metallocene sample was easily separated into six fractions in a single PTREF run. The results of cross-fractionations are presented below.

4.4.1. TREF-SEC Cross-Fractionation

Figure 4.17 shows the molar mass distribution of the collected PTREF fractions of the Ziegler-Natta LLDPE, PF0118F. The number and weight average molar masses as well as polydispersity index are given in Table 4.4. For all eight fractions, a broad molar mass distribution was observed. The polydispersity index M_w/M_n seemed to slightly decline as increasing elution temperature from 3.28 at 40°C to 2.28 at 95°C. It can also be seen from Figure 4.17 that all fractions had a similar shape of single-peaked molar mass distribution. The distribution curve shifted towards higher molar masses with increasing TREF elution temperature, as shown in Table 4.4.

Figure 4.18 shows the molar mass distribution of the PTREF fractions of metallocene LLDPE, Exact4033. The molar masses and polydispersity index of each
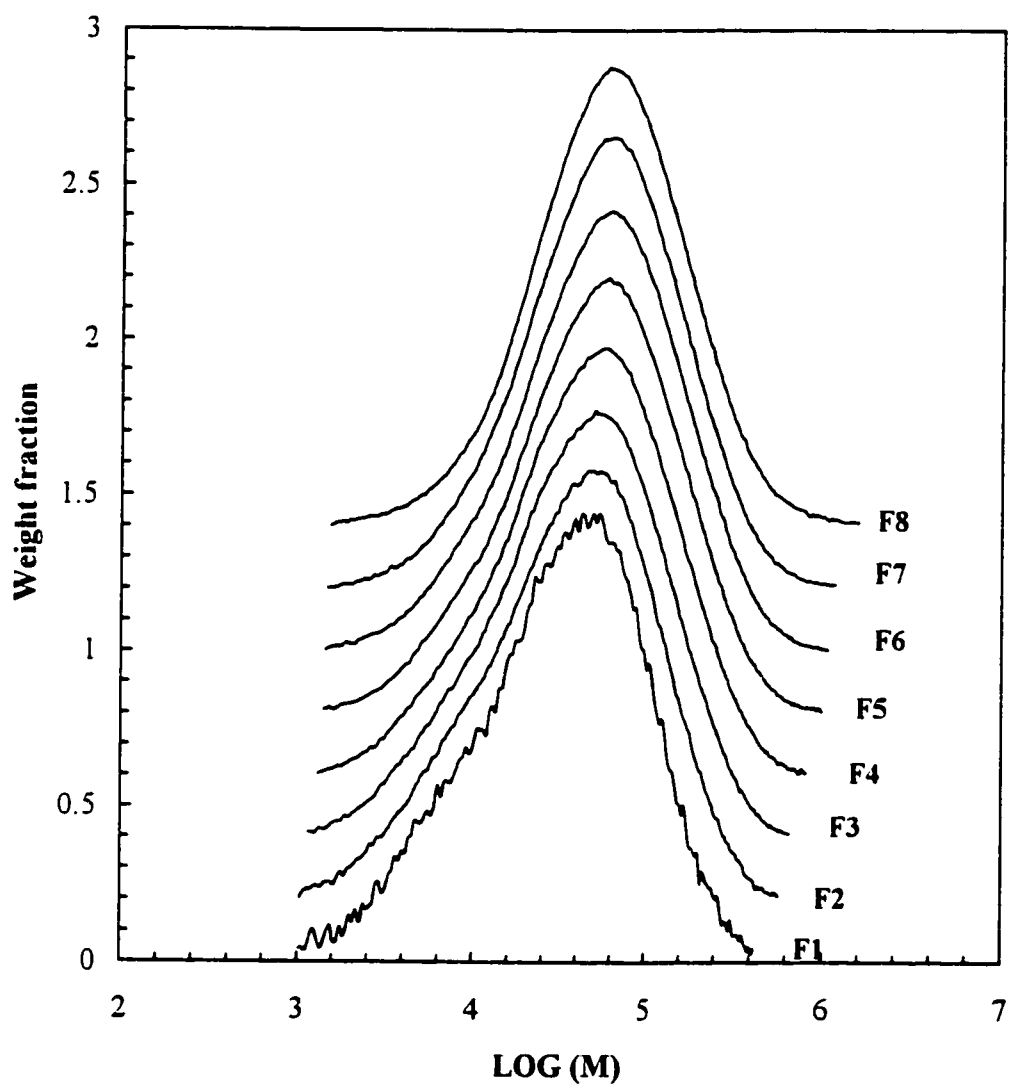
Figure 4.17. Molar mass distribution of PTREF fractions of Ziegler-Natta LLDPE (PF0118F) obtained at various temperature intervals: F1, 30-50; F2, 50-60; F3, 60-70; F4, 70-75; F5, 75-80; F6, 80-85; F7, 85-90; F8, 90-100 °C.
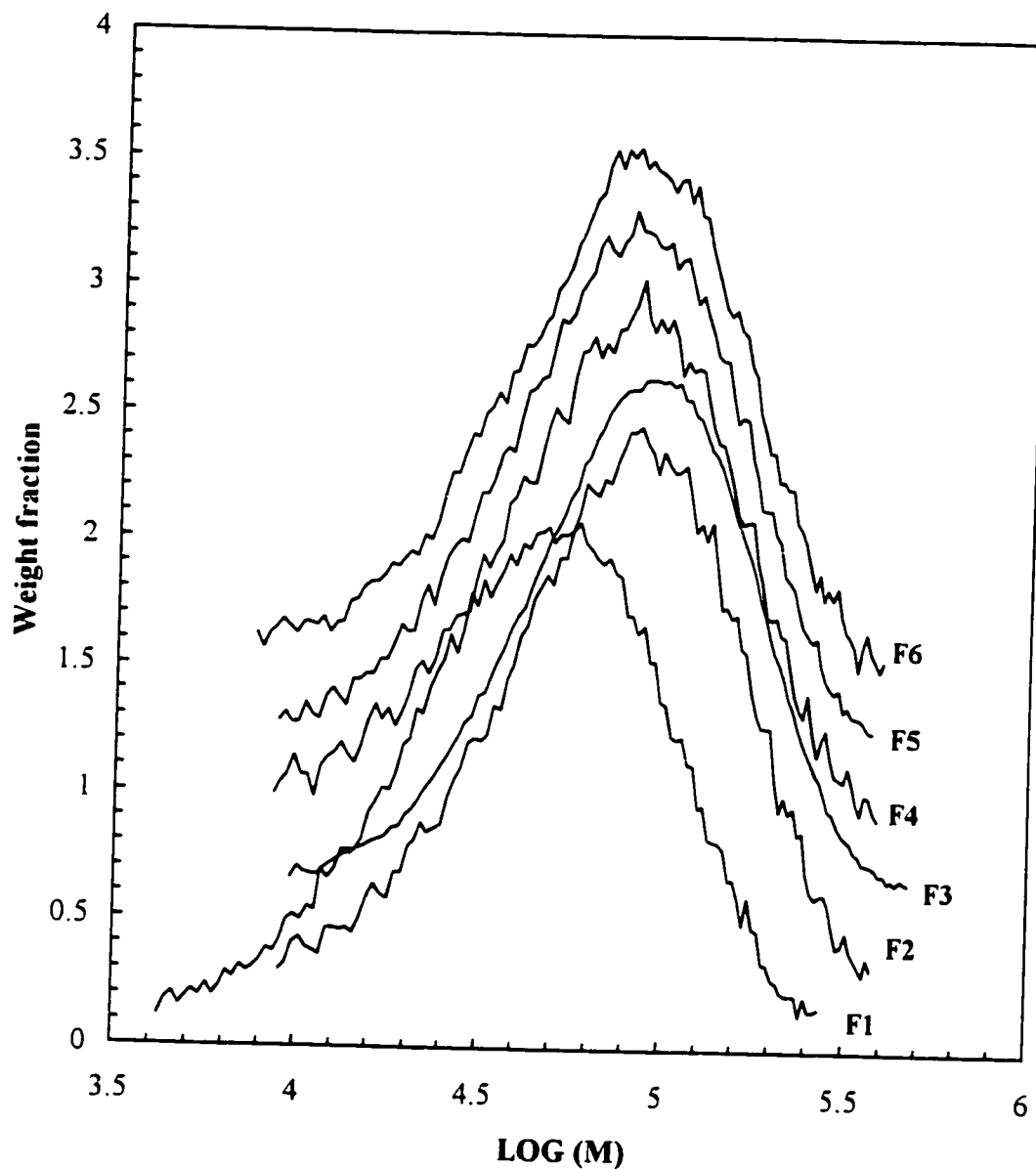
Figure 4.18. Molar mass distribution of PTREF fractions of metallocene LLDPE (Exact4033) obtained at various temperature intervals: F1, 20-30; F2, 30-40; F3, 40-45; F4, 45-50; F5, 50-55; and F6, 55-60°C.

Table 4.4. Molar masses and polydispersity of the PTREF fractions of the Ziegler-Natta LLDPE.

Fraction	T_e (°C)	$M_n \cdot 10^{-4}$	$M_w \cdot 10^{-4}$	P_d
F1	30-50	1.63	5.86	3.59
F2	50-60	1.86	6.70	3.60
F3	60-70	2.03	7.31	3.60
F4	70-75	2.42	8.46	3.50
F5	75-80	2.80	9.52	3.40
F6	80-85	3.07	9.87	3.21
F7	85-90	3.43	10.39	3.03
F8	90-100	3.82	10.94	2.86

T_e: elution temperature range of PTREF.

Table 4.5. Molar masses and polydispersity of the PTREF fractions of the metallocene LLDPE.

Fraction	T_e (°C)	$M_n \cdot 10^{-4}$	$M_w \cdot 10^{-4}$	P_d
F1	20-30	4.10	7.34	1.81
F2	30-40	5.81	10.07	1.73
F3	40-45	7.69	12.41	1.61
F4	45-50	7.04	10.50	1.50
F5	50-55	7.02	10.74	1.53
F6	55-60	6.75	10.81	1.60

fraction are also listed in Table 4.5. The molar mass distribution curves for the fractions eluted at temperatures above 30°C were very similar in shape. The curve for elution temperature of 20-30°C appeared at lowest molar mass. Notice from Table 4.5 that the fraction eluted between 40-45°C had the highest molar mass. The polydispersity for all the fractions was very similar in magnitude. In comparison, the TREF fractions of the

metallocene sample had narrower molar mass distributions than the Ziegler-Natta sample. The polydispersity indexes of the PTREF fractions of the Ziegler-Natta LLDPE were around 3.4, compared with about 1.6 for the PTREF fractions of metallocene LLDPE.

4.3.2. Relationship between Molar Mass and SCB of Ziegler-Natta and Metallocene LLDPEs

As indicated in Chapter 1, molar mass and short chain branching of a LLDPE are responsible for the variations in properties. For example, the processibility of a LLDPE is controlled mainly by molar mass and molar mass distribution, while the thermal and physical properties depend primarily on crystallinity or short chain branching (Kim et al., 1996). In the copolymerization of ethylene with α-olefins, particularly when Ziegler-Natta catalyst is used, controlling of molar mass and short chain branching is conflicting, since the low reactivity of α-olefins increases the probability of polymer chain transfer. As a result, copolymers of high SCB contents usually have lower molar mass and molar mass distribution, that is equivalent to say the processibility has to be compromised in order to achieve some other physical properties possessed by LLDPE of high SCB contents. For this reason, the characterization of the relationship between molar mass and SCB is of practical importance.

The relationship between molar mass and short chain branches can be elucidated by plotting the weight average molar mass of PTREF fractions against the degree of short chain branch. Figure 4.19 shows the calculated curves for the Ziegler-Natta LLDPE (PF0118F) and four metallocene LLDPEs. It can be seen that the M_w of the Ziegler-Natta sample increased monotonically with the decrease in the degree of short chain branching. This result is in good agreement with results generally found on commercial Ziegler-Natta samples (Mirabella and Ford, 1990; Karbashewski et al., 1992; Mingozzi et al., 1996). However, for the metallocene samples there appeared to be a maximum in the plot of M_w versus SCB. TREF-SEC cross-fractionation was done on three other metallocene samples besides Exact4033 to ensure that the maximum in molar mass was not a peculiarity of Exact4033. As shown in Figure 4.19, the TREF-SEC cross-fractionation of
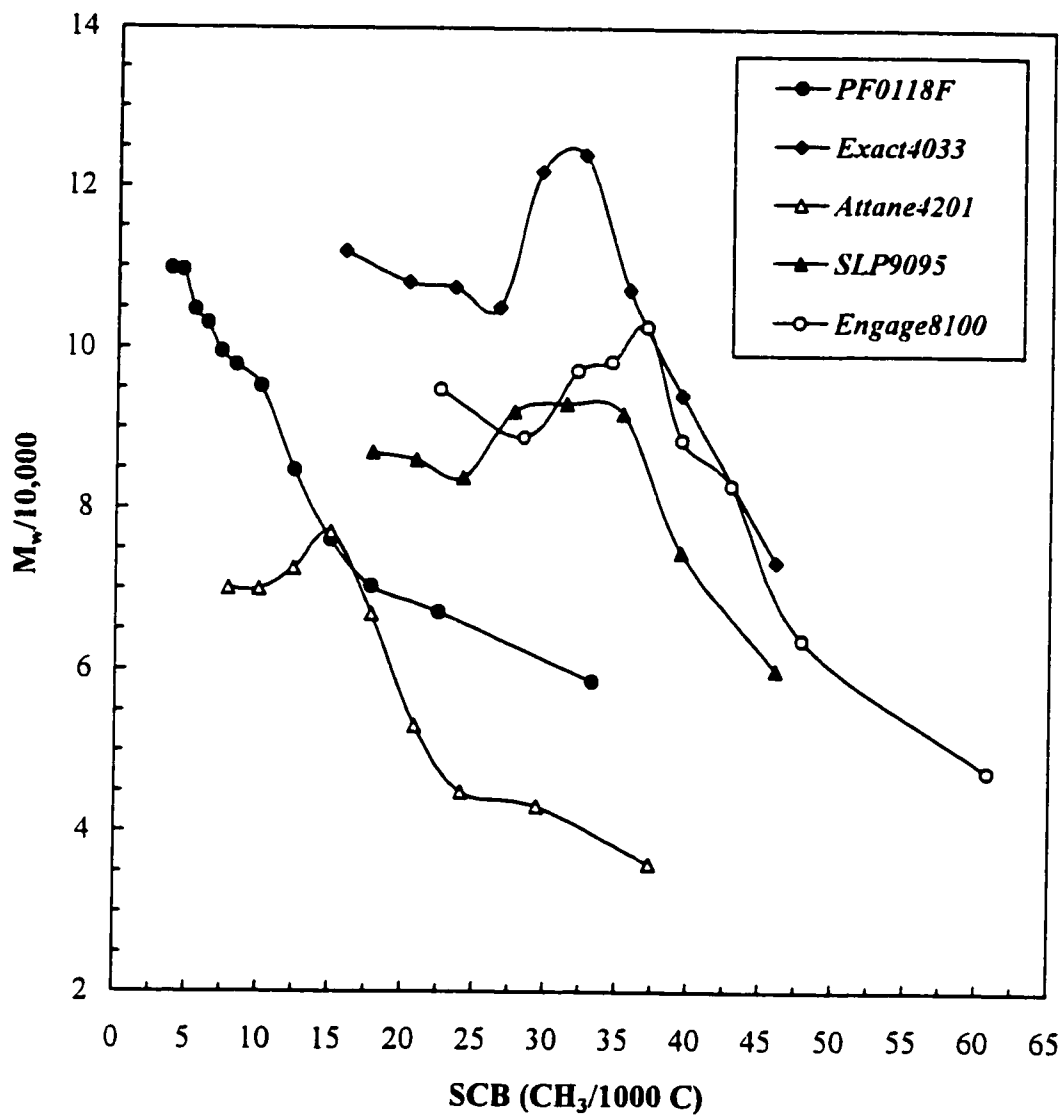
Figure 4.19. M_w as a Function of SCB for Ziegler-Natta and metallocene LLDPEs.

all four commercial metallocene LLDPEs utilized in this study resulted in the same trend, suggesting that the observed relationship of a maximum in the plot of M_w versus SCB could be characteristic of metallocene LLDPEs.

4.4.3. TREF-SNA-DSC Cross-Fractionation

The heterogeneity of the comonomer or short chain branch distribution is an important characteristic in describing the molecular structure of LLDPE. The characterization of the heterogeneity of SCB distribution is of importance since it not only affects the melting and thermodynamic properties of LLDPE, but also provides useful information on the mechanism of copolymerization. It is important to recognize that two types of heterogeneity exist for LLDPE: intramolecular and inter-molecular heterogeneity. Intramolecular heterogeneity means that the SCB distribution of individual macromolecule in the system is not uniform along the chain backbone, but all the molecules possess the same SCB distribution. Intermolecular heterogeneity means that the SCB distribution differs from one molecule to another. The concepts of intermolecular and intramolecular heterogeneities are schematically illustrated in Figure 4.20.

As a result of intramolecular and intermolecular SCB distributions, a LLDPE sample can be intermolecularly or intramolecularly heterogeneous or both. The classifications in terms of intermolecular or intramolecular heterogeneity are less ambiguous than the commonly-used classification of simply heterogeneous or homogeneous polymers (Mathot, 1994; Fu et al., 1997). To differentiate between the types of heterogeneity, it is necessary to fractionate and segregate the polymer in two dimensions according to average SCB content and methylene sequence distribution.

As indicated above, SNA-DSC segregates LLDPE molecules according to methylene sequence length. Therefore, unlike TREF which can only evaluate intermolecular heterogeneity, the SNA-DSC is able to assess both intramolecular and
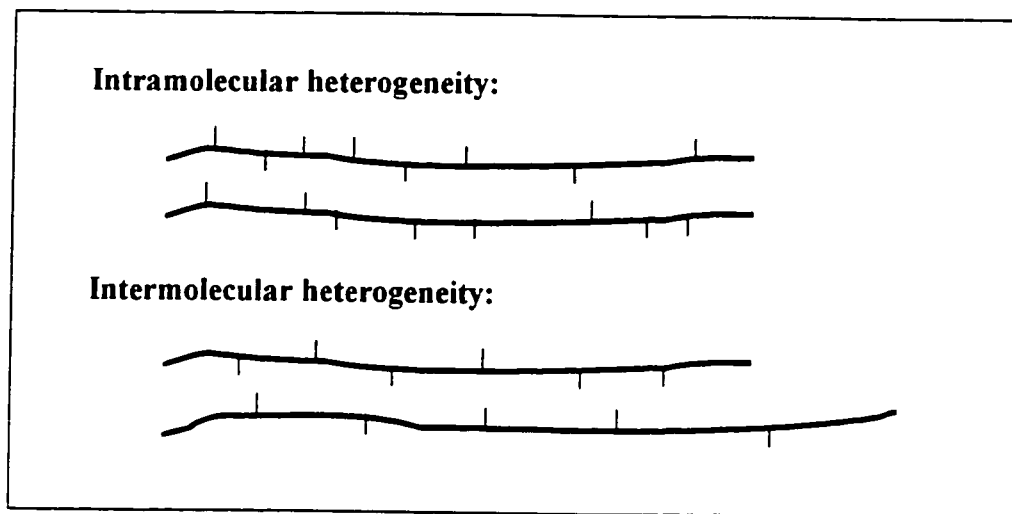
Figure 4.20. Schematical representation of chain structure of copolymer having intramolecular and intermolecular heterogeneity.

intermolecular heterogeneity. Hence, the PTREF-SNA-DSC cross-fractionation should be able to provide information about the intramolecular and intermolecular heterogeneity of SCB distribution.

Figure 4.21 shows the SNA-DSC endotherms of PTREF fractions of Ziegler-Natta LLDPE, PF0118F. The TREF elution temperature range and the SNA-DSC results are summarized in Table 4.6. Note that the crystallinity of TREF fractions increased with elution temperature, as expected. Given the fact that the TREF fractions were collected at relatively narrow temperature intervals, it is reasonable to assume that the macromolecules represented by each TREF fraction have similar SCB distributions, and so similar average short chain branch content. Thus, the DSC endotherm of each fraction represents the methylene sequence distribution of all the molecules in the fraction regardless of molar mass. It is clear from Figure 4.21 that the molecules eluted at each temperature interval had different methylene sequence distributions, indicating that the Ziegler-Natta LLDPE was intramolecularly heterogeneous. Also shown in Figure 4.21, the methylene sequence distribution considerably varied among fractions. The SNA-DSC

Figure 4.21. DSC endotherms of PTREF fractions of Ziegler-Natta LLDPE (PF0118F) obtained at various temperature intervals: F1, 30-50; F2, 50-60; F3, 60-70; F4, 70-75; F5, 75-80; F6, 80-85; F7, 85-90; F8, 90-100 °C.

endotherm of the fraction eluted between 30 and 50°C showed multiple peaks and a nearly symmetrical distribution of methylene sequence. With the increase in the elution temperature, the peaks of higher melting temperature became dominant in intensity. Moreover, the spectrum of the endotherms shifted toward high temperature. Clearly, theZiegler-Natta LLDPE was intermolecularly heterogeneous in terms of methylene sequence distribution as well. The results suggest that the Ziegler-Natta LLDPE is a mixture of macromolecules of very different SCB distribution, and a single distribution function as reported in literature (Stockmayer, 1945; Soares and Hamielec, 1995; Thomunn et al., 1997) may not be sufficient to describe the heterogeneity.

Table 4.6. PTREF and SNA-DSC results of the Ziegler-Natta ethyiene-butene copolymer.

Fraction	T_e (°C)	T_{onset} (°C)	T_{peak} (°C)	ΔH_f (J/g)	X_c (%)
F1	30-50	86.6	88.3	58.0	20.2
F2	50-60	96.3	98.0	84.2	29.3
F3	60-70	104.2	105.7	106.5	37.1
F4	70-75	106.6	108.6	113.1	39.4
F5	75-80	110.6	112.8	119.7	41.7
F6	80-85	115.1	117.5	124.1	43.2
F7	85-90	119.5	121.6	138.4	48.2
F8	90-100	127.9	129.6	156.1	54.4

T_{onset}: onset temperature of the primary peak on DSC endotherm.
T_{peak}: peak temperature of the primary peak on DSC endotherm.
ΔH_f: heat of fusion.
X_c: crystallinity.

The results also provide another possible interpretation of TREF mechanism which has not yet been fully understood (Karbashewski et al., 1993; Bonner et al., 1993; and Elicabe et al., 1996). Although it is generally agreed that TREF fractionates semicrystalline polymer based on crystallizability, and so most of the TREF calibrations have been based on the average SCB content generated from PTREF (Wild, 1991; Soares

and Hamielec, 1995), there have been suggestions that TREF separates macromolecules based on the length of crystallizable sequence (Bonner et al., 1993; and Elicabe et al., 1996). This can be easily understood by considering a crystallized molecule in TREF column, only when the longest sequence in the molecule dissolves does the whole molecule elutes from the column. As shown in Figure 4.21, the shifting of the methylene sequences toward high elution temperatures or long sequences implies that the longest methylene sequence length may dictate the separation by TREF.

Upon the cooling of the melt of PTREF fractions following the first heating, the DSC exotherms of the PTREF fractions were recorded and are shown in Figure 4.22. It is apparent that the crystallization behaviors of these PTREF fractions varied considerably. The low-temperature fractions crystallized at lower temperatures with a relatively broad crystallization peak, which is associated with the high SCB contents and more uniform composition. With the elution temperature increasing, the crystallization temperature became higher and the crystallization peak became sharper, resulting from the lower SCB contents and more heterogeneous distribution. The results well reflect the variation of crystallization behaviors with the SCB contents of Ziegler-Natta LLDPE.

DSC endotherms of the second heating runs of PTREF fractions of the Ziegler-Natta LLDPE are shown in Figure 4.23. Unlike those of the first heating runs, the DSC endotherms of the second heating runs only showed a single peak with long low-temperature tail for all the fractions. The melting temperature was appreciably shifted toward high temperatures with increasing TREF elution temperature. Nevertheless, the DSC endotherms did not seem to reflect the difference in MSL distribution as shown in Figure 4.21. This again shows that the SNA treatment is effective in separating LLDPE according to methylene sequence length.

The SNA-DSC endotherms of PTREF fractions of metallocene LLDPE, Exact4033, are shown in Figure 4.24, and the TREF elution temperature and the SNA-DSC results are listed in Table 4.7. The methylene sequence distribution was narrow for all the molecules in each fraction. Also, it is very intriguing to see all TREF fractions appeared

Figure 4.22. DSC exotherms of PTREF fractions of Ziegler-Natta LLDPE (PF0118F). Temperature range for each fraction is the same as in Figure 4.21.

Figure 4.23. DSC endotherms of PTREF fractions of Ziegler-Natta LLDPE (PE0118F). Temperature range for each fraction is the same as in Figure 4.21.
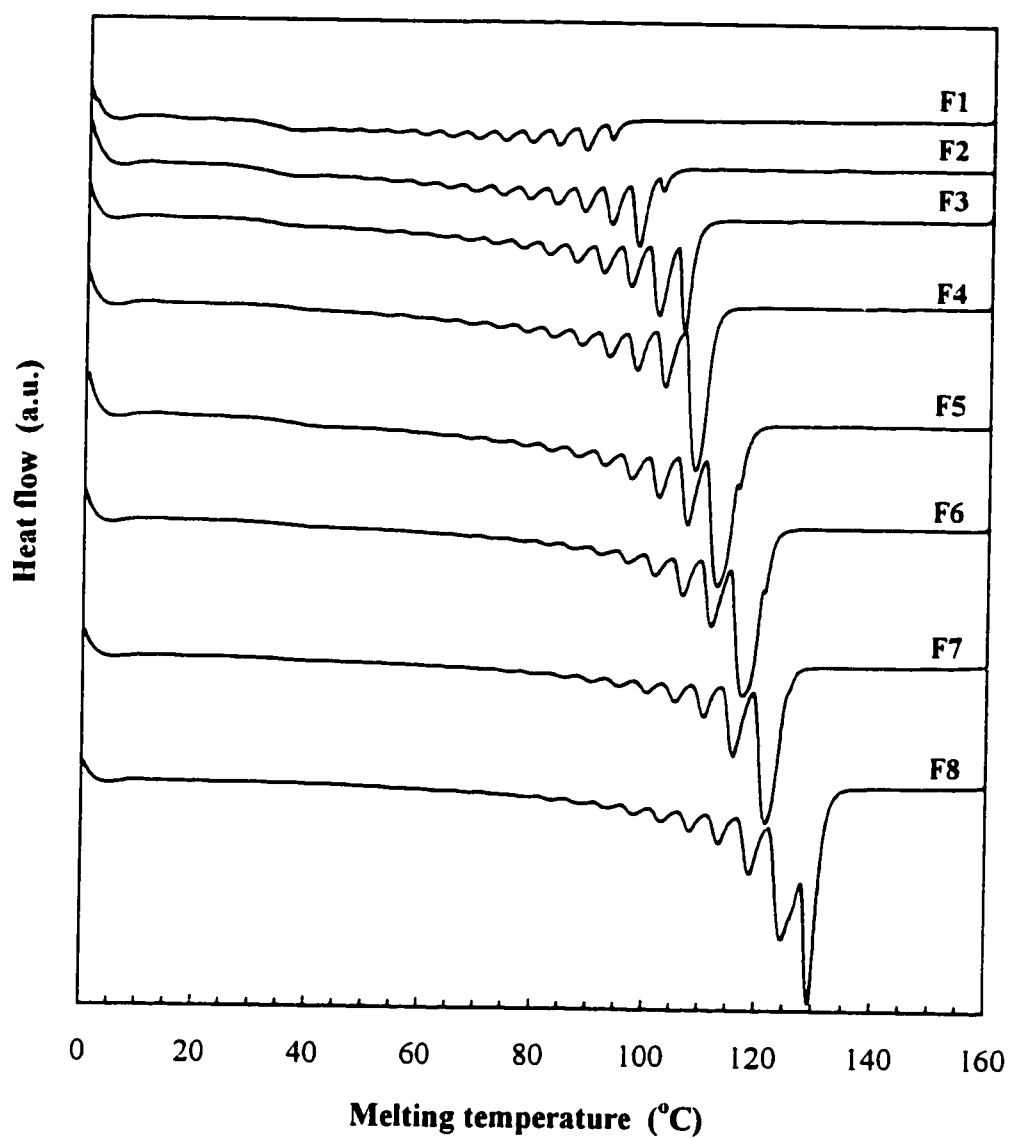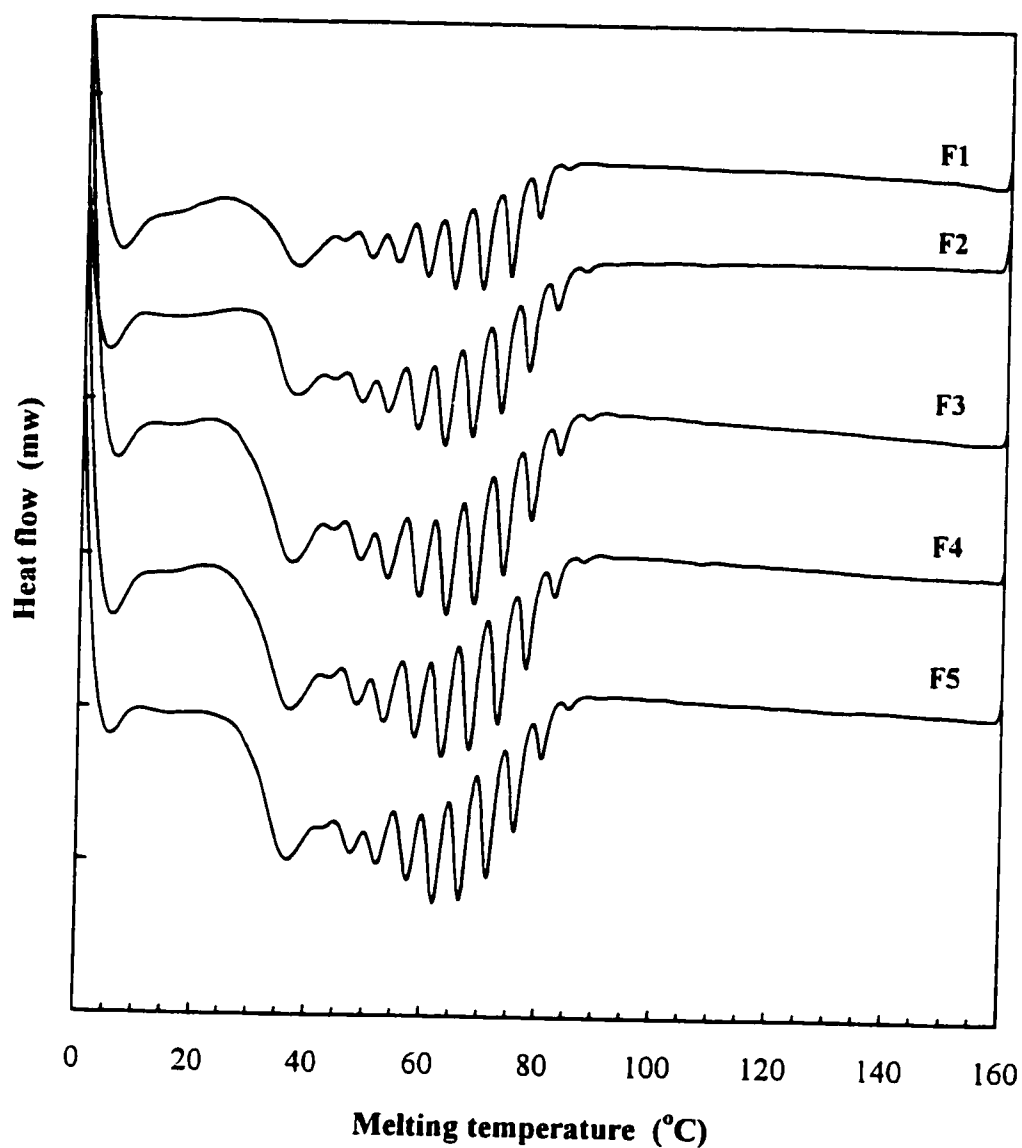
Figure 4.24. DSC Endotherms of PTREF Fractions of metallocene LLDPE (Exact4033) obtained at various temperature intervals: F1, 30-40; F2, 40-45; F3, 45-50; F4, 50-55; F5, 55-65°C.

to show the same distribution. These results strongly suggest, in a rather direct fashion, that the metallocene LLDPE has only intramolecular heterogeneity in chemical composition. In other words, the metallocene LLDPE is composed of macromolecules possessing the same SCB distribution, and therefore one can probably use one distribution function to describe the compositional heterogeneity. Similar conclusion has been deduced recently from TREF-^{13}C NMR of metallocene LLDPE (Balbontin et al., 1995).

Table 4.7. PTREF and SNA-DSC results of the metallocene ethylene-butene copolymer.

Fraction	T_c (°C)	T_{onset} (°C)	T_{peak} (°C)	ΔH_f (J/g)	X_c (%)
F1	30-40	----	----	----	----
F2	40-45	59.7	62.7	33.10	11.5
F3	45-50	60.3	63.5	37.79	13.2
F4	50-55	60.0	63.2	38.65	13.5
F5	55-65	58.6	62.0	40.54	14.1

The DSC exotherms of the PTREF fractions following the first heating runs are shown in Figure 4.25. All the five fractions had very similar crystallization temperature and melting peak, which signifies the homogeneousness of SCB distributions among these fractions of metallocene LLDPE.

Upon the further heating of DSC crystallized samples, the DSC endotherms of the PTREF fractions were recorded again and are shown in Figure 4.26. A single, broad, and unsymmetrical peak was observed for all the fractions, indicating the similarity in composition and compositional distribution among the PTREF fractions of the metallocene LLDPE. Compared with the SNA-DSC endotherms in Figure 4.24, the DSC endotherms of the second heating showed a gradual melting curve starting at temperature
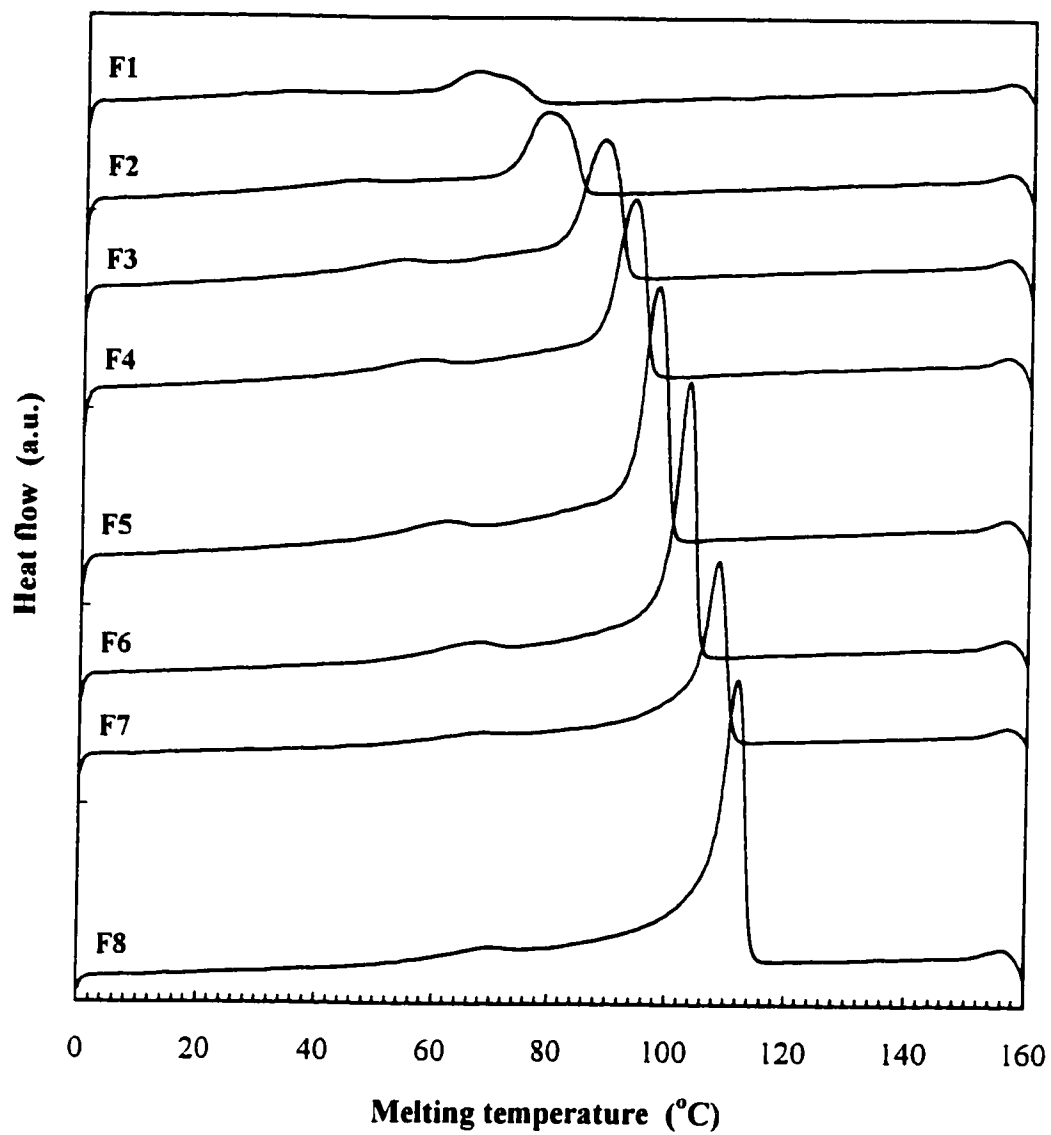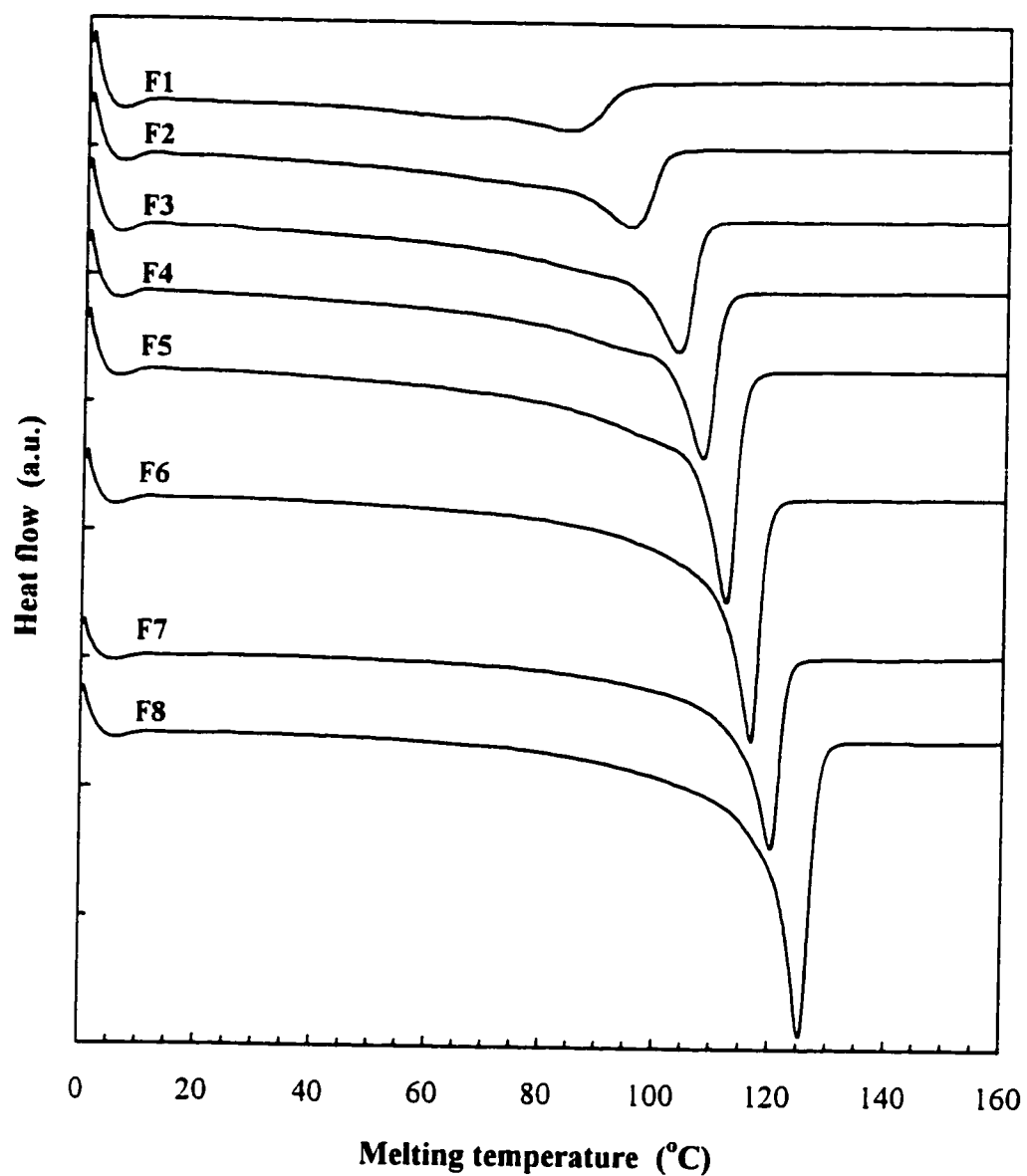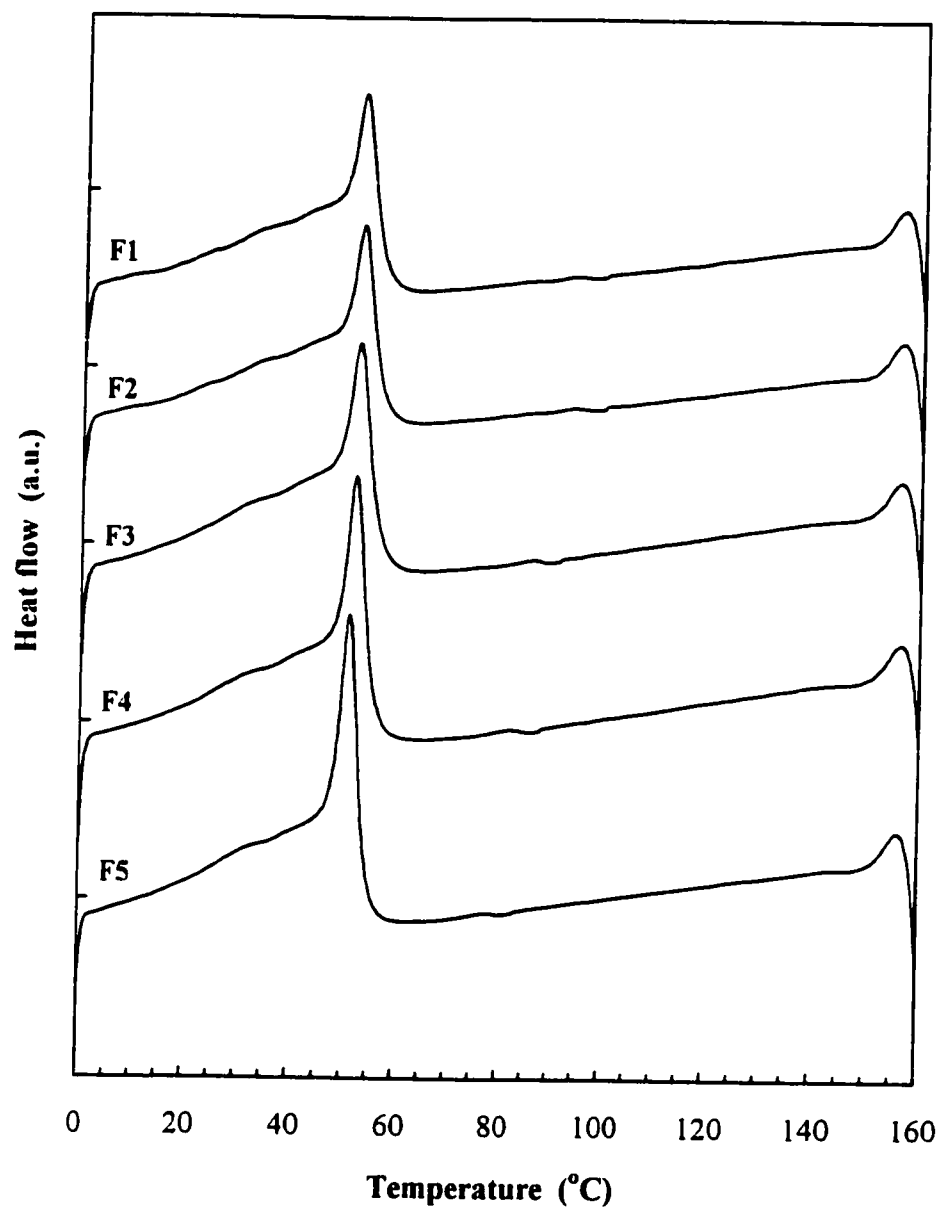
Figure 4.25. DSC exotherms of PTREF fractions of metallocene LLDPE (Exact4033). Temperature range for each fraction is the same as in Figure 4.24.
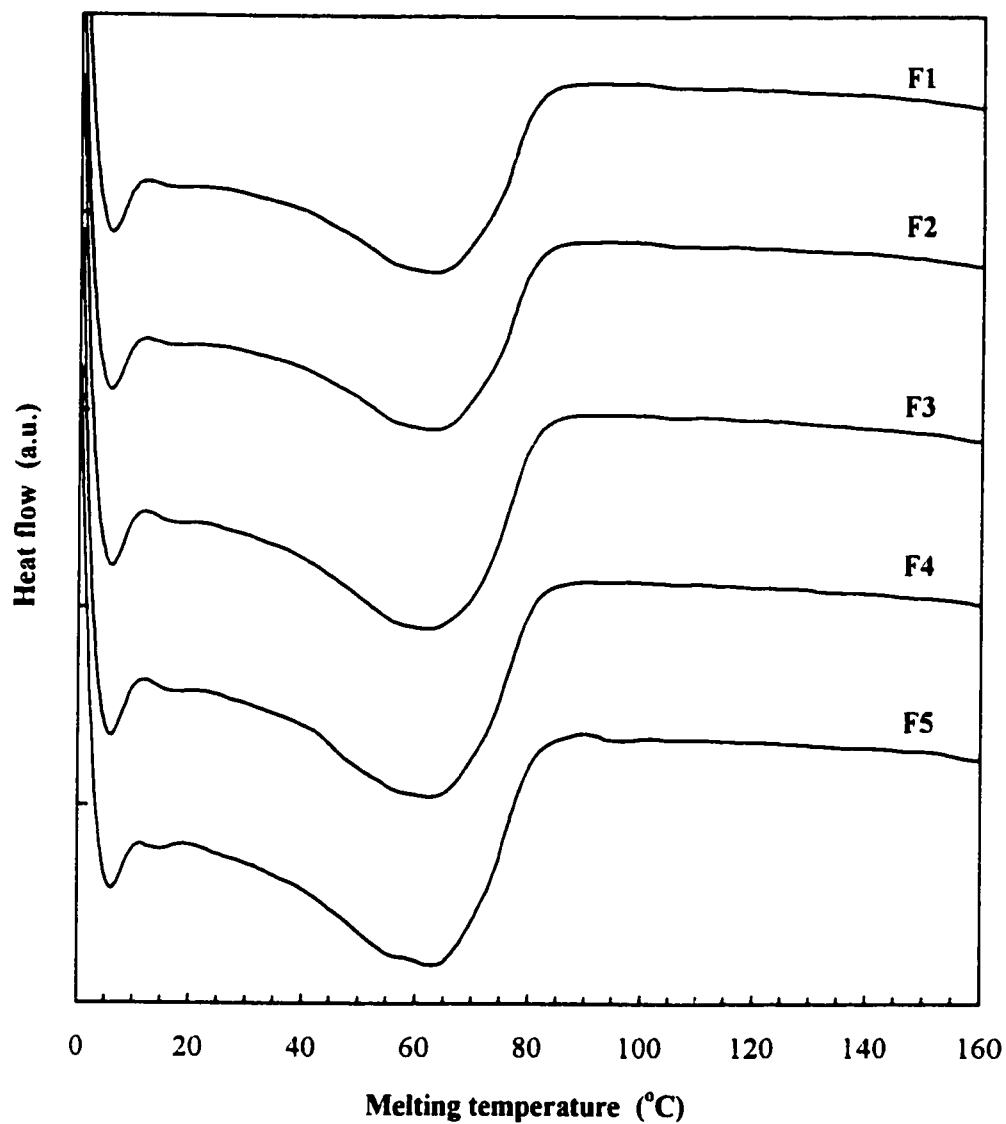
Figure 4.26. DSC endotherms of PTREF fractions of metallocene LLDPE (Exact4033). Temperature range for each fraction is the same as in Figure 4.24.

103

as low as about 15°C. The melting of SNA-treated fractions started at about 25°C with an intense peak centered at 35°C. It seemed that the SNA treatment could crystallize the highly branched molecule segments in a narrow temperature range which could not be crystallized by the usual cooling. This may explain the intense low-temperature peak on the SNA-DSC endotherms of other metallocene LLDPEs shown in Figure 4.11. The low-temperature peak representing highly branched molecule segments could not be detected by the SC-DSC or even by TREF due to the low melting temperatures or rather different fractionation mechanism, suggesting that the SNA-DSC is capable of providing complementary information on the molecular structure of LLDPEs.

The enthalpy of fusion for PTREF fractions of the Ziegler-Natta and metallocene LLDPEs from the SNA-DSC measurement are plotted against short chain branch content in Figure 4.27. It is interesting to note that the enthalpy of fusion of the Ziegler-Natta LLDPE declined substantially with increasing SCB content. Whereas that of metallocene LLDPE only slightly decreased. The enthalpy of fusion of the Ziegler-Natta sample was much higher than that of the metallocene sample even at high SCB contents where the Ziegler-Natta and metallocene fractions had similar average SCB contents. The difference may indicate that enthalpy of fusion of LLDPE is not only a function of composition, but also a strong function of compositional distribution.

The distinctive difference in methylene sequence distribution between the Ziegler-Natta and metallocene LLDPEs, as revealed above, can be better understood by considering the very different nature of the two catalyst systems. As mentioned above, there are multiple active sites present on the Ziegler-Natta catalyst (Soares and Hamielec, 1995; Balbontin et al., 1995; Starch, 1996), while the metallocene catalyst is generally believed to have a single type of catalytic site. According to the instantaneous bivariate distribution theory for the composition of linear copolymer proposed by Stockmayer (Stockmayer, 1945; Soares and Hamielec, 1995; Thomunn et al., 1997) a single catalytic site produces copolymer with a narrow distribution in both molar mass and composition. Thus, it is understandable that the LLDPE produced by single-sited metallocene catalyst shows only narrow molar mass distribution and intramolecular heterogeneity. For the
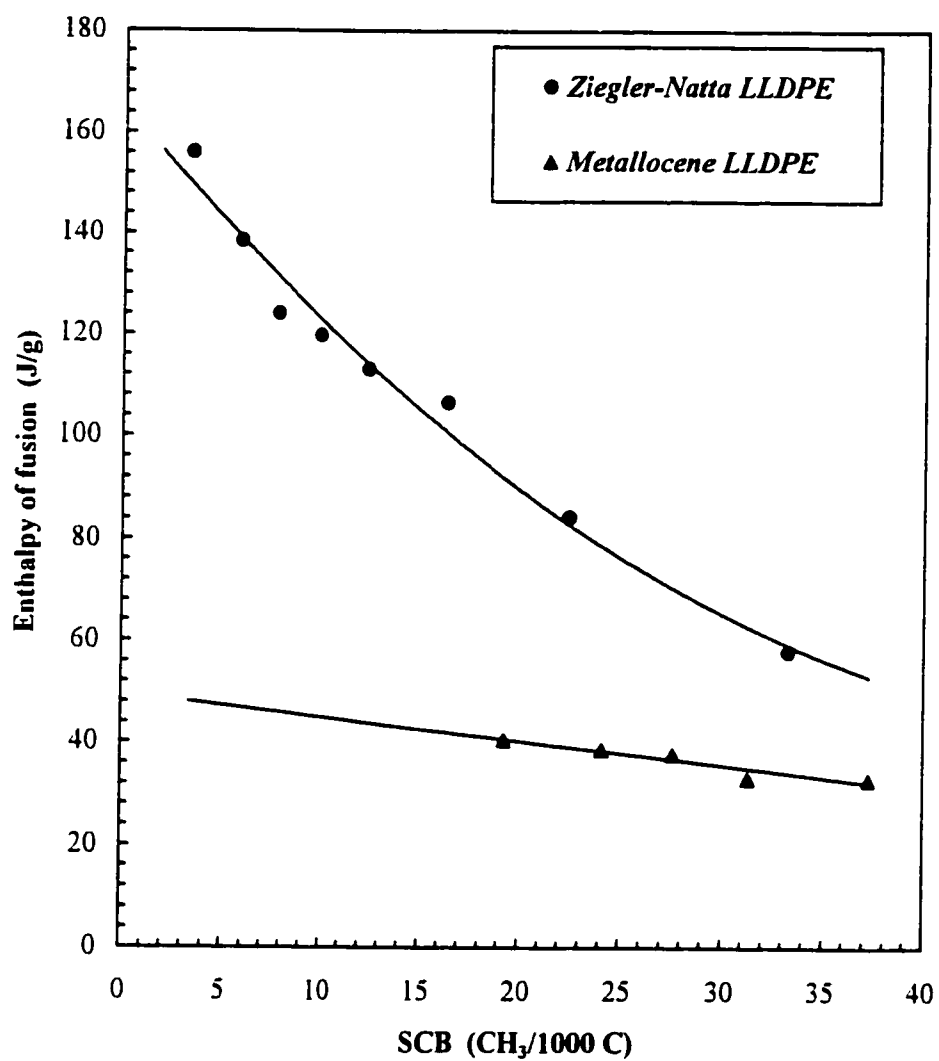
Figure 4.27. Enthalpy of fusion as a fuction of short chain branch contents for Ziegler-Natta and metallocene LLDPEs.

Ziegler-Natta catalyst having multiple sites, each site presumably produces molecules of intramolecular heterogeneity, while it is likely that different sites produces polymer with different SCB distributions. The very different methylene sequence distributions of the PTREF fractions for the Ziegler-Natta LLDPE are in agreement with the multiple site model for Ziegler-Natta catalysts.

CONCLUSIONS AND RECOMMENDATIONS

5.1. Conclusions

The molecular structure of various grades of Ziegler-Natta and metallocene LLDPEs was investigated in this study by TREF, thermally fractionated DSC, SEC, TREF-SEC cross-fractionation, and TREF-SNA-DSC cross-fractionation. Emphasis was placed on the effectiveness of different characterization techniques for the identification of the difference in short chain branch distribution (SCBD) in commercial LLDPEs, as well as on the elucidation of the heterogeity of SCBD.

ATREF analyses demonstrated that Ziegler-Natta LLDPEs show a characteristic bimodal SCB distribution, while the metallocene LLDPEs exhibit a narrower single-peaked distribution. The metallocene LLDPEs generally have high average SCB contents characterized by high weight-average and number-average SCB contents (C_w and C_n). The ratio of C_w to C_n is a good quantitative indication of the broadness of SCB distribution. The C_w/C_n ratios for the Ziegler-Natta LLDPEs are around 1.5, while those of the metallocene LLDPEs are about 1.0. The definition of C_w and C_n, and their use for describing the SCBD, is one of the contributions of the current work.

DSC results for different LLDPE samples treated with varied crystallization methods indicated that the DSC analyses of LLDPEs depend heavily on the thermal history of the LLDPE samples. The treatment of LLDPE samples using step-crystallization (SC) or successive nucleation/annealing (SNA) prior to DSC analysis is necessary to get reliable SCB distribution, particularly for the Ziegler-Natta LLDPEs with low SCB contents. It has been shown that the SNA is more effective and resolved than SC for segregating LLDPEs with respect to methylene sequence length (MSL), and the SNA-DSC can provide similar information on SCB distribution to ATREF. For metallocene LLDPEs, the SNA-DSC endotherms showed an intense peak centered at a melting temperature of

about 40°C. The low-temperature peak represents highly branched chain segments with the MSL of about 18 carbons. Such short MSL seemed not to be crystallized by the SC or detected by TREF due to the low melting temperatures or rather different fractionation mechanism, implying that the SNA-DSC is capable of providing complementary information on the SCBD of LLDPEs to TREF.

Quantitative analysis of the SNA-DSC showed that the average SCB contents estimated from the normalized heat of fusion are close to those obtained by TREF for the Zieger-Natta LLDPEs, but the average SCB contents for the metallocene LLDPEs are higher than those obtained from TREF. The low-temperature peak on the DSC endotherms of the metallocene LLDPEs is probably the major reason for the discrepancy.

TREF-SEC cross-fractionation showed that the M_w of the Ziegler-Natta sample increases monotonically with the decrease in the degree of short chain branching. However, the TREF-SEC cross-fractionation of all the commercial metallocene LLDPEs consistently indicated a maximum in the plot of M_w versus SCB, suggesting that the observed relationship of a maximum in the M_w versus SCB plot is characteristic of metallocene LLDPEs.

TREF-SNA-DSC cross-fractionation was used to obtain further insight into the heterogeneity of SCBD. The obtained results indicate that the two-dimentional fractionation according to composition is an effective way of fractionating semicrystalline polymer based on both crystallizability and methylene sequence length. It provides, in a rather direct fashion, detailed information about intramolecular and intermolecular distribution of SCBs of different types of LLDPEs.

TREF-SNA-DSC cross-fractionation demonstrated that the metallocene LLDPE possesses only intramolecular heterogeneity characterized by similar MSL distribution for all PTREF fractions. The Ziegler-Natta LLDPE shows both intramolecular and intermolecular heterogeneity, as revealed by the very different MSL distribution on the SNA-DSC endotherms of the PTREF fractions. The pronounced difference in molar mass

and short chain branch distribution between the two types of LLDPEs well reflects the characteristics of Ziegler-Natta and metallocene LLDPEs and is useful in explaining the difference in their properties.

5.2. Recommendations

As shown above, TREF is a reliable technique for the characterization of LLDPE in terms of short chain branching. Although there have been several different ways of constructing TREF calibration, it appears that the calibration curve presented in this study yields good results. It should be pointed out that the interpretation of any TREF calibration relies on the TREF separation mechanism. With the current lack of the complete understanding of TREF mechanism, the calibration of this study using MSL of known elution temperature to approximate the governing MSL for differential TREF fractions seems to be a reliable choice. The validity of the calibration can, however, be verified by some other ways. For instance, the use of dual IR detectors in future studies may help quantify the dependence of TREF calibration on the types of LLDPE, particularly for metallocene LLDPEs for which the dual IR detectors may sensitively measure the concentration of $-CH_2$ and $-CH_3$ due to the high SCB contents. Also, TREF analysis of LLDPE samples with well-defined structures (e.g., homogeneous LLDPE) will help to interpret the validity of the calibration and the mechanism of TREF separation.

The crystallization step is very crucial for TREF analysis. Even though this issue has rarely been addressed in literature, care needs to be taken when TREF is used to analyze ethylene copolymers with long branches (e.g. C_6 branches). It is recommended that an appropriate amount of support materials such as glass beads be used in crystallization solution. As well, for the elucidation of short chain branch distribution, it should be better to run the samples more than twice to ensure the reproducibility of TREF analysis.

Successive nucleation/annealing (SNA) is very effective for crystallizing highly branched polyethylene segments (methylene sequence lengths as low as 18 carbons)

which cannot be crystallized by other crystallization procedures such as the step-crystallization and the solution crystallization for TREF. Thus, the SNA-DSC is particularly suitable for the analysis of metallocene LLDPEs which generally contain high fraction of highly branched ethylene segments, and should be utilized as a complementary technique for TREF analysis. In addition, since the SNA-DSC is effective in differentiating different types of polyethylenes, it might be useful for the analysis of the blend of polyethylenes.

The quantitative analysis of the SNA-DSC endotherms using the normalized heat flow, as shown in section 4.2.2, provides a quick solution for the estimation of the average SCB content and SCBD of LLDPEs. The results can be improved by transforming the heat flow into mass fraction using another calibration that relates the enthalpy of fusion to melting temperature. However, as shown in section 4.4.3, such calibration is a strong function of SCBD, and therefore varies from sample to sample. As a consequence, the generation of the calibration requires employing other techniques such as the PTREF-SNA-DSC cross-fractionation, which makes the estimation method very tedious and almost impractical. Hence, the simplified method proposed by the present study can be adopted for the quick estimation of the average SCB content and SCBD. Similar studies on LLDPEs with well-defined structures can be conducted to check the validity of the method.

For the detailed characterization of molecular structure of LLDPE, the two-dimensional fractionation in terms of molar mass and short chain branching is quite necessary. The methodology used in this study, especially the TREF-SNA-DSC cross-fractionation, is very informative in elucidating the heterogeneity of SCBD. It is also interesting to see that the SNA-DSC analysis not only provides structural but also morphological information on LLDPEs. These studies can be complemented by other techniques such as small-angle X-ray scattering (SAXS) or wide-angle X-ray diffraction (WAXD).

REFERENCES

Abiru, T., A. Mizuno, and F. Weigand, "Microstructural Characterization of Propylene-Butene-1 Copolymer Using Temperature Rising Elution Fractionation", *Journal of Applied Polymer Science*, 68, 1493-1501 (1998).

Adisson, E., M. Ribeiro, A. Deffieux, and M. Fontanille, "Evaluation of the Heterogeneity in Linear Low-Density Polyethylene Comonomer Unit Distribution by Differential Scanning Calorimetry Characterization of Thermally Treated Sample", *Polymer*, 33, 4337 (1992).

Alamo, R., R. Domszy, and L. Mandelkern, "Thermodynamic and Structural Properties of Copolymers of Ethylene", *Journal of Physical Chemistry*, 88, 6587-6595 (1984).

Balbontin, G., I. Camurati, T. Dall'Occo, R. C. Ziegler, "Linear Low Density Polyethylene: Catalyst System Effect on Polymer Microstructure", *Journal of Molecular Catalysis A: Chemical*, 98, 123 (1995).

Bonner, J. G., C. J. Frye, and G. Capaccio, "A Novel Calibration for the Characterization of Polyethylene Copolymers by Temperature Rising Elution Fractionation", *Polymer*, 34, 3532-3534 (1993).

Borrajo, J., C. Cordon, J.M. Carella, S. Toso, and G. Goizueta, "Modelling the Fractionation Process in TREF System: Thermodynamic Simple Approach", *Journal of Polymer Science: Part B: Polymer Physics*, 33, 1627-1632 (1995).

Cheng, H. N., B.T. Stanley, and L.J. Kasehagen, "Compositional Heterogeneity in Polymer: Computer Simulation Approaches", *Macromolecules*, 25, 3779-3785 (1992).

Cheng, H. N., M. Kakugo, "^{13}C NMR Analysis of Compositional Heterogeneity in Ethylene-Propylene Copolymers", *Macromolecules*, 24, 1724-1726 (1991).

Defoor, F., G. Groeninckx, P. Schouterden, and B. Van der Heijden, "Molecular, Thermal and Morphological Characterization of Narrowly Branched Fractions of 1-Octene Liear Low-Density Polyethylene: 1. Molecular and Thermal Characterization", *Polymer*, 33(18), 3878 (1992).

Defoor, F., G. Groeninckx, H. Reynaers, P. Schouterden, and B. Van der Heijden, "Thermal and Morphological Characterization of Binary Blends of Fractions of 1-Octene LLDPE", *Journal of Applied Polymer Science*, 47, 1839-1848 (1993).

Desreux, V. and M.C. Spiegels, "Fractionation and Extraction of polyethylene", *Bulletin of Society of Chemistry, Belgium*, 59, 476-489 (1950).

Elicabe, G., C. Cordon, J. Carella, "Modelling the Fractionation Process in TREF System. III. Model Validation With Low Molar mass Homopolymers", *Journal of Polymer Science: Part B: Polymer Physics*, 34, 1147-1154 (1996).

Feng, Y. and X. Jin, "Fractionation and Characterization of a LLDPE Synthesized by a Metallocene Catalyst", *Polymer-Plastics Technology Engineering*, 37(3), 271-283 (1998).

Feng, Y. and X. Jin, "Effect of Self-Nucleation on Crystallization and Melting Behavior of Polypropylene and Its Copolymers", *Journal of Applied Polymer Science*, 72, 1559-1564 (1999).

Fillon, B., J.C. Wittmann, B. Lotz, and A. Thierry, "Self-Nucleation and Recrystallization of Isotactic Polypropylene (α Phase) Investigated by Differential Scanning Calorimetry", *Journal of Polymer Science: Part B: Polymer Physics*, 31, 1383-1393 (1993).

Francuskiewicz, F., "Temperature Rising Elution Fractionation", in *Polymer Fractionation*, Springer-Verlag, Berlin Heidelberg, (1994).

Fu, Q., F. Chiu, K. W. McCreight, M. Guo, W. W. Tseng, S. Z. D. Cheng, M. Y. Keating, E. T. Hsieh, and P. J. DesLauriers, "Effects of the Phase-Separated Melt on Crystallization Behavior and Morphology in Short Chain Branched Metallocene Polyethylenes", *Journal of Macromolecular Science - Physics*, B36(1), 41-60 (1997).

Galli, P., "The Breakthrough in Catalysis and Processes for Olefin Polymerization: Innovative Structures and a Strategy in the Materials Area for the Twenty-First Century", Progress in Polymer Science, 19, 159 (1994).

Glockner, G., "Temperature Rising Elution Fractionation: A Review", *Journal of Applied Polymer Science, Applied Polymer Symposium*, 45, 1-24 (1990)

Hamielec, A. E. and J. B. P. Soares, "Polymerization Reaction Engineering — Metallocene Catalyst", *Progress in Polymer Science*, 21, 651 (1996).

Hosoda, S., "Structural Distribution of Linear Low-Density Polyethylenes", *Polymer Journal*, 20(5), 383-397 (1988).

Huang, J. and G. L. Rempel, "Ziegler-Natta Catalysts for Olefin Polymerization: Mechanistic Insights from Metallocene Systems", *Progress in Polymer Sciences*, 20, 459 (1995).

Huang, J. C.-K., Y. Lacombe, D.T. Lynch, and S.E. Wanke, "Effects of Hydrogen and 1-Butene Concentrations on the Molecular Properties of Polyethylene Produced by Catalytic Gas-Phase Polymerization", *Industrial & Engineering Chemistry Research*, 36(4), 1136-1143 (1997).

Kakugo, M., T. Miyatake, K. Mizunuma, and Y. Kawai, "Characteristics of Ethylene-Propylene and Propylene-1-Butene Copolymerization over TiCl₃·1/3AlCl₃ - Al(C₂H₅)₂Cl", *Macromolecules*, 21, 2309-2313 (1988).

Kale, L.T., T.A. Plumley, R.M. Patel, O.D. Redwine, and P. Jain, "Structure-Property Relationships of Ethylene/1-Octene and Ethylene/1-Butene Copolymers Made Using INSITE Technology", *Journal of Plastic Film & Sheeting*, 12, 27-40 (1996).

Kapoglanlan, S. A. and I. R. Harrison, "The Similarity of Compositional Distribution Information Generated by DSC and TREF", *Thermochimica Acta*, 288, 239-245 (1996).

Kapoglanlan, S. A. and I. R. Harrison, "A Temperature Rising Elution Fractionation Study of Short Chain Branching Behavior in Ultra Low Density Polyethylene", *Polymer Engineering and Science*, 36(5), 731 (1996).

Karbashewski, E., L. Kale, A. Rudin, W. J. Tchir, D.G. Cook, and J.O. Pronovost, "Characterization of Linear Low Density Polyethylene by Temperature Rising Elution Fractionation and by Differential Scanning Calorimetry", *Journal of Applied Polymer Science*, 44, 425 (1992).

Karbashewski, E., A. Rudin, L. Kale, and W. J. Tchir, D.G. Cook, "A Note on the Effect of Comonomer Sequence Distribution on TREF Branching Distribution", *Polymer Engineering and Science*, 33(20), 1370-1371 (1993).

Keating, M., I. H., Lee, and C. S., Wong, "Thermal Fractionation of Ethylene Polymers in Packaging Application", *Thermochimica Acta*, 284, 47 (1996).

Keating, M. Y. and E. F. McCord, "Evaluation of the Comonomer Distribution in Ethylene Copolymers Using DSC Fractionation", *Thermochimica Acta*, 243, 129 (1992).

Kelusky, E. C., C.T. Elston, and R. E. Murray, "Characterizing Polyethylene-Based Blends with Temperature Rising Fractionation (TREF) Techniques", *Polymer Engineering and Science*, 27(20), 1562-1571 (1987).

Kim, Y. S., Chan II Chung, Shin Yaw Lai, and Kun Sup Hyun, "Processability of Polyethylene Homopolymers and Copolymers with Respect to Their Molecular Structure", *Korean Journal of Chemical Engineering*, 13(3), 294-303 (1996).

Lacombe, Y., "TREF and SEC Characterization of Ethylene/1-Butene Copolymers Produced at Various 1-Butene and Hydrogen Pressures", *M.Sc. Thesis, University of Alberta*, Edmonton, Canada (1995).

Mandelkern, L., "Crystallization and Melting", in *Comprehensive Polymer Science: The Synthesis, Characterization, Reactions & Applications of Polimers*, Vol. 2: Polymer Properties, 415-458, Pergamon Press, New York, (1989).

Mandelkern, L. and G. Stack, "Equilibrium Melting Temperature of Long-Chain Molecules", *Macromolecules*, 17, 871-878 (1984).

Marigo, A., R. Zannetti, and Federico Milan, "A Small- and Wide-Angle X-Ray Scattering Study of the 1-Butene LLDPE Obtained by Metallocene and Ziegler-Natta Catalysis", *European Polymer Journal*, 33(5), 595-598 (1997).

Marigo, A., C. Marega, R. Zannetti, and P. Sgarzi, "A Study of the Lamellar Thickness Distribution in 1-Butene, 4-Methyl-1-Pentene and 1-Hexene LLDPE by Small and Wide Angle X-Ray Scattering and Transmission Electron Microscopy", *European Polymer Journal*, 34(5/6), 597-603 (1998).

Mathot, V. B. F., "The Crystallization and Melting Region", in *Calorimetry and Thermal Analysis of Polymers*, Edited by Vincent B. F. Mathot, Hanser Publishers, New York (1994).

Mathot, V. B. F., and M.F.J., Pijpers, "Molecular Structure, Melting Behavior, and Crystallinity of 1-Octene-Based Very Low Density Polyethylenes (VLDPEs) as Studied by Fractionation and Heat Capacity Measurements with DSC", *Journal of Applied Polymer Science*, 39, 979-994 (1990).

Mills, P. J., and J.N. Hay, "The Lamella Size Distribution in Non-Isothermally Crystallized Low Density Polyethylene", *Polymer*, 25, 1277-1280 (1984).

Mingozzi, I. and S. Nascetti, "Chemical Composition Distribution and Molecular Weight Distribution Determination of Ethylene, 1-Butene Linear Low-Density Polyethylene (LLDPE)", *International Journal of Polymer Analysis & Characterization*, 3, 59 (1996).

Mirabella, F. M., Jr. and E. A. Ford, "Characterization of Linear Low Density Polyethylene: Cross-Fractionation According to Copolymer Coposition and Molecular Weight", *Journal of Polymer Science: Part B: Polymer Physics*, 25, 777 (1990).

Monrabal, B., "Crystallization Analysis Fractionation: A New Technique for the Analysis of Branching Distribution in Polyolefins", *Journal of Applied Polymer Science*, 52, 491-499 (1994).

Monrabal, B., "Crystallization Analysis Fractionation. A New Approach for the Composition Analysis of Semicrystalline Polymers", *Macromolecular Symposium*, 110, 81-86 (1996).

Monrabal, B., J. Blanco, J. Nieto, and J.B.P. Soares, "Characterization of Homogeneous Ethylene/1-Octene Copolymers Made with a Single-Site Catalyst. CRYSTAF Analysis and Calibration", *Journal of Polymer Science, Part A: Polymer Chemistry*, 37, 89-93 (1999).

114

Morse, P. M., "New Catalysts Renew Polyolefins", *Chemical & Engineering News*, July 6, 11 (1998).

Muller, A. J., Z. H. Hernandez, M. L. Arnal, and J. J. Sanchez, "Successive Self-Nucleation/Annealing (SSA): A Novel Technique to Study Molecular Segregation During Crystallization", *Polymer Bulletin*, 39, 465 (1997).

Nakano, S. and Y. Goto, "Development of Automatic Cross fractionation: Combination of Crystallinity Fractionation and Molar Mass Fractionation", *Journal of Applied Polymer Science*, 26, 4217 (1981).

Peeters, M., B. Goderis, C. Vonk, H. Reynaers, and V. Mathot, "Morphology of Homogeneous Copolymers of Ethene and 1-Octene. I. Influence of Thermal History on Morphology", *Journal of Polymer Science: Part B: Polymer Physics*, 35, 2689-2713 (1997).

Peeters, M., B. Goderis, H. Reynaers, and V. Mathot, "Morphology of Homogeneous Copolymers of Ethene and 1-Octene. II. Structural Changes on Annealing", *Journal of Polymer Science: Part B: Polymer Physics*, 37, 83-100 (1997).

Pigeon, M. G. and A. Rudin, "Comparison of Analytical and Preparative TREF Analysis: A Mathematical Approach to Correcting Analytical TREF Data", *Journal of Applied Polymer Science*, 47, 685-696 (1993).

Pigeon, M. G. and A. Rudin, "Branching Measurement by Analytical TREF: A Fully Quantitative Technique", *Journal of Applied Polymer Science*, 51, 303-311 (1994).

Prasad, A., "A Quantitative Analysis of Low Density Polyethylene and Linear Low Density Polyethylene Blends by Differential Scanning Calorimetry and Fourier Transform Infrared Spectroscopy Methods", *Polymer Engineering and Science*, 38(10), 1716-1728 (1998).

Reddy, S. S. and S. Sivaram, "Homogeneous Metallocene-Methylaluminoxane Catalyst Systems for Ethylene Polymerization", *Progress in Polymer Sciences*, 20, 309 (1995).

Richards, C. T., "Overview of Recent Advances in Polyethylene Process and Product Technologies, *Plastics Rubber Composites Processing and Applications*, 27(1), 3-7 (1998).

Schouterden, P., and G. Groeninckx, "Fractionation and Thermal Behavior of Linear Low Density Polyethylene", *Polymer*, 28, 2099-2104 (1987).

Shaw, B. M., K.B. McAuley, and W. Bacon, "Similating Joint Chain Length and Composition Fractions from Semi-Batch Ethylene Copolymerization Experiments", *Polymer Reaction Engineering*, 6(2), 113-142 (1998).

Shiramaya, K., T. Okada, and S.I. Kita, "Distribution of Short Chain Branching in Low-Density Polyethylene", *Journal of Polymer Science*, Part A 3, 907-916 (1965).

Soares, J. B. P. and A. E. Hamielec, "Temperature Rising Elution Fractionation of Linear Polyolefins", *Polymer*, 36(8), 1639-1654 (1995a).

Soares, J. B. P. and Archie E. Hamielec, "Analyzing TREF Data by Stockmayer's Bivariate Distribution", *Macromolecule Theory Simulation*, 4, 305 (1995b).

Soares, J. B. P., R.F. Abbott, J.N. Willis, and X. Liu, "A New Methodology for Studying Multiple-Site-Type Catalysts for the Copolymerization of Olefins", *Macromolecular Chemistry Physics*, 197, 3383-3396 (1996).

Stack, G. M. and Mandelkern, "On the Crystallization of High Molecular Weight Normal Hydrocarbons", *Macromolecules*, 21, 510-514 (1988).

Starck, P., "Studies of the Comonomer Distributions in Low Density Polyethylenes Using Temperature Rising Elution Fractionation and Stepwise Crystallization by DSC", *Polymer International*, 40(2), 111 (1996).

Stockmayer, W. H., "Distribution of Chain Lengthes and Compositions in Copolymers", *Journal of Chemical Physiscs*, 13, 199-207 (1945).

Tacx, J. C. J., "Effect of Molar Maa Ratio of Monomers on the Mass Distribution of Chain Lengths and Compositions in Copolymers: Extension of the Stockmayer Theory", *Journal of Polymer Science: Part A: Polymer Chemistry*, 26, 61-69 (1988).

Takahashi, M., N. Kashiwa, A. Todo, and M. Ohgizawa, "Structure and Properties of Metallocene LLDPE in the Gas Phase Process", *Metallocene '95*, 61-73 (1995).

Thomann, Y., Friedrich G. Sernetz, Ralf Thomann, Jorg Kressler, and Rolf Mulhaupt, "Temperature Rising Elution Fractionation of a Random Ethene/Styrene Copolymer", *Macromolecular Chemistry and Physics*, 198, 739 (1997).

Todo, A. and N. Kashiwa, "Structure and Properties of New Olefin Polymers", *Macromolecular Symposium*, 101, 301-308 (1996).

Ungar, G. and A. Keller, "Inversion of the Temperature Dependence of Crystallization Rates Due to Onset of Chain Folding", *Polymer*, 28, 1989-1907 (1987).

Usami, T., "Branching Analysis for Polyethylenes", in *Handbook of Polymer Science and Technology*, Vol. II, 435-483, Marcel Dekker Inc., New York (1989).

Usami, T., Y. Gotoh, and S. Takayama, "Generation Mechanism of Short-Chain Branching Distribution in Liear Low-Density Polyethylenes", *Macromolecules*, 19, 2722 (1986).

Wild, L., "Temperature Rising Elution Fractionation", *Advances in Polymer Science*, 98, 1 (1991).

Wild, L., S. Chang, and M.J. Shankernarayanan, "Improved Method for Compositional Analysis of Polyolefins by DSC", *Polymer Preprints of American Chemical Society*, 31, 270-271 (1990).

Wild, L., and T. R. Ryle, "Crystallizability Distribution of Polymers: A New Analytical Technique", ", *Polymer Preprints of American Chemical Society*, 18, 182-188 (1977).

Wild, L., T. R. Ryle and D. C. Knobeloch, "Branching Distribution in LLDPEs", *Polymer Preprints of American Chemical Society*, 23(2), 133 (1982a).

Wild, L., T. R. Ryle, D. C. Knobeloch, and I.R. Peat, "Determination of Branching Distributions in Polyethylene and Ethylene Copolymers", *Journal of Polymer Science: Polymer Physics Edition*, 20, 441-455 (1982b).

Wilfong, D. L., "Crystallization Mechanism for LLDPE and Its Fractions", *Journal of Polymer Science: Part B: Polymer Physics*, 28, 861-870 (1990).

Wunderlich, B., *Macromolecular Physics*, Vol. 2, Academic Press, New York, 1976.

Zhang, M., J.C.K. Huang, D.T. Lynch, and S.E. Wanke, "Characterization of LLDPE by DSC", *ANTEC '98*, 2000-2002 (1998).

Zhou, H., and G.L. Wilkes, "Comparison of Lamellar Thickness and Its Distribution Determined from DSC, SAXS, TEM and AFM for High Density Polyethylene Films Having a Stacked Lamellar Morphology", *Polymer*, 38(23), 5735-5747 (1997).

Zhou, X. Q., and J.N. Hay, "Fractionation and Structural Properties of Linear Low Density Polyethylene", *European Polymer Journal*, 29, 291-300 (1993).

Appendix A. DESCRIPTION OF ATREF AND PTREF ANALYSES

The experimental details of TREF analyses conducted in this project are summarized in Appendix A. Table A.1 lists the crystallization and TREF operating conditions for ATREF experiments. In addition to the experimental conditions in the Table A.1, the sample size for ATREF runs was typically 5 to 7 mg for Ziegler-Natta LLDPEs and 10 to 11 mg for metallocene LLDPEs.

Table A.2 is a list of sample size, temperature range, and number of fractions collected for PTREF runs. All the LLDPE samples were crystallized in o-xylene solution. Other PTREF experimental conditions and procedures were similar for all LLDPE samples and were described in detail in Section 3.1.2.2.

Table A.1. Experimental details of the ATREF analyses

Sample	file	crystallizatin method	crystallization solvent	solvent flow rate (mL/min)	heating rate (°C/min)	comments
PF0118F	peb01	solution	o-xylene	1.0	1.0	Good run
PF0118F	peb02	solution	o-xylene	1.0	1.0	Good run (IR detector set 3.42 μm)
PF0118F	peb03	solution	o-xylene	1.0	1.0	Good run
PF0118F	Pebsna01	Solution-SNA	o-xylene	1.0	1.0	Good run
PF0118F	Pebsna01	Soluton-SNA	o-xylene	1.0	1.0	Good run
PF0118F	Pebsna01	Solution-SNA	o-xylene	1.0	1.0	Good run
TF0119F	Peh01	solution	o-xylene	1.0	1.0	Good run
TF0119F	Peh02	solution	o-xylene	1.0	1.0	Good run
TF0119F	Peh03	solution	o-xylene	1.0	1.0	Good run
TF0119F	Peh04	solution	o-xylene	1.0	1.0	Good run
Sclair13J7	Peo01	solution	o-xylene	1.0	1.0	Random bumps on TREF profile
Sclair13J7	Peo02	solution	o-xylene	1.0	1.0	Random bumps on TREF profile
Sclair13J7	Peo03	solution	o-xylene	1.0	1.0	Random bumps on TREF profile
Sclair13J7	Peo05	solution	o-xylene	1.0	1.0	Good run
Sclair13J7	Peo06	solution	o-xylene	1.0	1.0	Good run
Exact4033	exa40331	solution	o-xylene	1.0	1.0	Good run
Exact4033	exa40332	solution	o-xylene	1.0	1.0	Good run
Exact4033	exa40333	solution	o-xylene	1.0	1.0	Good run

Sample	file	crystallizatin method	crystallization solvent	solvent flow rate (mL/min)	heating rate (°C/min)	comments
Exact4033	exsna01	solution-SNA	o-xylene	1.0	1.0	Good run
Exact4033	exsna02	solution-SNA	o-xylene	1.0	1.0	Good run
SLP9095	SLP90951	solution	o-xylene	1.0	1.0	Good run
SLP9095	SLP90952	solution	o-xylene	1.0	1.0	Good run
SLP9029	SLP90291	solution	o-xylene	1.0	1.0	Good run
SLP9029	SLP90292	solution	o-xylene	1.0	1.0	Good run
Engage8100	eng81001	solution	o-xylene	1.0	1.0	Good run
Engage8100	eng81002	solution	o-xylene	1.0	1.0	Good run
Engage8100	eng81003	solution	o-xylene	1.0	1.0	Good run
Engage8100	eng81004	solution	o-xylene	1.0	1.0	Good run
Attane4201	att42011	solution	o-xylene	1.0	1.0	Good run
Attane4201	att42012	solution	o-xylene	1.0	1.0	Good run
Attane4201	att42013	solution	o-xylene	1.0	1.0	Good run
Attane4201	att42014	solution	o-xylene	1.0	1.0	Good run
Attane4201	dowsna01	solution-SNA	o-xylene	1.0	1.0	Good run
Attane4201	dowsna02	solution-SNA	o-xylene	1.0	1.0	Good run

Table A.2. Experimental details of the PTREF runs

Sample	file	sample size (mg)	temperature range (°C)	number of fractions	comments
GC93048	ptref01	300	30-90	9	Good run
GC93048	ptref02	300	30-95	12	Good run
PF0118F	ptref03	300	30-90	8	Good run
PF0118F	ptref05	300	30-95	12	Good run for SEC
PF0118F	ptref08	320	30-90	6	Samples overlapping
PF0118F	ptref09	320	30-85	6	Good run for DSC
PF0118F	Ptref20	68	85-110	3	Good run for SEC
Exact4033	Ptref10	119	0-60	7	Good run
Exact4033	Ptref13	20	20-65	8	Good run for SEC
Exact4033	Ptref15	68	0-50	7	bad run (power failure)
Exact4033	Ptref16	37	0-70	10	Good run
Exact4033	Ptref18	103	0-65	7	Good run for DSC
SLP9095	Ptref11	103	20-65	8	Good run for SEC
Engage8100	Ptref17	35	0-60	9	Good run for SEC
Attane4201	Ptref14	122	20-85	10	Good run for SEC

Appendix B. DESCRIPTION OF DSC ANALYSES

Table B.1 lists the sample size, crystallization method, and DSC operating conditions for various LLDPE samples, standard samples, and PTREF fractions. The sample size for commercial LLDPE samples was normally about 11 mg. For standard linear hydrocarbon and polyethylene samples, a smaller sample size of about 5 mg was used due to the limitation of the volume of DSC pans. The sample size of PTREF fractions was also about 5 mg, depending on the amount of sample collected. Other experimental details were given in Section 3.2.

Table B.1. Experimental details of DSC analyses.

Sample	sample size (mg)	file	crystallization method	heating rate (°C/min)	cooling rate (°C/min)	comments
PF0118F	12.7	Z-PE0.001	SC	10.0	10.0	Good run
PF0118F	12.9	Z-PE0.014	SC	10.0	10.0	Good run
PF0118F	12.0	Z-PE0.018	As-received	10.0	10.0	Good run
PF0118F	8.3	Z-PE0.025	Solution	10.0	10.0	Good run
PF0118F	11.2	Z-PE0.032	SC	5.0	10.0	Good run
PF0118F	11.2	Z-PE0.033	SC	1.0	10.0	Good run
PF0118F	11.2	Z-PE0.038	Slow-melt	10.0	10.0	Good run
PF0118F	12.8	Z-PE0.041	SNA	10.0	10.0	DSC failure, bad run
PF0118F	11.9	Z-PE0.044	SNA	10.0	10.0	Good run
PF0118F	11.0	Z-PE0.050	SNA	10.0	10.0	Good run
PF0118F	11.5	Z-PE0.110	As-received	10.0	10.0	Good run
PF0218F	12.8	Z-PE0.003	SC	10.0	10.0	Good run
PF0218F	8.3	Z-PE0.026	Solution	10.0	10.0	Good run
PF0218F	12.0	Z-PE0.051	SNA	10.0	10.0	Good run
TF0119F	11.4	Z-PE0.002	SC	10.0	10.0	Good run
TF0119F	12.9	Z-PE0.011	SC	10.0	10.0	Good run
TF0119F	11.8	Z-PE0.034	Slow-melt	10.0	10.0	Good run
TF0119F	12.6	Z-PE0.042	SNA	10.0	10.0	Good run

123

Sample	sample size (mg)	file	crystallization method	heating rate (°C/min)	cooling rate (°C/min)	comments
TF0119F	13.0	Z-PE0.055	SNA	10.0	10.0	Good run
Sclair13J7	12.4	Z-PE0.004	SC	10.0	10.0	Good run
Sclair13J7	11.2	Z-PE0.035	Slow-melt	10.0	10.0	Good run
Sclair13J7	12.2	Z-PE0.043	SNA	10.0	10.0	Good run
Sclair13J7	12.7	Z-PE0.044	SNA	10.0	10.0	Good run
Sclair13J7	11.1	Z-PE0.108	As-received	10.0	10.0	Good run
Exact4033	11.8	Z-PE0.005	SC	10.0	10.0	Good run
Exact4033	11.6	Z-PE0.028	SC	10.0	10.0	Good run
Exact4033	12.6	Z-PE0.030	Solution	10.0	10.0	Good run
Exact4033	11.5	Z-PE0.046	SNA	10.0	10.0	Good run
Exact4033	9.4	Z-PE0.097	As-received	10.0	10.0	Good run
SLP9095	12.4	Z-PE0.006	SC	10.0	10.0	Good run
SLP9095	11.6	Z-PE0.008	SC	10.0	10.0	Good run
SLP9095	10.9	Z-PE0.017	As-received	10.0	10.0	Good run
SLP9095	10.8	Z-PE0.031	Solution	10.0	10.0	Good run
SLP9095	10.8	Z-PE0.047	SNA	10.0	10.0	Good run
Engage8100	12.0	Z-PE0.009	SC	10.0	10.0	Good run
Engage8100	11.7	Z-PE0.016	As-received	10.0	10.0	Good run
Engage8100	10.7	Z-PE0.048	SNA	10.0	10.0	Good run
Attane4201	11.8	Z-PE0.027	SC	10.0	10.0	Good run

Sample	sample size (mg)	file	crystallization method	heating rate (°C/min)	cooling rate (°C/min)	comments
Attane4201	10.7	Z-PE0.045	SNA	10.0	10.0	Good run
Attane4201	10.7	Z-PE0.098	As-received	10.0	10.0	Good run
SLP9029	12.4	Z-PE0.007	SC	10.0	10.0	Good run
SLP9029	10.5	Z-PE0.049	SNA	10.0	10.0	Good run
S221 (HDPE)	12.2	Z-PE0.013	SC	10.0	10.0	Good run
S221 (HDPE)	12.2	Z-PE0.053	SNA	10.0	10.0	Good run
S216 (LDPE)	12.4	Z-PE0.012	SC	10.0	10.0	Good run
S216 (LDPE)	12.4	Z-PE0.052	SNA	10.0	10.0	Good run
C$_{20}$	12.6	Z-PE0.024	SC	10.0	10.0	Good run
C$_{20}$	12.6	Z-PE0.024	SC	10.0	10.0	Good run
C$_{20}$	12.6	Z-PE0.024	SNA	10.0	10.0	Good run
C$_{40}$	5.9	Z-PE0.023	SC	10.0	10.0	Good run
C$_{40}$	5.9	Z-PE0.089	SNA	10.0	10.0	Good run
C$_{60}$	4.7	Z-PE0.022	SC	10.0	10.0	Good run
C$_{60}$	4.7	Z-PE0.093	SNA	10.0	10.0	Good run
LP1482	5.3	Z-PE0.021	SC	10.0	10.0	Good run
LP1482	5.3	Z-PE0.084	SNA	10.0	10.0	Good run
LP1482	5.3	Z-PE0.094	SNA	10.0	10.0	Good run
LP1483	4.9	Z-PE0.020	SC	10.0	10.0	Good run
LP1483	4.9	Z-PE0.085	SNA	10.0	10.0	Good run

125

Sample	sample size (mg)	file	crystallization method	heating rate (°C/min)	cooling rate (°C/min)	comments
LP1483	4.9	Z-PE0.090	SNA	10.0	10.0	Good run
LP1484a	5.8	Z-PE0.019	SC	10.0	10.0	Good run
LP1484a	5.8	Z-PE0.086	SNA	10.0	10.0	Good run
LP1484a	5.8	Z-PE0.091	SNA	10.0	10.0	Good run
$C_{40}+C_{60}$	4.7 (50/50)	Z-PE0.082	SNA	10.0	10.0	Good run
$C_{40}+C_{60}$	4.7 (50/50)	Z-PE0.088	SNA	10.0	10.0	Good run
$C_{60}+LP1482$	4.8 (50/50)	Z-PE0.082	SNA	10.0	10.0	Good run
$C_{60}+LP1482$	4.8 (50/50)	Z-PE0.095	SNA	10.0	10.0	Good run
$C_{60}+LP1482$	3.6 (50/50)	Z-PE0.099	SNA	10.0	10.0	Good run
PF0118F-F1[a]	5.0	Z-PE0.067	SNA	10.0	10.0	Good run
PF0118F-F2[a]	6.3	Z-PE0.064	SNA	10.0	10.0	Good run
PF0118F-F3[a]	6.4	Z-PE0.063	SNA	10.0	10.0	Good run
PF0118F-F4[a]	6.2	Z-PE0.066	SNA	10.0	10.0	Good run
PF0118F-F5[a]	7.3	Z-PE0.068	SNA	10.0	10.0	Good run
PF0118F-F6[a]	6.4	Z-PE0.069	SNA	10.0	10.0	Good run
PF0118F-F7[a]	4.2	Z-PE0.121	SNA	10.0	10.0	Good run
PF0118F-F8[a]	5.7	Z-PE0.120	SNA	10.0	10.0	Good run
Exact4033-F1[b]	1.0	Z-PE0.100	SNA	10.0	10.0	Good run
Exact4033-F2[b]	5.2	Z-PE0.103	SNA	10.0	10.0	Good run
Exact4033-F3[b]	6.3	Z-PE0.104	SNA	10.0	10.0	Good run

Sample	sample size (mg)	file	crystallization method	heating rate (°C/min)	cooling rate (°C/min)	comments
Exact4033-F4[b]	6.2	Z-PE0.105	SNA	10.0	10.0	Good run
Exact4033-F5[b]	6.2	Z-PE0.106	SNA	10.0	10.0	Good run

SC: Step-crystallization.
SNA: Successive nucleation annealing.
[a]: PTREF fraction of PF0118F.
[b]: PTREF fraction of Exact4033

Appendix C. REPRODUCIBILITY OF ATREF

Reproducibility required of TREF analyses is to be considered reliable. The crystallization conditions were the key to the good reproducibility. Figure C.1 shows the TREF profiles of Ziegler-Natta LLDPE (ethylene-1-octene copolymer Sclair13J7). The crystallization conditions for the four samples were the same except that the amount of glass beads contained in the crystallization solutions was different. It follows that when a small amount of glass beads was used, the obtained TREF profile deviated significantly from the bimodal TREF profile normally observed for Ziegler-Natta LLDPE. Therefore, the amount of glass beads added in the crystallization solution should be 1.4 to 1.6 g for about 6 mg of sample size (profiles C and D in Figure C.1).

It should be pointed out that for ethylene-1-butene copolymers (e.g., PF0118F). The reproducibility of ATREF analyses is generally good, even if no glass beads were added in the crystallization solution.
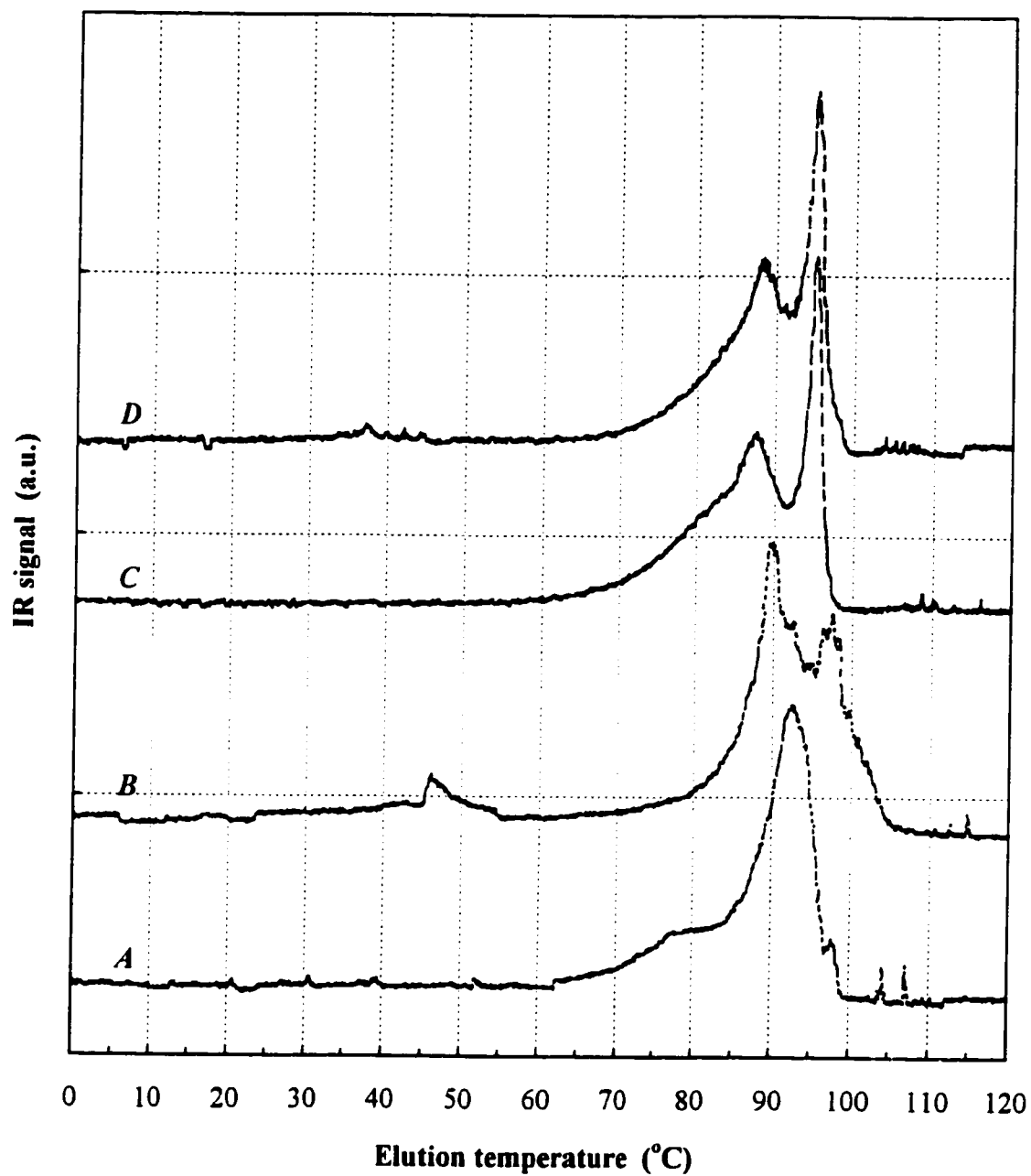
Figure C.1. Effect of crystallization conditions on TREF reproducibility: (A) without glass bead; (B) with 0.5 g of glass beads; (C) with 1.4 g of glass beads; and (D) with 1.6 g of glass beads in crystallization solution.

129

Appendix D. PROCEDURE FOR CALCULATING AVERAGE SCB CONTENTS FROM SNA-DSC ENDOTHERMS

The calculation of average SCB contents was based on the peak temperatures and peak areas, which were obtained by fitting the SNA-DSC endotherm using the Peakfit software (see Section 4.3.5). The procedure described below was used to calculate average SCB contents from the obtained peak temperatures and areas:

1. Peak temperature (T_i) was converted into mole fraction of crystallizable ethylene units (X_i) by using the calibration equation (in Figure 3.7), that is:

$$X_i = \exp(0.3451 - 142.2/T_i)$$

2. The mole fraction of crystallizable ethylene units which melted at temperature T_i were translated into methylene sequence length (MSL) by the following equation:

$$(MSL)_i = \frac{2X_i}{(1 - X_i)}$$

3. Since each MSL is connected with the other two MSLs in a molecule, each MSL is counted as one short chain branch. Hence, MSL was converted to SCB content (branches in 1,000 carbons) by the following equation:

$$C_i = \frac{1000}{(MSL)_i}$$

where C_i is the SCB content.

130

4. Knowing the SCB content (C_i) and peak area (A_i) for each peak of the DSC endotherms, the number-average SCB content (C_n) and weight-average SCB content (C_w) were calculated by using Equations 3.3 and 3.4:

$$C_n = \frac{\sum A_i C_i}{\sum A_i}$$

$$C_w = \frac{\sum A_i C_i^2}{\sum A_i C_i}$$

It should be mentioned that the above treatment missed counting one end SCB for each molecule. The error is, however, negligible considering the large molar mass of the LLDPE samples.